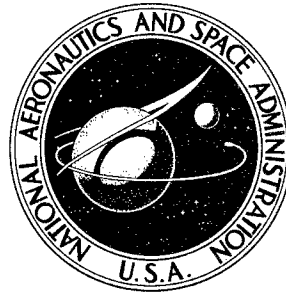


**NASA CONTRACTOR
REPORT**



NASA CR-243

NASA CR-243

AMPTIAC

60810

DISTRIBUTION STATEMENT A
Approved for Public Release
Distribution Unlimited

**BOILING HEAT TRANSFER
FOR CRYOGENICS**

by J. D. Seader, W. S. Miller, and L. A. Kalvinskas

Prepared under Contract No. NAS 8-5337 by
ROCKETDYNE
Canoga Park, Calif.
for

20010823 131

BOILING HEAT TRANSFER FOR CRYOGENICS

By J. D. Seader, W. S. Miller, and L. A. Kalvinskas

Distribution of this report is provided in the interest of information exchange. Responsibility for the contents resides in the author or organization that prepared it.

Prepared under Contract No. NAS 8-5337 by
ROCKETDYNE
Canoga Park, Calif.

for

NATIONAL AERONAUTICS AND SPACE ADMINISTRATION

FOREWORD

Rocketdyne, a Division of North American Aviation, Inc., has prepared this final report which documents in detail all of the work performed in fulfillment of the program "Boiling Heat Transfer for Cryogenics" sponsored by the National Aeronautics and Space Administration, George C. Marshall Space Flight Center, Huntsville, Alabama, under Contract No. NAS8-5337. The work was performed by the Heat Transfer and Fluid Dynamics Unit of the Research Department during a 9-month period extending from 16 May 1963 to 15 February 1964.

ACKNOWLEDGMENT

This report was written by J. D. Seader, W. S. Miller, and L. A. Kalvinskas of the Rocketdyne Research Department. The Project Engineer was J. D. Seader. R. J. Ingram, A. S. Okuda, and D. M. Trebes assisted in the graphical preparation of data. Informal translations of foreign references were rendered by J. E. Snowden, Jr., H. F. Bauer, and I. Lysyj.

ABSTRACT

An extensive survey of available information from the literature on heat transfer to boiling hydrogen, nitrogen, and oxygen is presented. Included are a bibliography of available experimental data, a summary of boiling theory, graphical comparisons of the experimental data, and compilations of pertinent physical properties for each of the three cryogenic fluids. Based upon the results of the survey, recommendations are made for a test program to provide critical information where data are lacking.

CONTENTS

| | |
|---|-----|
| Foreword | iii |
| Abstract | v |
| Summary | 1 |
| Introduction | 3 |
| Literature Survey | 7 |
| Coding Scheme | 11 |
| Physical Properties | 19 |
| Density, ρ_L and ρ_V | 20 |
| Specific Heat at Constant Pressure, C_L and C_V | 22 |
| Viscosity, μ_L and μ_V | 23 |
| Thermal Conductivity, k_L and k_V | 24 |
| Vapor Pressure, P_V | 25 |
| Surface Tension, σ | 25 |
| Heat of Vaporization, λ | 26 |
| Boiling Theory | 27 |
| Pool Nucleate Boiling | 29 |
| Pool Nucleate Boiling Maximum Heat Flux | 44 |
| Pool Film Boiling Minimum Heat Flux | 55 |
| Pool Stable Film Boiling | 60 |
| Forced Convection Subcooled Nucleate Boiling | 67 |
| Forced Convection Subcooled Nucleate Boiling Maximum Heat Flux | 75 |
| Forced Convection Saturated Boiling | 80 |
| Forced Convection Film Boiling | 86 |
| Experimental Data | 89 |
| Pool Boiling | 89 |
| Subcooled Forced Convection Boiling | 97 |

| | |
|---|-----|
| Saturated Forced Convection Boiling | 102 |
| Conclusions | 107 |
| Pool Nucleate Boiling | 107 |
| Pool Nucleate Boiling Maximum Heat Flux | 109 |
| Pool Film Boiling Minimum Heat Flux | 111 |
| Stable Pool Film Boiling | 111 |
| Subcooled Forced Convection Boiling | 113 |
| Saturated Forced Convection Boiling | 113 |
| Recommendations | 115 |
| Nomenclature | 117 |
| Experimental Data Bibliography | 121 |
| Subject Cross References | 137 |
| Physical Property References | 143 |
| General References | 145 |
| Theory References | 147 |
| <u>Appendix A</u> | |
| Physical Property Graphs | 153 |

ILLUSTRATIONS

| | |
|--|----|
| 1. Comparison of Pool Boiling Curves | 4 |
| 2. Typical Theoretical Pool Boiling Curve | 28 |
| 3. Correlation Factor of Levy | 36 |
| 4. Pool Nucleate Boiling of Hydrogen at 12.0 psia | 37 |
| 5. Pool Nucleate Boiling of Nitrogen at 15.2 psia | 38 |
| 6. Pool Nucleate Boiling of Oxygen at 12.8 psia | 39 |
| 7. Predicted Pool Nucleate Boiling Heat Flux For Hydrogen According to Forster and Zuber Equation | 40 |
| 8. Predicted Pool Nucleate Boiling Heat Flux For Nitrogen According to Forster and Zuber Equation | 41 |
| 9. Predicted Pool Nucleate Boiling Heat Flux For Oxygen According to Forster and Zuber Equation | 42 |
| 10. Correlation Parameter of Addoms and Noyes (Alternate) | 50 |
| 11. Correlation Parameter of Griffith | 51 |
| 12. Comparison of Theories For Pool Nucleate Boiling Maximum Heat Flux for Hydrogen | 52 |
| 13. Comparison of Theories For Pool Nucleate Boiling Maximum Heat Flux for Nitrogen | 53 |
| 14. Comparison of Theories For Pool Nucleate Boiling Maximum Heat Flux for Oxygen | 54 |
| 15. Pool Film Boiling Minimum Heat Flux For Hydrogen | 57 |
| 16. Pool Film Boiling Minimum Heat Flux For Nitrogen | 58 |
| 17. Pool Film Boiling Minimum Heat Flux For Oxygen | 59 |
| 18. Stable Pool Film Boiling of Hydrogen | 68 |
| 19. Stable Pool Film Boiling of Nitrogen | 69 |
| 20. Stable Pool Film Boiling of Oxygen | 70 |
| 21. Typical Forced Convection Subcooled Nucleate Boiling Curve | 72 |

| | | |
|-------|---|-----|
| 22. | Generalized Forced Convection Nonboiling Heat Transfer Coefficient at Saturated Conditions | 79 |
| 23. | Flow Regimes Along Boiler | 81 |
| 24. | Reynolds Number Factor, F, of Chen | 84 |
| 25. | Suppression Factor, S, of Chen | 85 |
| 26. | Experimental Pool Boiling Data For Hydrogen | 90 |
| 27. | Experimental Pool Boiling Data For Nitrogen | 91 |
| 28. | Experimental Pool Boiling Data For Oxygen | 92 |
| 29. | Experimental Subcooled Forced Convection Boiling Data | 98 |
| A-1. | Density of Para-Hydrogen | 154 |
| A-2. | Density of Nitrogen | 155 |
| A-3. | Density of Oxygen | 156 |
| A-4. | Specific Heat at Constant Pressure of Para-Hydrogen | 157 |
| A-5. | Specific Heat at Constant Pressure of Nitrogen | 158 |
| A-6. | Specific Heat at Constant Pressure of Oxygen | 159 |
| A-7. | Viscosity of Para-Hydrogen | 160 |
| A-8. | Viscosity of Nitrogen | 161 |
| A-9. | Viscosity of Oxygen | 162 |
| A-10. | Thermal Conductivity of Para-Hydrogen | 163 |
| A-11. | Thermal Conductivity of Nitrogen | 164 |
| A-12. | Thermal Conductivity of Oxygen | 165 |
| A-13. | Vapor Pressure of Para-Hydrogen | 166 |
| A-14. | Vapor Pressure of Nitrogen and Oxygen | 167 |
| A-15. | Surface Tension of Para-Hydrogen | 168 |
| A-16. | Surface Tension of Nitrogen and Oxygen | 169 |
| A-17. | Heat of Vaporization of Para-Hydrogen | 170 |
| A-18. | Heat of Vaporization of Nitrogen and Oxygen | 171 |

TABLES

| | |
|---|-----|
| 1. Coding Scheme | 12 |
| 2. Experimental Studies Reported in More Than One Reference . . | 15 |
| 3. Over-all Scope of Conditions Covered in Experimental Cryogenic Boiling Studies | 16 |
| 4. Melting, Normal Boiling, and Critical Conditions for Hydrogen, Nitrogen, and Oxygen | 19 |
| 5. Summary of Pool Nucleate Boiling Equations | 33 |
| 6. Summary of Pool Nucleate Boiling Theories in Generalized Stanton Number Form | 45 |
| 7. Summary of Pool Nucleate Boiling Maximum Heat Flux Theories | 48 |
| 8. Summary of Pool Film Boiling Minimum Heat Flux Theories | 56 |
| 9. Saturated Forced Convection Boiling Experiments | 104 |

SUMMARY

This report presents an extensive survey of the available information from the literature on heat transfer to boiling hydrogen, nitrogen, and oxygen for both pool and flow conditions. A comprehensive bibliography of 74 literature articles, reports, unpublished papers, and theses concerning experimental data is presented. Each data reference is coded with respect to boiling regime, flow condition, geometry, unusual conditions, and method of data presentation. From this coding, a large number of convenient cross-reference bibliography lists were prepared for specific conditions of boiling. In addition to the coding, each data reference is rated with respect to the experimental technique description.

A review of all the available theoretical approaches to the prediction of boiling phenomena is presented. In general, empirical expressions are not considered. Calculations based on the theories are given graphically for each of the three cryogenic fluids for several types of boiling. Computations with the equations were made possible by an extensive compilation of all the physical properties pertinent to boiling.

The available experimental data are presented in graphical form and compared to theoretical predictions where possible. The effects of the many boiling parameters involved are discussed. Based on the results of the literature survey, recommendations are made for additional analytical and experimental studies that are required to provide an adequate knowledge of heat transfer to boiling cryogenics.

INTRODUCTION

Interest in heat transfer to boiling cryogenic fluids such as hydrogen, nitrogen, and oxygen has increased rapidly during the past 15 years. This interest has been due primarily to a growing number of space applications. Compared to the boiling of ordinary fluids such as water at temperatures near or above ambient, cryogenic boiling is characterized by smaller temperature driving forces, smaller heat fluxes, and the practicability of operation in the stable film boiling regime. This is illustrated graphically in Fig. 1 where the atmospheric pool boiling curve of water is compared to hydrogen and oxygen for horizontal wires. As can be seen, nucleate boiling of hydrogen occurs for ΔT values to only about 5 F and to heat fluxes on the order of 10,000 Btu/hr-sq ft. For oxygen, the nucleate boiling range is extended to a ΔT of about 20 F and a heat flux of about 50,000 Btu/hr-sq ft. For water, the nucleate boiling ΔT is greatly extended to approximately 50 F and the heat flux to approximately 400,000 Btu/hr-sq ft. The direct transition of nucleate boiling to stable film boiling for hydrogen and oxygen results in surface temperatures below 1000 F, which is attainable with many materials. Thus, heat fluxes greater than the pool nucleate-boiling maximum heat flux can be achieved without burnout. With water, however, direct transition to stable film boiling can lead to surface temperatures in excess of 2000 F. For many materials this will result in a burnout, and operation consequently is restricted to the nucleate boiling regime.

These characteristics of cryogenic boiling complicate and make difficult the acquisition of accurate and complete experimental data. Therefore, it seems appropriate to survey the available data and determine the status of knowledge of cryogenic boiling.

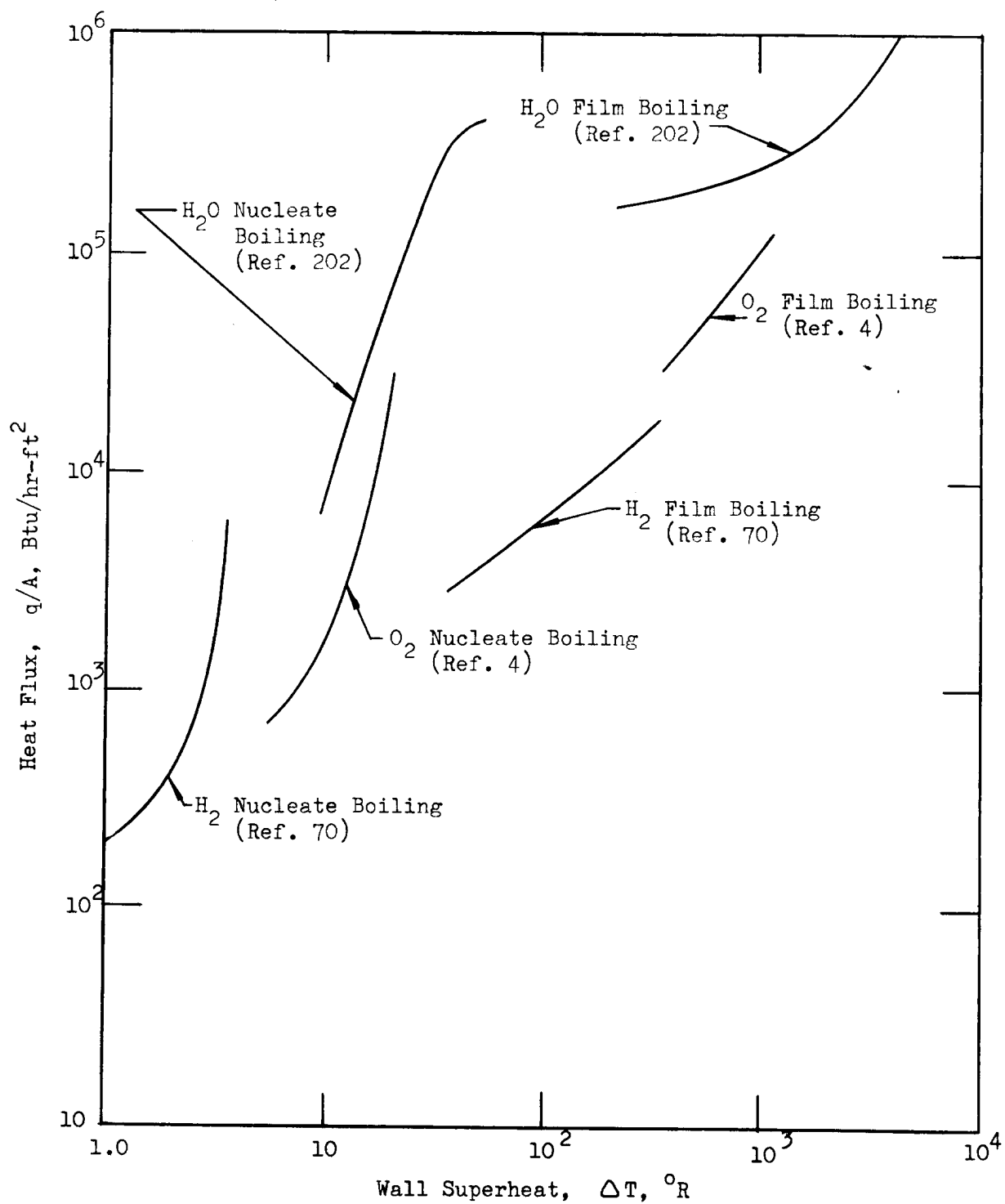


FIGURE 1 COMPARISON OF POOL BOILING CURVES

This report presents such a survey. Included is a complete bibliography of available experimental data. The references are coded and cross-referenced to facilitate searches for specific information. Also included are compilations of pertinent physical properties, a summary of available boiling theory, and graphical presentations of the available data. Based upon the results of the survey, recommendations are made for a test program to provide critical information for regions where data are lacking.

LITERATURE SURVEY

An exhaustive search of the literature was conducted for all literature articles, reports, unpublished papers and theses concerning experimental data for boiling heat transfer from solid surfaces to hydrogen, nitrogen, and oxygen. Most of the available literature to 1960 was surveyed by Richards, Steward, and Jacobs (Ref.201). The present survey includes all articles to January 1964. The sources consulted in the literature survey were:

Chemical Abstracts (1907-June 1962)

Heat Transfer

Each Compound

Nuclear Science Abstracts (1946-December 1963)

Heat Transfer

Boiling

Each Compound

Engineering Index (1944-February 1964)

Heat Transfer-Boiling Liquids

Applied Science and Technology Index (1958-January 1964)

Boiling

Low Temperature

Heat Transmission

Each Compound

Industrial Arts Index (1941-1957)

Boiling

Heat Transmission

Each Compound

Aeronautical Engineering Index (1947-1956)

Heat Transfer

Aerospace Engineering Index (1957-1958)

Heat Transfer

International Aerospace Abstracts (1961-January 1964)
Heat Transfer

Refrigeration Abstracts (1949-1957)

Dissertation Abstracts (1955-December 1963)

Liquid Propellant Information Agency (1958-1962)
Heat Transfer
Cryogenic Liquids
Each Compound

Chemical Propulsion Information Agency (1963)

Armed Services Technical Information Agency (ASTIA)
Special bibliography was requested on Boiling Heat Transfer.
The bibliography was compiled from ASTIA holdings from 1952 to
January 1964.

NASA-NACA:

NASA Scientific and Technical Aerospace Reports (STAR)
January 1963 to January 1964

NASA Technical Announcement Bulletin
April-December 1962

NASA Index to NASA Technical Publications
1957-1961

NACA Index to NACA Technical Publications
1950-1956

Heat Transfer Reviews
Industrial and Engineering Chemistry (1948-1962)
Mechanical Engineering (1960-1962)

International Journal of Heat and Mass Transfer (1960-1963)
Including Heat Transfer Bibliography

American Rocket Society Journal (1954-1963)
(Now AIAA Journal)
Including Technical Literature Digest

Cryogenics (1962-1963)
Including Bibliography on Heat Transfer

Journal of Heat Transfer (ASME) (1959-February 1964)

Advances in Cryogenic Engineering
Vol. 1-8 (1955-1962)

International Developments in Heat Transfer
Papers of 1st International Heat Transfer Conference 1961; ASME

Jet Propulsion Laboratory
Publications of the Jet Propulsion Laboratory (July 1938-June 1962)

Applied Cryogenic Engineering
Vance, R. W. and W. M. Duke, Ed. John Wiley & Sons Inc., New
York, 1962

A Survey of the Literature on Heat Transfer from Solid Surfaces to
Cryogenic Fluids
Richards, R. J., W. G. Steward, and R. B. Jacobs
National Bureau of Standards
Technical Note 122
October 1961

A Bibliography of Low Temperature Engineering and Research
Mendelssohn, K., R. B. Scott, and L. Weil
1944-1960
Heywood and Co. Ltd., London
Published as a special issue of "Cryogenics"

A Brief Review of the Literature on Boiling Heat Transfer
Hawkins, G. A.
University of California, Department of Engineering, Los Angeles
June 1950

Problems in Heat Transfer During a Change of State
A collection of articles
Kutateladze, S. S.
State Power Press, Moscow, 1953
(AEC-translation-AEC-tr-3405)

Current Contents (1962-January 1964)

Papers from 9th Annual Cryogenic Engineering Conference
Boulder, Colorado (August 1963)

Papers from ASME-AIChE Heat Transfer Conference
Boston, Massachusetts (August 1963)

A total of 74 applicable references were found, including replies to letters sent to various authors requesting tabulated data. These references are listed alphabetically according to author in the Experimental Data Bibliography. It is believed that the literature search is the most complete available for boiling heat transfer to cryogenic fluids from solid surfaces.

Special attention was given to articles in foreign languages. Informal oral translations were obtained from experienced scientists and engineers to determine the content of each of these references.

Of the 74 references, 62 were in English and 12 were in foreign languages as follows:

| <u>Language</u> | <u>Reference No.</u> |
|-----------------|----------------------------------|
| Czechoslovakian | 61 |
| French | 4, 58, 68, 69, 70, 71, 72, 73 |
| German | 28, 29 |
| Russian | 65 |

It is interesting to note that although the Russians have devoted much effort to the development of basic boiling theories, they have shown little apparent interest in obtaining fundamental experimental data for boiling cryogenics. The only Russian papers found (Ref. 48 and 65) were concerned with obtaining rather specialized boiling data.

CODING SCHEME

Because of the numerous geometric configurations and operating conditions for which experimental boiling data may be obtained, it was considered desirable to devise a coding scheme to allow rapid determination of the boiling conditions for a given reference. Accordingly, 73 of the 74 references were coded as given in the Experimental Data bibliography. Reference 64 was not coded because it contains only over-all coefficients for a condensing-boiling system.

The coding scheme developed is given in Table 1.

As part of the coding scheme, each reference was also rated with respect to the extent to which the experimental technique was described. The following rating scheme was used:

- X : Little or no discussion of experimental technique
- XX : Some discussion of experimental technique, but
insufficient detail concerning preparation of
surface and/or instrumentation
- XXX : Relatively complete details of experiments

This rating was applied to the entire individual reference and was placed to the right of the coding for the boiling conditions.

TABLE 1
CODING SCHEME

- A. Boiling Regime
 - 1. Nucleate
 - 2. Transition (or partial film)
 - 3. Stable Film
 - 4. Peak Nucleate (or burnout condition)

 - B. Flow Condition
 - 1. Pool
 - 2. Forced Convection--subcooled (surface boiling)
 - 3. Forced Convection--saturated (bulk boiling)
 - 4. Natural Circulation

 - C. Geometry
 - 1. Above Horizontal Plates
 - 2. Below Horizontal Plates
 - 3. Vertical Plates
 - 4. Inside Vertical Tubes
 - 5. Outside Vertical Tubes
 - 6. Inside Horizontal Tubes
 - 7. Outside Horizontal Tubes
 - 8. Horizontal Wires
 - 9. Vertical Wires
 - 10. Inclined Plates
 - 11. Miscellaneous Geometry
 - a. Circular Passage
 - b. Annular Passage
 - c. Other Shaped Passage
- } Pertains to items
4 and 6 only

TABLE 1
(Continued)

D. Other Pertinent Conditions

1. Surface Effects
2. Vortices
3. G-field
4. Agitation
5. Electrical Field

E. Data Presentation

1. Tabulated Only
2. Plotted Only
3. Plotted and Tabulated
4. Complete Data Available From Another Listed Source

An example of the application of the coding scheme as applied to Ref. 15 is as follows:

Class, C. R., De Haan, J. R., Piccone, M., and Cost, R.: "Pool Boiling Heat Transfer to a Cryogenic Liquid," Beechcraft Research and Development, Inc., Engineering Dept. 6154, WADC TR 58-528, AD214256, 1958

H₂:A1-B1-C1,C3,C10-D1-E3

H₂:A3-B1-C1,C3,C10-D1-E3 XXX

H₂:A4-B1-C1,C3,C10-D1-E3

From the coding, it is immediately apparent that this work was concerned with nucleate, peak nucleate, and stable film pool boiling. The heating surface was a flat plate in horizontal, vertical, and inclined positions. Surface condition effects were studied, and the data are both plotted and tabulated. Relatively complete details of the experiments were given.

Detailed study of the 74 references in conjunction with the coding scheme indicated that, in a number of cases, the same experimental study was reported in more than one reference. The cases where this occurred are listed in Table 2. It was determined that the 73 coded references corresponded to only 43 separate experimental studies.

The over-all scope of the general conditions covered in the 43 separate cryogenic boiling studies is given in Table 3. It is evident that experimental data are completely lacking in a number of cases. This lack of data in certain areas is discussed in detail in the subsequent section on Recommendations.

TABLE 2

EXPERIMENTAL STUDIES REPORTED IN MORE THAN ONE REFERENCE

| Reference Numbers | Principal Investigator(s) |
|-------------------------------------|---------------------------------|
| 1, 56, 62 | O'Hanlon and Sherley |
| 2, 3 | Banchero, Barker and Boll |
| 5, 6, 7 | Bromley |
| 8, 9, 10, 11, 12, 13, 14, 50, 51 | Clark and Merte |
| 15, 16 | Class, DeHaan, Piccone and Cost |
| 20, 21 | Dean and Thompson |
| 22, 23 | Drayer and Timmerhaus |
| 24, 25 | Fenster and Clark |
| 27, 31, 32 | Frederking |
| 28, 29, 30 | Frederking |
| 34, 59 | Giaque |
| 35, 39, 40 | Graham, Hendricks and Hsu |
| 41, 42 | Hsu and Westwater |
| 44, 66 | Lewis |
| 46, 47 | Lyon, Kosky and Harmon |
| 60, 61 | Ruzicka |
| 67, 74 | Wright and Walters |
| 68, 70 | Weil |

TABLE 5

OVER-ALL SCOPE OF CONDITIONS COVERED IN
EXPERIMENTAL CRYOGENIC BOILING STUDIES

| Conditions | Number of Studies | | |
|-----------------------------|-------------------|----------|--------|
| | Hydrogen | Nitrogen | Oxygen |
| Nucleate Boiling: | | | |
| Pool | 7 | 20 | 11 |
| Subcooled Forced Convection | 2 | 2 | 0 |
| Saturated Forced Convection | 5 | 4 | 0 |
| Stable Film Boiling: | | | |
| Pool | 3 | 14 | 3 |
| Subcooled Forced Convection | 2 | 1 | 0 |
| Saturated Forced Convection | 4 | 1 | 0 |
| Maximum Heat Flux: | | | |
| Pool | 3 | 11 | 2 |
| Forced Convection | 1 | 2 | 0 |

In addition to the alphabetical listing by author in the Experimental Data Bibliography, a large number of convenient cross-reference bibliography lists were prepared. This was facilitated by typing the references on Keysort cards, using the coding scheme in punching the cards. These listings, by reference number only, allow rapid determination of the references applicable to specific conditions of boiling. The cross-reference lists are included after the Experimental Data Bibliography.

PHYSICAL PROPERTIES

In connection with the evaluation of the various theoretical boiling predictions to be presented in the next section, an extensive compilation of pertinent thermodynamic and transport properties of hydrogen, nitrogen, and oxygen was completed. Saturation properties were compiled from the melting point to the critical temperature. Superheated vapor properties were tabulated from the normal boiling temperature to 3000 R and for pressures from one atmosphere to the critical pressure. The melting, normal boiling, and critical conditions for the three cryogenic fluids are listed in Table 4.

TABLE 4

MELTING, NORMAL BOILING, AND CRITICAL CONDITIONS FOR
HYDROGEN, NITROGEN, AND OXYGEN

| Property | Hydrogen | Nitrogen | Oxygen |
|-------------------------------|----------|----------|--------|
| Melting Temperature, R | 25.0 | 113.8 | 98.5 |
| Normal Boiling Temperature, R | 36.5 | 139.2 | 162.3 |
| Critical Temperature, R | 59.4 | 227.3 | 278.6 |
| Critical Pressure, psia | 187.7 | 492.9 | 736.0 |

The following saturation properties were compiled:

| | |
|---|----------|
| Liquid Density | ρ_L |
| Vapor Density | ρ_V |
| Liquid Specific Heat at Constant Pressure | C_L |

| | |
|-----------------------------|-----------|
| Liquid Viscosity | μ_L |
| Liquid Thermal Conductivity | k_L |
| Vapor Pressure, | P_V |
| Surface Tension | σ |
| Heat of Vaporization | λ |

The following superheated vapor properties were compiled:

| | |
|--|----------|
| Vapor Density | ρ_V |
| Vapor Specific Heat at Constant Pressure | C_V |
| Vapor Viscosity | μ_V |
| Vapor Thermal Conductivity | k_V |

All properties are presented in graphical form in Appendix A. A discussion of the methods employed for the compilation of each property is given below. The references are included in the Physical Property References section.

DENSITY, ρ_L AND ρ_V

Hydrogen

Values of the density of saturated liquid and saturated vapor from 35 R to the critical temperature were taken from the tabulated values of NBS TN-130 (Ref. 101). Values down to 25 R were extrapolated from a plot of the above values. The superheated vapor densities were calculated from various equations of state, as summarized below.

| <u>Temperature Range,</u> <u>R</u> | <u>Reference</u> |
|---------------------------------------|-----------------------|
| 36-180 | 102 |
| 180-540 | 101 |
| 540-2500 | 104 |
| 2500-3000 | perfect gas relations |

Nitrogen

All saturation properties, both liquid and vapor, were taken from Johnson (Ref. 104). The superheated vapor values to 1000 R were calculated from the equation of state recommended by NBS (Ref. 105). Above this temperature, the perfect gas relationships were assumed to apply.

Oxygen

Values of saturated liquid density from 110 to 275 R were taken from Johnson (Ref. 104). The lower temperature values were extrapolated from those values. The values of saturated vapor density were taken from the Battelle Handbook (Ref. 106). Superheated vapor values to 1000 R were calculated from the equation of state recommended by NBS (Ref. 107). From 1000 to 3000 R the perfect gas relations were assumed to be applicable.

SPECIFIC HEAT AT CONSTANT PRESSURE, C_L AND C_V

Hydrogen

The values of saturated liquid specific heat at constant pressure were taken from Johnson (Ref. 104), except for a small extrapolation down to 25 R. The superheated vapor values to 2500 R were taken from Ref. 102. Above this temperature, values were taken from Ref. 103.

Nitrogen

The saturated liquid values from 115 to 210 R were taken from Johnson (Ref. 104). Above this temperature, the above data were graphically extrapolated. The superheated vapor values to 1000 R were calculated by the NBS recommended equations (Ref. 105). Above this temperature, the values were taken from Ref. 113.

Oxygen

Specific heat values of the saturated liquid from 105 to 160 R were taken from Johnson (Ref. 104). Above 160 R, no values could be obtained. However, values of C_{sL} , the heat capacity of the liquid along the saturation line, were available (Ref. 108). The values of C_{sL} were converted to C_L by the method of Hougen and Watson (Ref. 109). The specific heat of the saturated vapor was taken from Ref. 107 up to 1000 R. Above this temperature, the values were taken from Ref. 113.

VISCOSITY, μ_L AND μ_V

Hydrogen

Values of saturated liquid viscosity from 30 to 35 R were taken from Johnson (Ref. 104). The remainder of the saturated liquid values and the superheated vapor values were obtained from the residual method first suggested by Abas-Zade (Ref. 110). This method states that the viscosity is composed of an ideal low-pressure contribution, μ^* which is a function of temperature only and a residual value due to pressure ($\mu - \mu^*$). The residual is a function of pressure alone. The μ^* values were taken from Starrett (Ref. 111) and the ($\mu - \mu^*$) values from the correlation of Thodos (Ref. 112).

Nitrogen

Values of saturated liquid viscosity from 115 to 210 R were taken from Johnson (Ref. 104). From 210R to the critical point, the values were extrapolated. The superheated vapor values were obtained by the residual method. The μ^* values were taken from NBS circular 564 (Ref. 113) and ($\mu - \mu^*$) values from Thodos (Ref. 114).

Oxygen

The values of saturated liquid viscosity were taken from Johnson (Ref. 104). The superheated vapor values were calculated by the residual method with μ^* values from Ref. 113 and ($\mu - \mu^*$) from Ref. 114.

THERMAL CONDUCTIVITY, k_L AND k_V

Hydrogen

All values of thermal conductivity were taken from the reduced state plot of Thodos (Ref. 115), where k_r is plotted against T_r with P_r as a parameter.

Nitrogen

Values of saturated liquid thermal conductivity from 125 R to 160 R were taken from Johnson (Ref. 104). The remainder of the liquid values were obtained from Thodos (Ref. 115) and smoothed to fit the tabulated data of Johnson (Ref. 104). The superheated vapor thermal conductivity was calculated by the residual method, with k^* taken from Ref. 113 and $(k-k^*)$ from Ref. 116.

Oxygen

The values of liquid thermal conductivity from 130 R to the critical point were taken from Johnson (Ref. 104). The values from 160 to 125 R were extrapolated. Superheated vapor thermal conductivity was obtained by the residual method, with k^* from Ref. 113 and the residual from Ref. 116.

VAPOR PRESSURE, P_V

Hydrogen, Nitrogen, Oxygen

The vapor pressure of hydrogen, nitrogen, and oxygen over the entire temperature range was obtained from Johnson (Ref. 104).

SURFACE TENSION, σ

Hydrogen

The surface tension of hydrogen was obtained from NBS 7616 (Ref. 117).

Nitrogen

The surface tension of nitrogen was obtained by the equation of Guggenheim (Ref. 118) where:

$$\sigma = \sigma_o (1 - T/T_c)^{11/9}$$

and σ_o is a constant for a given fluid. The value of σ_o was determined at the normal boiling point value given by Johnson (Ref. 104).

Oxygen

The surface tension of oxygen was obtained in the same manner as that for nitrogen.

HEAT OF VAPORIZATION, λ

Hydrogen

The heat of vaporization of hydrogen from 35 R to the critical was taken from the tabulated values in NBS TN130 (Ref. 101). Values down to 25 R were obtained from Roder, et al. (Ref. 119).

Nitrogen

The heat of vaporization of nitrogen over the entire saturation curve was obtained from Johnson (Ref. 104).

Oxygen

The heat of vaporization of oxygen was obtained from the Watson equation (Ref. 120):

$$\lambda = \lambda_1 \left(\frac{1 - T_r}{1 - T_{r1}} \right)^{0.38}$$

where λ_1 is the heat of vaporization at any reduced temperature, T_{r1} . The reference value of λ_1 was taken at the atmospheric boiling point from Ref. 120.

BOILING THEORY

Prior to 1950, only a few empirical correlations of boiling data were available. Since then, however, a considerable number of theoretical and semitheoretical equations have been developed to predict boiling phenomena in both the nucleate and stable film boiling region, as well as at the burnout point. This has been particularly true for pool boiling. This is illustrated in Fig. 2 where a complete boiling curve for a specific case of hydrogen is constructed solely on the basis of theories to be discussed below. Some notable theoretical progress has also been made for subcooled forced convection (surface) boiling. However, for saturated forced convection (bulk) boiling and the accompanying complex two-phase flow phenomena, only a start has been made and little is known.

This section presents a review of all of the available theoretical approaches to boiling phenomena. In all cases the theories are general and are not restricted to cryogenic fluids. However, applications of the equations in this report are made only to the cryogenic fluids of interest. In general, empirical expressions are not considered. Included are equations covering the following areas of boiling:

- Pool Nucleate Boiling

- Pool Nucleate Boiling Maximum Heat Flux

- Pool Film Boiling Minimum Heat Flux

- Pool Stable Film Boiling

- Forced Convection Subcooled Nucleate Boiling

- Forced Convection Subcooled Nucleate Boiling Maximum Heat Flux

- Forced Convection Saturated Boiling

- Forced Convection Film Boiling

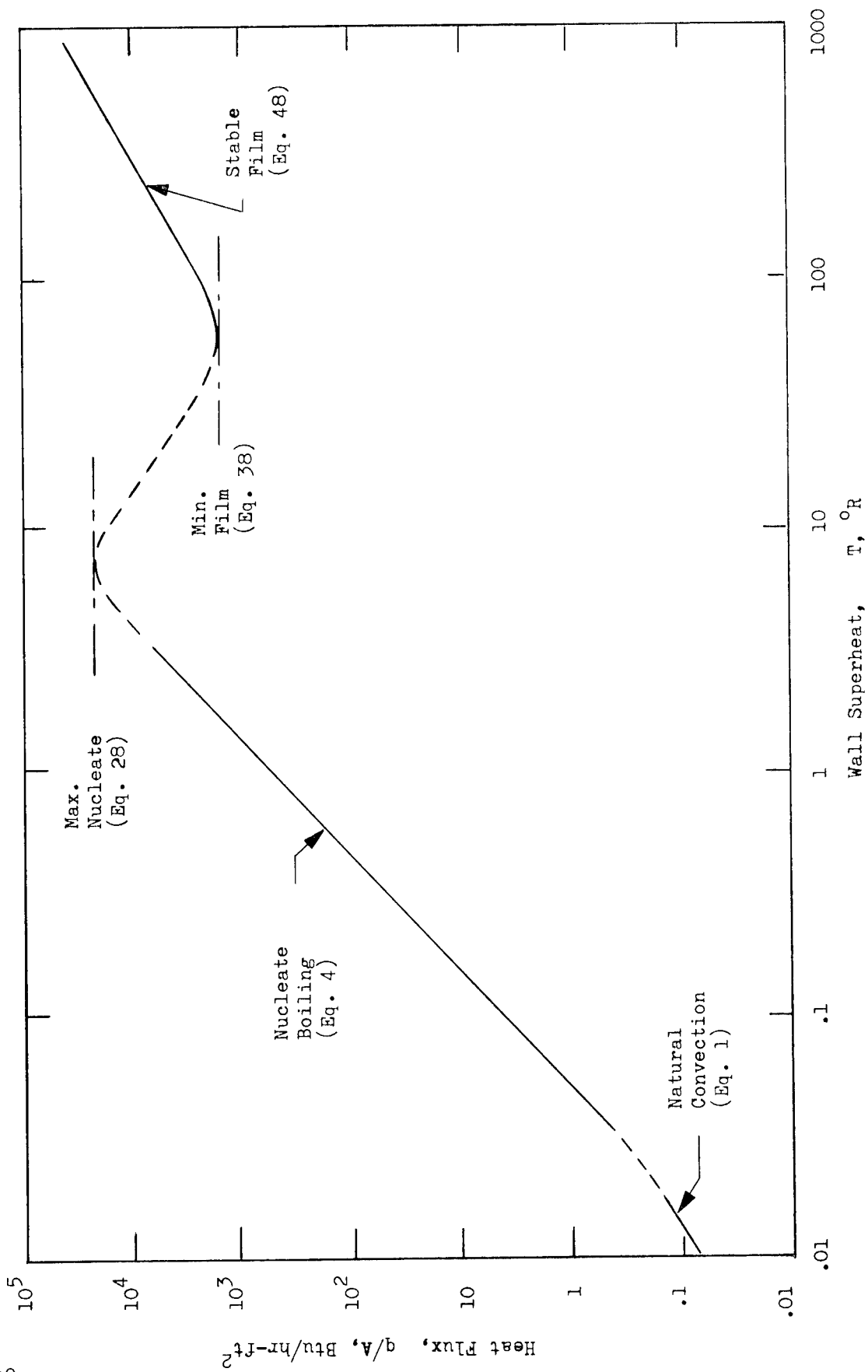


FIGURE 2 TYPICAL THEORETICAL POOL BOILING CURVE, HYDROGEN - 12 psia - HORIZONTAL PLATE FACING UP

A fundamental discussion of boiling is not included in this report, but may be found in a number of excellent references including McAdams (Ref. 202), Jakob (Ref. 203), Grober, Erk and Grigull (Ref. 204), Rohsenow (Ref. 205), and Westwater (Ref. 206). For the most part, comparison of theory with experimental data is discussed in the next section of this report.

POOL NUCLEATE BOILING

To initiate pool boiling, the heat transfer surface temperature must be somewhat higher than the saturation temperature of the fluid at the existing pressure. If the surface temperature is less than the value required to initiate boiling, then heat transfer will occur by natural convection only. This process is governed by equations similar to the following for natural convection above a horizontal flat plate, as given by McAdams (Ref. 202):

$$q/A = 0.14 \left[g (\Delta T)^4 \left(\frac{k_L^3 \rho_L^2 \beta}{\mu_L^2} \right)_f \left(\frac{c_L \mu_L}{k_L} \right)_f \right]^{1/3} \quad (1)$$

Thus, the heat flux is proportional to the temperature difference raised to an exponent somewhat greater than one. Nonboiling relations for other geometrical configurations are also given in Ref. 202 and are not discussed here.

When a sufficient superheat exists to cause nucleate boiling then, as shown in Fig. 2, the heat flux becomes a stronger function of the temperature difference. With increasing ΔT , the bubble population grows

until it reaches a maximum density corresponding to the maximum pool nucleate boiling heat flux. For the ΔT region between the initiation of boiling and this maximum, a number of theories have been proposed for saturated pool nucleate boiling. These are summarized in Table 5 as Eq. 2 through 10. In general, these equations can be arranged into the following general boiling Nusselt number form suggested by Rohsenow (Ref. 301) and discussed by Zuber and Fried (Ref. 302):

$$\text{Nu}_B = C_1 \text{Re}_B^m \text{Pr}^n \quad (11)$$

or, better, in an equivalent boiling Stanton number form to separate the heat flux, q/A , from the superheat, ΔT :

$$\text{Re}_B = \frac{C_2}{\text{St}_B^a \text{Pr}^b} \quad (12)$$

$$\text{where: } \Delta T = T_w - T_s \quad (13)$$

$$\text{Nu}_B = \frac{hL^*}{k_L} \quad (14)$$

$$\text{Re}_B = \frac{L^*G^*}{\mu_L} \quad (15)$$

$$\text{Pr} = \frac{C_L \mu_L}{k_L} \quad (16)$$

$$\text{St}_B = \frac{h}{C_L G^*} = \frac{(q/A)}{(\Delta T)C_L G^*} \quad (17)$$

In effect, the boiling Stanton number is a ratio of the latent heat effect to the sensible heat effect. The characteristic length, L^* , in the Reynolds number is, in most cases, based on an initial bubble radius,

the bubble diameter at departure such as in Eq. 2, 3, and 7, a bubble diameter referred to some time constant such as in Eq. 4, or a vapor front advance distance such as in Eq. 8. The characteristic superficial mass velocity, G^* , in the Reynolds number is, in most cases, based on the liquid assuming either $G_L = G_V$ as in Eq. 2, or $V_L = V_V$ as in the other equations of Table 5. Table 6 compares, in Stanton number form, the equations listed in Table 5. In developing Table 6, the following assumptions were made to simplify the relations:

$$\Delta P = \frac{(\Delta T) \rho_V \lambda}{T_s} \quad (18)$$

$$(\rho_L - \rho_V) \approx \rho_L \quad (19)$$

In all cases, $G^* \propto (q/A)$. Thus, the Reynolds number $Re_B \propto (q/A)$ and $1/St_B \propto (\Delta T)^a$, thus separating out the effects of q/A and ΔT as noted above.

In general, the theories predict:

$$q/A \propto (\Delta T)^n \quad 2 \leq n \leq 3-1/3$$

$$\text{and} \quad q/A \propto (Pr_L)^{-b}$$

with the exponent, $-b$, ranging from -5.1 to $-19/24$. The effect of liquid viscosity cancels out in the equations of Levy (Ref. 306), Michenko (Ref. 307), Chang and Snyder (Ref. 309) and Nishikawa and Yamagata (Ref. 310). The predicted variation of the heat flux with the surface tension is given by:

$$q/A \propto (\sigma)^c$$

with c ranging from $-10/6$ to $-1/2$.

The pool nucleate boiling equations listed in Table 5 were programmed for the IBM 7094 to facilitate calculations for the cryogenic fluids of interest.

Values of the required physical properties for H_2 , N_2 , and O_2 , given in Appendix A, were included in the computer program to permit direct application of the equations to these fluids. Results of calculations for a pressure of about 1 atmosphere are given in Fig. 4, 5, and 6 for hydrogen, nitrogen, and oxygen, respectively. A value of $C_{sf} = 0.015$ for the Rohsenow equation was used. Calculations were also carried out for a wide range of pressure. Results from the Forster and Zuber equation are shown in Fig. 7, 8, and 9. This equation appeared to give results representative of the better nucleate boiling equations. The increase in heat flux with increasing pressure for a given ΔT is typical of the trends of experimental data as is discussed in the following section. The curves in Fig. 7, 8, and 9 are terminated at approximately the pool nucleate boiling maximum heat fluxes as determined from the limited experimental data of Class, et al. (Ref. 15 and 16) for hydrogen and Lyon, et al. (Ref. 46) for nitrogen and oxygen for boiling above horizontal plates.

In general, the greatest shortcoming of the above theories for pool nucleate boiling is their failure to theoretically account for variables which are not easily controlled. These include amounts of dissolved and adsorbed gases, and impurities, contamination, and nature of the heating surface. Also of importance are the size, geometry and orientation of the heating surface. This is discussed more fully in the next section where experimental data are presented. These effects can influence both the slope and position of the boiling curve. Consequently, the equations

TABLE 5

SUMMARY OF POOL NUCLEATE BOILING EQUATIONS

| Reference | Equation | Equation No. |
|-------------------------|--|--------------|
| Rohsenow (301) | $\frac{C_L (\Delta T)}{\lambda} = C_{sf} \left\{ \frac{(q/A)}{\mu_L \lambda} \left[\frac{g_c \sigma}{g (\rho_L - \rho_V)} \right]^{1/2} \right\}^{0.33}$ $(C_L \mu_L / k_L)^{1.7}$ <p>Typically C_{sf} varies from 0.0027 to 0.015 depending upon fluid-heater surface combination.</p> | 2 |
| Kutateladze (303) | $\frac{h}{k_L} \left[\frac{g_c \sigma}{g (\rho_L - \rho_V)} \right]^{1/2} = 7.0 \times 10^{-4}$ $\left\{ \frac{\rho_L (q/A)}{\mu_L \rho_V \lambda} \cdot \left[\frac{g_c \sigma}{g (\rho_L - \rho_V)} \right]^{1/2} \right\}^{0.7}$ $(C_L \mu_L / k_L)^{0.35} \left\{ \frac{P}{\left[\sigma \frac{g}{g_c} (\rho_L - \rho_V) \right]^{1/2}} \right\}^{0.70}$ | 3 |
| Forster and Zuber (304) | $\left[\frac{(q/A) C_L \rho_L}{k_L \lambda \rho_V} \right] (\pi \alpha_L)^{1/2} (2 \sigma / \Delta P)^{1/2}$ $(\rho_L / g_c \Delta P)^{1/4} = 0.0015 \left\{ \frac{\rho_L}{\mu_L} \left[\frac{(\Delta T) C_L \rho_L}{\rho_V \lambda} \right]^2 \pi \alpha_L \right\}^{5/8}$ $(C_L \mu_L / k_L)^{1/3}$ | 4 |

TABLE 5
(Continued)

| Reference | Equation | Equation No. |
|-------------------------|---|--------------|
| Forster and Greif (305) | $q/A = 0.0012 (k_L T_s/J \lambda \rho_V \sigma^{1/2}) \cdot$ $(C_L T_s \alpha_L^{1/2} g_c/J \lambda^2 \rho_V^2)^{1/4} \cdot$ $\left[(\rho_L/\mu_L)^{5/8} (C_L \mu_L/k_L)^{1/3} (\Delta P)^2 \right]$ | 5 |
| Levy (306) | $q/A = \frac{J k_L C_L \rho_L^2 (\Delta T)^3}{\sigma T_s (\rho_L - \rho_V)} \varphi (\rho_V \lambda)$ <p>The function $\varphi (\rho_V \lambda)$ is given in Fig. 3</p> | 6 |
| Michenko (307) | $\frac{h}{k_L} \left[\frac{g_c \sigma}{g (\rho_L - \rho_V)} \right]^{1/2} = 8.7 \times 10^{-4} \cdot$ $\left\{ \frac{(q/A)}{\alpha_L \rho_V \lambda} \left[\frac{g_c \sigma}{g (\rho_L - \rho_V)} \right]^{1/2} \right\}^{0.7} \cdot$ $\left\{ \frac{P}{\left[\sigma \frac{g}{g_c} (\rho_L - \rho_V) \right]^{1/2}} \right\}^{0.70}$ | 7 |

TABLE 5
(Continued)

| Reference | Equation | Equation No. |
|---------------------------------------|---|--------------|
| Labountzov (308) | $\frac{h C_L \rho_L \sigma T_s}{k_L (\rho_V \lambda)^2 J} = C_1 \left[\underbrace{\frac{\rho_L (q/A) C_L \rho_L \sigma T_s}{\mu_L \rho_V \lambda (\rho_V \lambda)^2 J}}_{\text{Re}} \right]^m \left(\frac{C_L \mu_L}{k_L} \right)^{1/3}$ <p>For $\text{Re} > 10^{-2}$, $m = 0.65$, $C_1 = 0.125$ For $\text{Re} < 10^{-2}$, $m = 0.50$, $C_1 = 0.0625$</p> | 8 |
| Chang and Snyder (309) | $h = 4 \times 10^{-4} \left[\frac{k_L (\Delta P)^{1.4}}{J^{0.4} (\rho_V \lambda)^{0.8} \sigma} \right]$ $\left[C_L T_s (\rho_L - \rho_V) \right]^{0.4}$ | 9 |
| Nishikawa and Yamagata (310) | $\frac{h L}{k_L} = 8.0 \left\{ \left[\frac{C_L \rho_L^2 g}{M^2 B k_L \sigma \lambda \rho_V g_c} \right]^{1/2} (q/A) \right\}^{2/3} L \cdot$ $(P/P_{\text{atm}})^2 f_c$ <p>$m = 274.32 \text{ ft}^{-1}$ $B = 6.742 \text{ Btu/hr}$</p> | 10 |

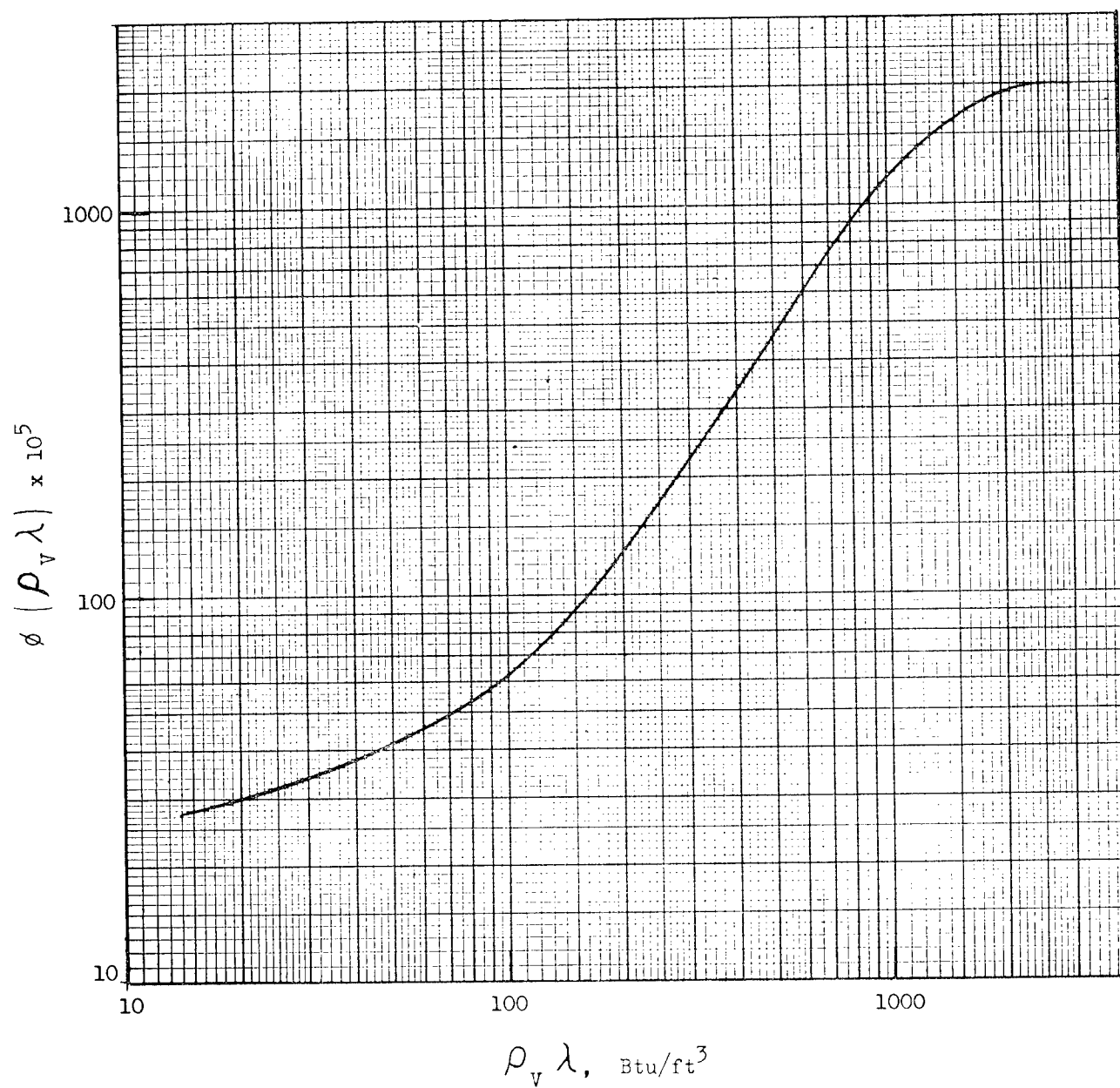


FIG. 3 CORRELATION FACTOR OF LEVY

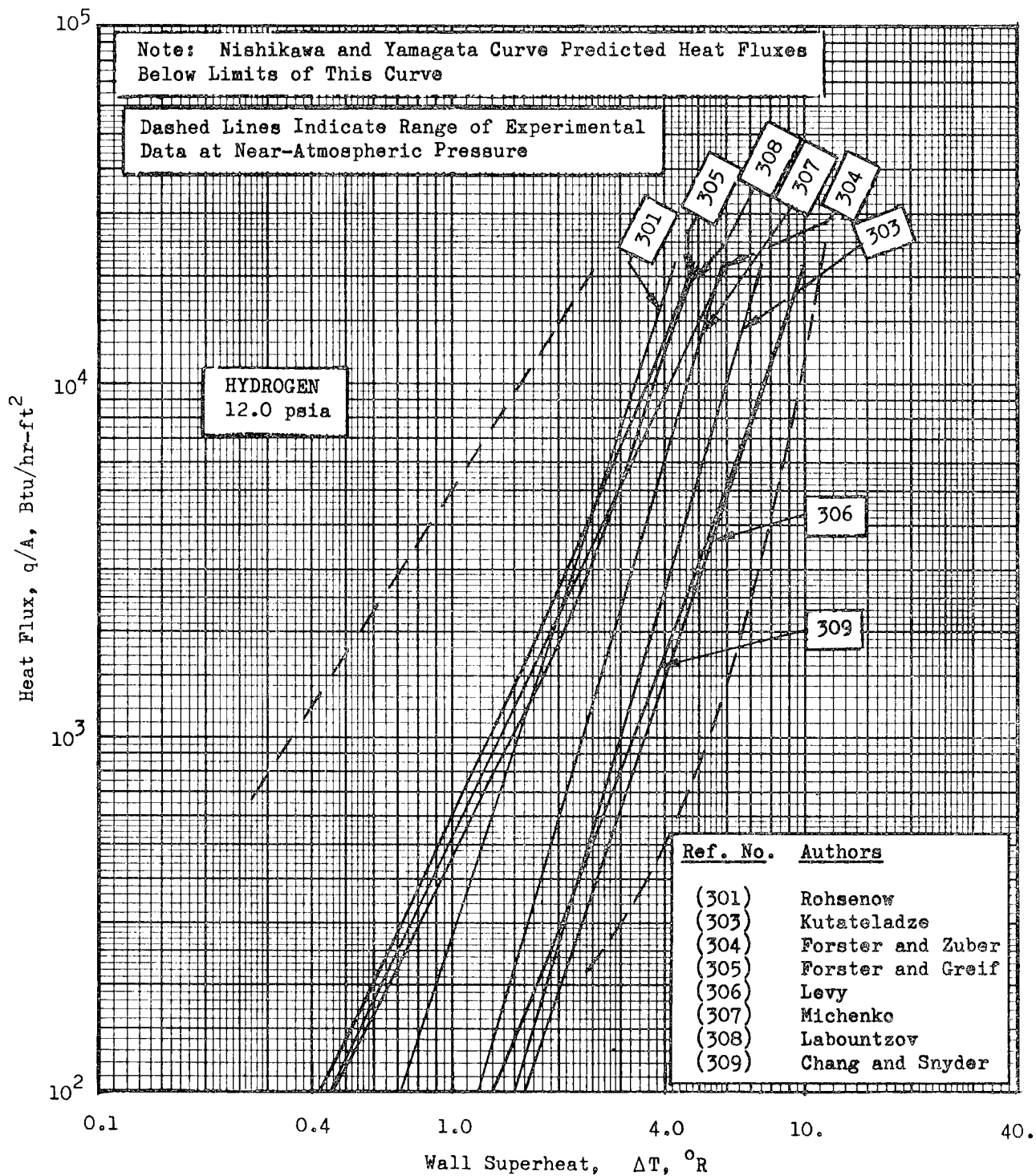


FIG. 4 POOL NUCLEATE BOILING OF HYDROGEN AT 12.0 PSIA

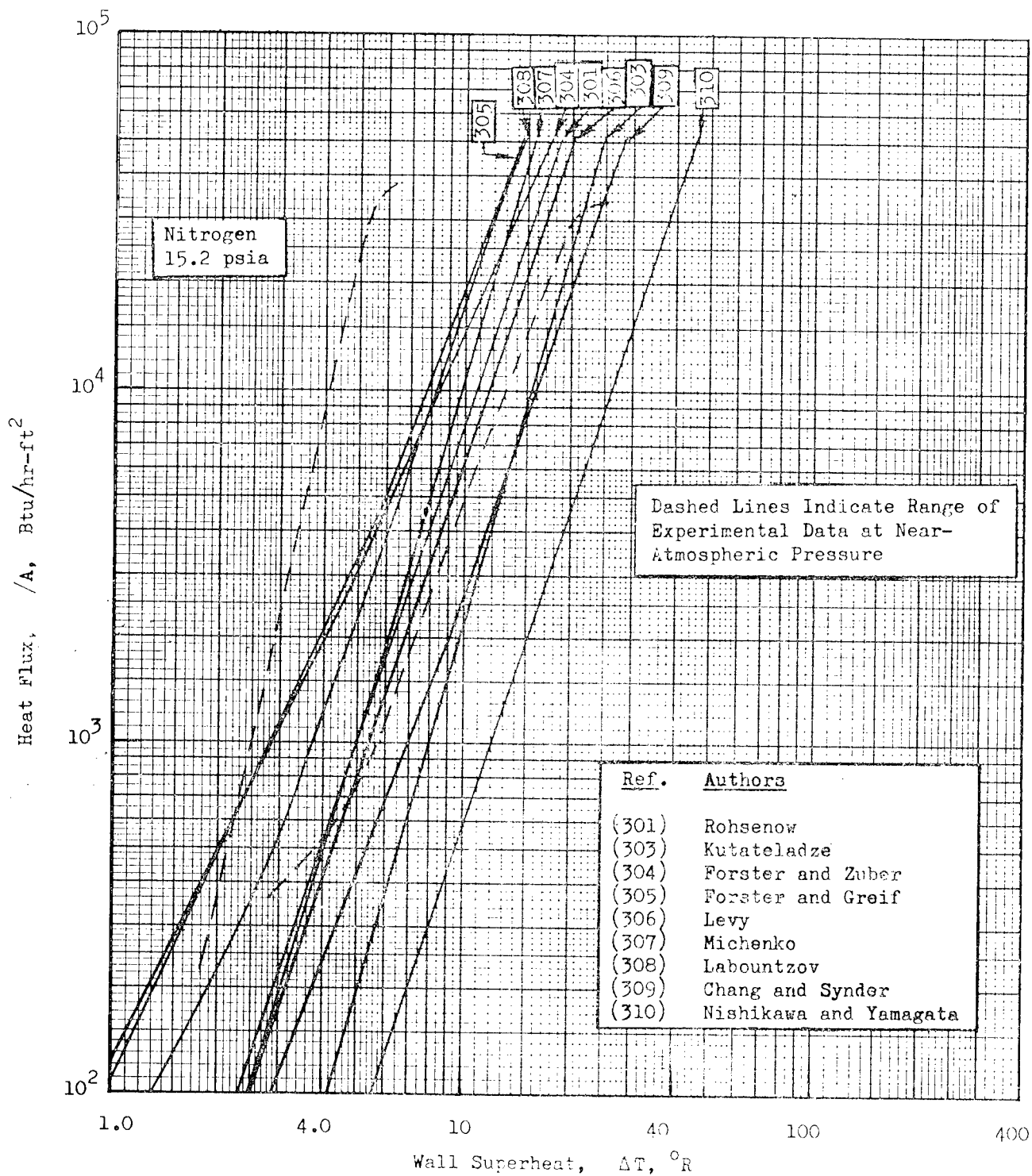


FIG. 5 POOL NUCLEATE BOILING OF NITROGEN AT 15.2 PSIA

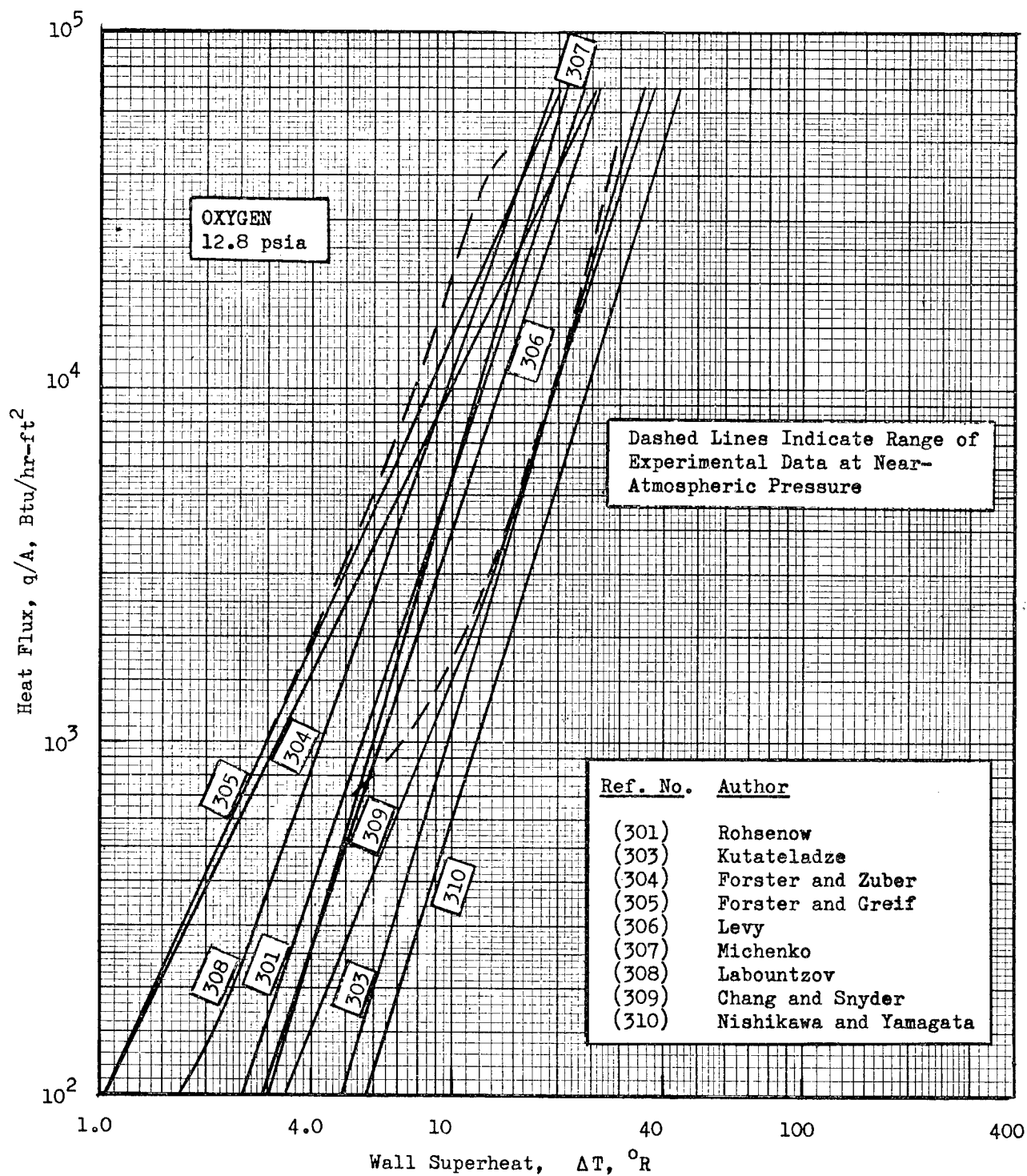


FIG. 6 POOL NUCLEATE BOILING OF OXYGEN AT 12.8 PSIA

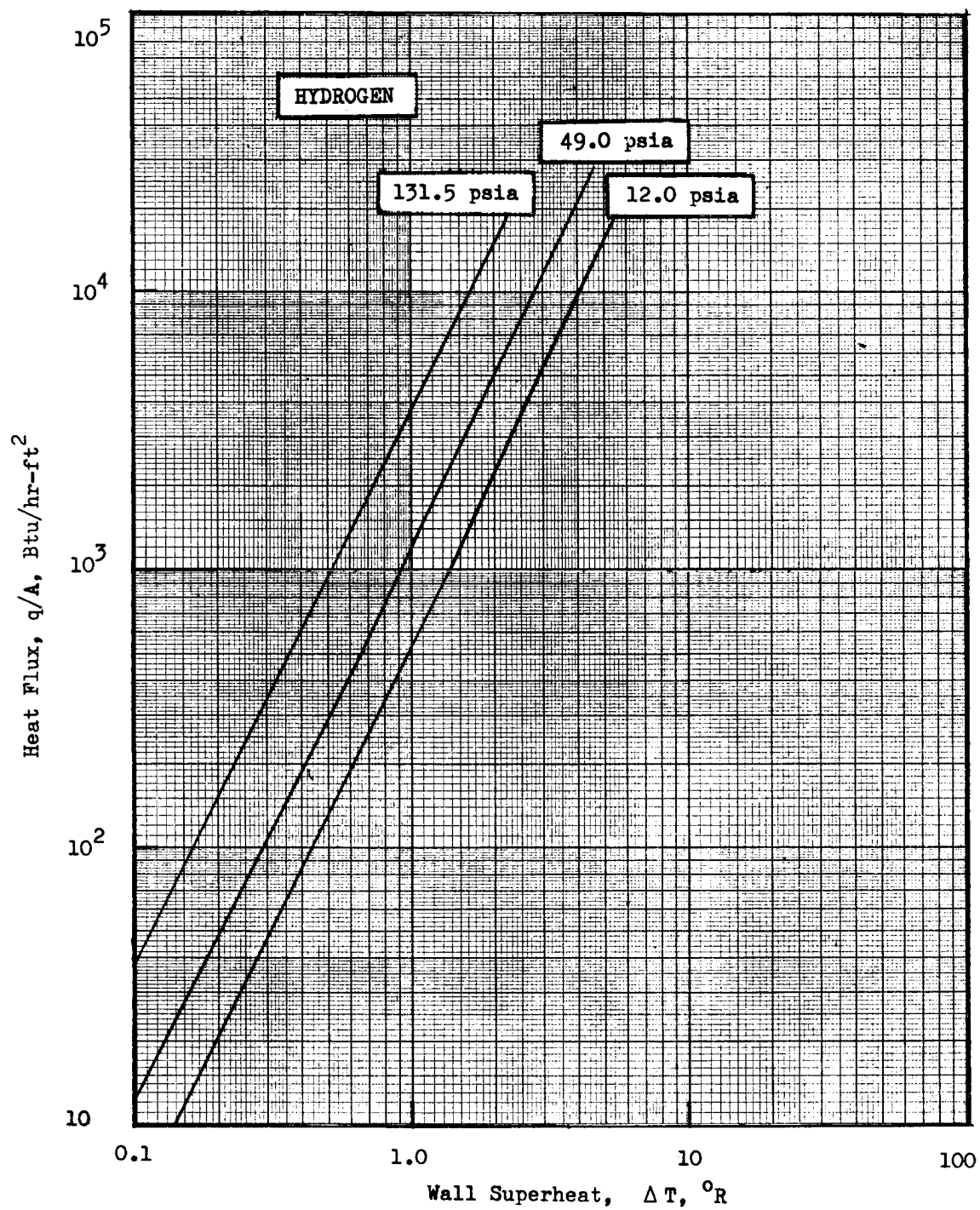


FIG. 7 PREDICTED POOL NUCLEATE BOILING HEAT FLUX FOR HYDROGEN ACCORDING TO FORSTER AND ZUBER EQUATION

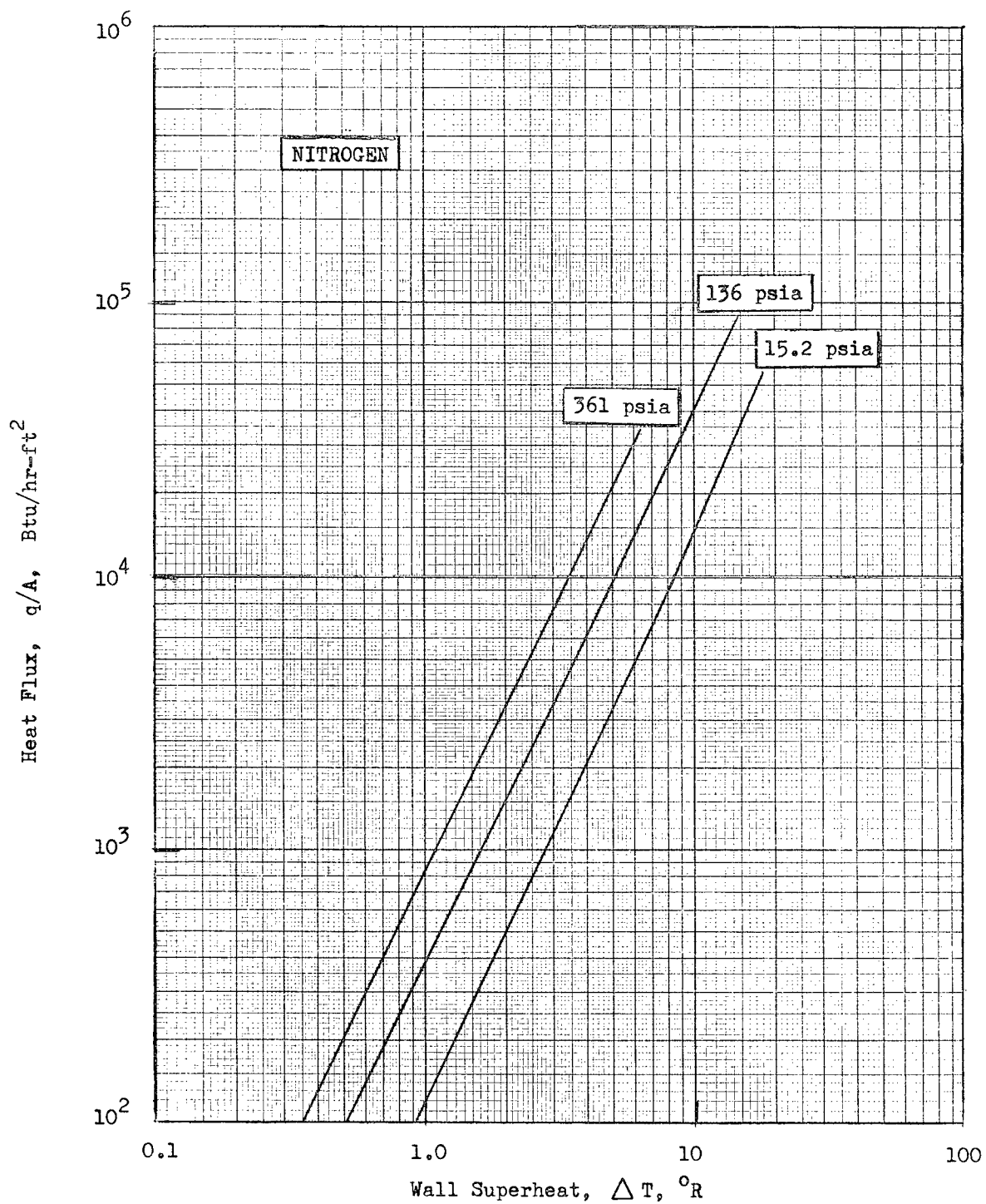


FIG. 8 PREDICTED POOL NUCLEATE BOILING HEAT FLUX FOR NITROGEN ACCORDING TO FORSTER AND ZUBER EQUATION

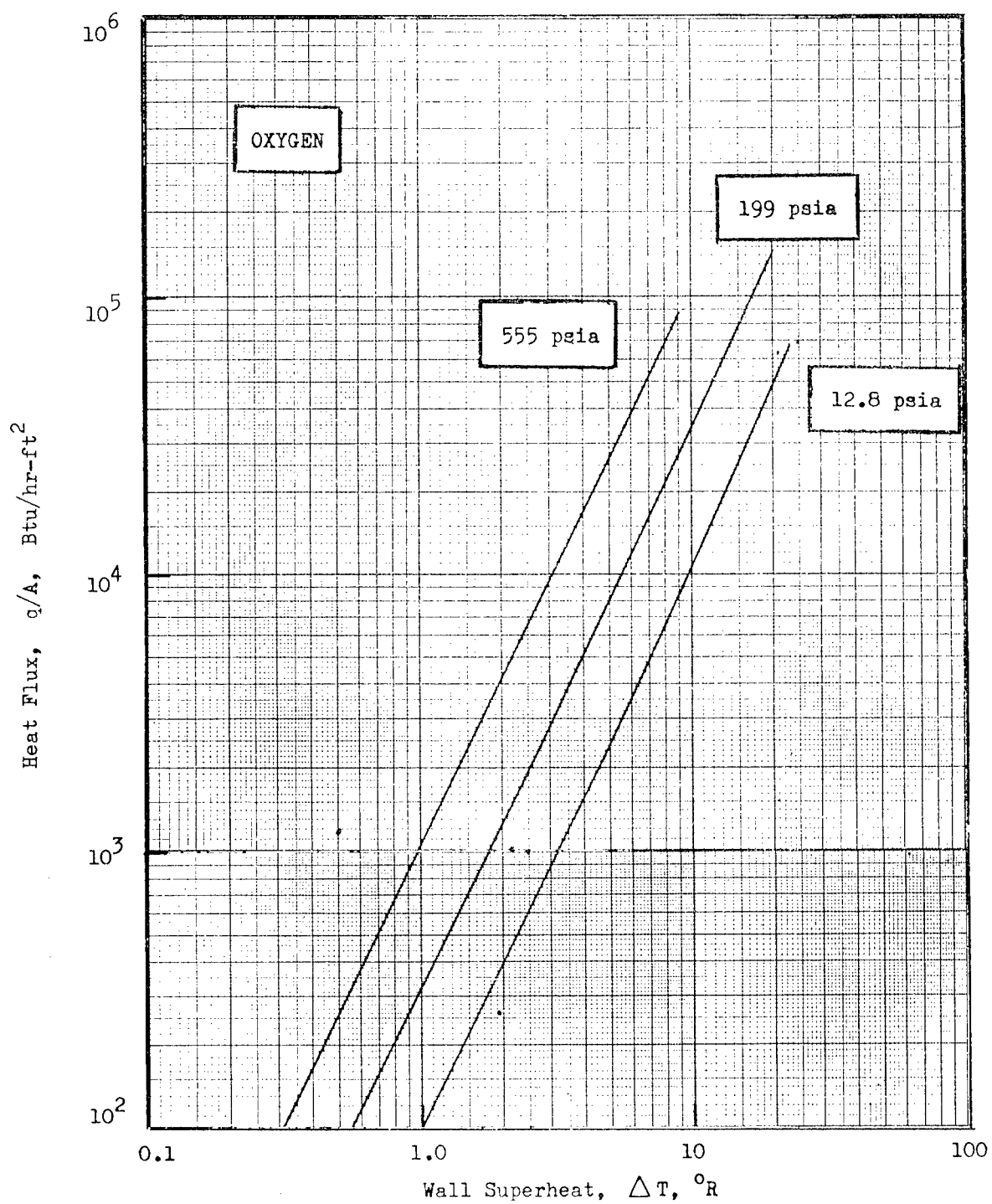


FIG. 9 PREDICTED POOL NUCLEATE BOILING HEAT FLUX FOR OXYGEN
ACCORDING TO FORSTER AND ZUBER EQUATION

are not general and cannot be expected to predict the heat transfer condition accurately for any heater-fluid combination. Some recent work on improved theories which accounts for the nature of the heating surface and its relationship to active sites has been presented by Kurihara and Myers (Ref. 311), Tien (Ref. 312), and Lienhard (Ref. 313). For example, the latter equation is of the form:

$$q/A = B k_L \left(\frac{C_L \mu_L}{k_L} \right)^{1/3} \left[\frac{\sigma_g g_c (\rho_L - \rho_V)}{\rho_V^2} \right]^{1/2} (\Delta T)^{5/4} n^{1/3}$$

The number of active sites, n , is a function of the nature of the surface and, in general, increases as the temperature of the surface increases.

Furthermore, theoretical development of pool nucleate boiling for cryogenic fluids will also be limited unless detailed boiling mechanism studies, specifically for cryogenic fluids, are conducted. An initial start in this important area has been made by McFadden and Grassman (Ref. 314). Their study concerned bubble frequency and diameter at a given nucleation site. Experimental data were obtained with liquid nitrogen and were compared with the correlation of Zuber (Ref. 323):

$$f D = 0.59 \left[\frac{\sigma_g g_c (\rho_L - \rho_V)}{\rho_L^2} \right]^{1/4} \quad (20)$$

This correlation had been shown to work reasonably well for water, carbon tetrachloride, and methyl alcohol. The nitrogen data, however, did not fit the Zuber correlation. Accordingly, it was shown by dimensional analysis that:

$$\frac{f D^2 \rho_L^{1/2}}{(\sigma g_c D)^{1/2}} \propto \left(\frac{g (\rho_L - \rho_V) D^2}{\sigma g_c} \right)^d \quad (21)$$

and a plot of all data, including nitrogen, was best represented by:

$$f D^{1/2} = 0.56 \left(\frac{g (\rho_L - \rho_V)}{\rho_L} \right)^{1/2} \quad (22)$$

Far from the critical temperature $(\rho_L - \rho_V) \approx \rho_L$, and accordingly:

$$f D^{1/2} = 0.56 (g)^{1/2} \quad (23)$$

Equation 23 correlated all available results more closely than Eq. 20; however, the authors felt that more experimental work is needed to extend the diameter range and a wider variety of fluids should be studied. Relations such as Eq. 23 will be useful in developing more exact nucleate boiling theories for cryogenics based on active sites.

POOL NUCLEATE BOILING MAXIMUM HEAT FLUX

The regime of pool nucleate boiling is limited to a maximum heat flux and a corresponding maximum ΔT . As with other fluids, the maximum heat flux and maximum ΔT for cryogenic fluids both depend on the particular fluid, the pressure and, to some extent, the geometry and

TABLE 6

SUMMARY OF POOL NUCLEATE BOILING THEORIES IN
GENERALIZED STANTON NUMBER FORM

$$\text{Re}_B = \frac{C_2}{(\text{St})_B^a (\text{Pr})^b} \quad \text{or} \quad \frac{L^* G^*}{\mu_L} = \frac{C_2}{\left[\frac{(q/A)}{\Delta T C_L G^*} \right]^a (\text{Pr})^b} \quad (\text{consistent units})$$

| Reference | L^* | G^* | C_2 | a | b |
|---|---|---------------------------------------|--|----------------|-----------------|
| Rohsenow (301) | $\left[\frac{g_c \sigma}{g (\rho_L - \rho_V)} \right]^{1/2}$ | $\frac{(q/A)}{\lambda}$ | $2.97 \times 10^5 \text{ to } 5.08 \times 10^7$ | 3 | 5.1 |
| Kutateladze (303) | $\left[\frac{g_c \sigma}{g (\rho_L - \rho_V)} \right]^{1/2}$ | $\frac{(q/A) \rho_L}{\lambda \rho_V}$ | $3.05 \times 10^{-11} \left\{ \left[\frac{\sigma \frac{g_c}{g_c} (\rho_L - \rho_V)}{P} \right]^{1/2} \right\}^{7/3}$ | $\frac{10}{3}$ | $\frac{6.5}{3}$ |
| Forster and Zuber (304) and Forster and Greif (305) | $\frac{C_L (\rho_L - \rho_V) T_s \sigma}{(\rho_V \lambda)^2 J}$ | $\frac{(q/A) \rho_L}{\lambda \rho_V}$ | $0.0012 \left[\frac{C_L \rho_L^2 T_s \sigma^2 g_c}{\mu^2 \rho_V^2 \lambda^2 J} \right]^{1/4} \left(\frac{\rho_L}{\rho_L - \rho_V} \right)$ | 2 | $\frac{19}{24}$ |
| Levy (306) | $\frac{C_L (\rho_L - \rho_V) T_s \sigma}{(\rho_V \lambda)^2 J}$ | $\frac{(q/A) \rho_L}{\lambda \rho_V}$ | $\varphi (\rho_V \lambda)$ from graph of Fig. 3 | 3 | 1 |

TABLE 6

(Continued)

| Reference | L* | G* | C ₂ | a | b |
|---------------------------------------|---|---------------------------------------|--|---|--|
| Michenko (307) | $\left[\frac{g_c \sigma}{g (\rho_L - \rho_V)} \right]^{1/2}$ | $\frac{(q/A) \rho_L}{\lambda \rho_V}$ | $6.3 \times 10^{-11} \left\{ \frac{P}{\sigma \frac{g_c}{g_c} (\rho_L - \rho_V)} \right\}^{1/2}$ $7/3$ | $\frac{10}{3}$ | 1.0 |
| Labountzov (308) | $C_L \frac{(\rho_L - \rho_V) T_s \sigma}{(\rho_V \lambda)^2 J}$ | $\frac{(q/A) \rho_L}{\lambda \rho_V}$ | $\begin{cases} \text{Re} < 10^{-2}: & 0.00391 \\ \text{Re} > 10^{-2}: & 0.00260 \end{cases}$ | $\begin{matrix} 2 \\ 2.86 \end{matrix}$ | $\begin{matrix} 4/3 \\ 1.9 \end{matrix}$ |
| Chang and Snyder (309) | $C_L \frac{(\rho_L - \rho_V) T_s \sigma}{(\rho_V \lambda)^2 J}$ | $\frac{(q/A) \rho_L}{\lambda \rho_V}$ | 57.2×10^{-4} | 2.4 | 1 |
| Nishikawa and Yamagata (301) | $C_L \frac{(\rho_L - \rho_V) T_s \sigma}{(\rho_V \lambda)^2 J}$ | $\frac{(q/A) \rho_L}{\lambda \rho_V}$ | $\frac{1}{512} \left[\frac{(\rho_L - \rho_V) k_L T_s g_c}{M^2 B \rho_V \lambda J g_c} \right] (P/p_{atm})^2 f \zeta$ $M = 274.32 \text{ ft}^{-1}$ $B = 6.742 \text{ Btu/hr}$ | 3 | 1 |

orientation of the surface. The maximum heat flux is essentially independent of the nature of the surface (except if it is greased) but the maximum ΔT is highly dependent on this factor.

A number of theories have been proposed recently to estimate the pool nucleate boiling maximum heat flux. Some postulate that this maximum occurs at the point where the vapor formation rate is of such magnitude that hydrodynamic instabilities begin to impede the counterflow of the liquid toward the heating surface. All the theories proposed can be rearranged easily in terms of the superficial vapor disengaging velocity:

$$\frac{(q/A)_{\max}}{\lambda \rho_V} = \Phi_1 \quad * \quad (24)$$

*It should be noted that this is not a dimensionless parameter.

where Φ_1 includes buoyancy, acceleration and/or other physical property effects. Expressions for Φ_1 of the theories reviewed are summarized in Table 7. The importance of certain liquid properties such as C_L , k_L , μ_L and ρ_L appears to be a major point of contention among the theories.

Calculations were carried out for the pool nucleate boiling maximum heat flux as a function of pressure using the theories summarized in Table 7. The results are plotted in Fig. 12, 13, and 14 for H_2 , N_2 , and O_2 , respectively. In general, considerable disagreement between the various theories exists over the entire pressure range. As is typical with all fluids, a maximum pool nucleate boiling maximum heat flux is predicted at a pressure about one-third the critical pressure. Comparison with experimental data is discussed in the next section.

TABLE 7

SUMMARY OF POOL NUCLEATE BOILING MAXIMUM
HEAT FLUX THEORIES

$$\frac{(q/A)_{\max}}{\lambda \rho_V} = \Phi_1 \text{ (consistent units except as noted)}$$

| Reference | Φ_1 | Equation No. |
|-----------------------------|--|--------------|
| Addoms (315) | $\left[g \left(\frac{k_L}{\rho_L c_L} \right) \right]^{1/3} \left[\varphi \left(\frac{\rho_L - \rho_V}{\rho_V} \right) \right] \text{ (see Fig. 10)}$ | 25 |
| Rohsenow and Griffith (316) | $143 \left(\frac{\rho_L - \rho_V}{\rho_V} \right)^{0.6}, \text{ ft/hr}$ | 26 |
| Griffith (317) | $\left[\frac{g (\rho_L - \rho_V)}{\mu_L} \left(\frac{k_L}{\rho_L c_L} \right)^2 \right]^{1/3} \left[\varphi \left(\frac{P}{P_c} \right) \right] \text{ (see Fig. 11)}$ | 27 |
| Zuber and Tribus (318) | $\frac{\pi}{24} \left[\frac{\sigma g g_c (\rho_L - \rho_V)}{\rho_V^2} \right]^{1/4} \left(\frac{\rho_L}{\rho_L + \rho_V} \right)^{1/2}$ | 28 |
| Kutateladze (319) | $0.16 \left[\frac{\sigma g g_c (\rho_L - \rho_V)}{\rho_V^2} \right]^{1/4}$ | 29 |

TABLE 7
(Continued)

| Reference | Φ_1 | Equation No. |
|--|--|----------------------|
| Borishanskii (320) | $\left[\frac{\sigma \, g g_c (\rho_L - \rho_V)}{\rho_V^2} \right]^{1/4}$ $\left\{ 0.13 + \frac{\mu_L^2 \left[g (\rho_L - \rho_V) \right]^{1/2}}{\rho_L (\sigma g_c)^{3/2}} \right\}^{0.4}$ | 30 |
| Noyes (321) | $0.144 \left[\frac{g g_c \sigma}{\rho_L} \right]^{1/4} \left(\frac{\rho_L - \rho_V}{\rho_V} \right)^{1/2} \left(\frac{C_L \mu_L}{k_L} \right)^{-0.245}$ | 31 |
| Noyes (321) (alternate correlation) | $\left[g \left(\frac{k_L}{\rho_L C_L} \right) \right]^{1/3} \left[\frac{C_L \mu_L}{k_L a g} \right]^{1/12} \left[\varphi \left(\frac{\rho_L - \rho_V}{\rho_V} \right) \right]$ | 31a (see Fig. 10) |
| Chang and Snyder (309) | $0.145 \left[\frac{\sigma \, g g_c (\rho_L - \rho_V)}{\rho_V^2} \right]^{1/4} \left(\frac{\rho_L + \rho_V}{\rho_L} \right)^{1/2}$ | 32 |
| Chang (322) | $K \left[\frac{\sigma \, g g_c (\rho_L - \rho_V)}{\rho_V^2} \right]^{1/4}, \begin{cases} K = 0.098 & \text{vertical} \\ K = 0.13 & \text{horizontal} \end{cases}$ | 33 |
| Moissis and Berenson (323) | $0.18 \frac{\left[\sigma \, g g_c (\rho_L - \rho_V) \right]^{1/4} \left[\frac{\rho_L + \rho_V}{\rho_L \rho_V} \right]^{1/2}}{1 + 2 (\rho_V/\rho_L)^{1/2} + (\rho_V/\rho_L)}$ | 34 |

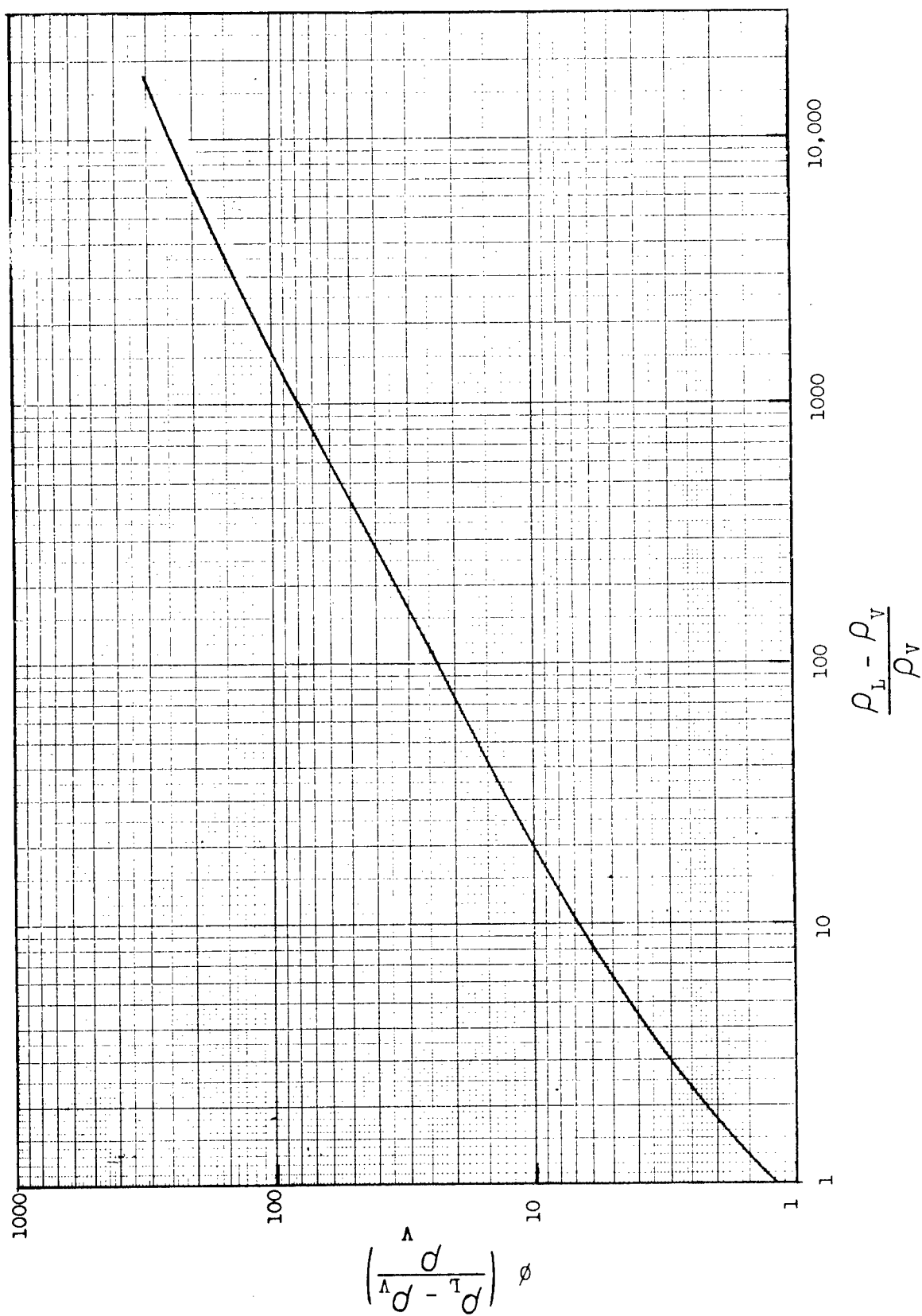


FIG. 10 CORRELATION PARAMETER OF ADDONS AND NOYES (ALTERNATE)

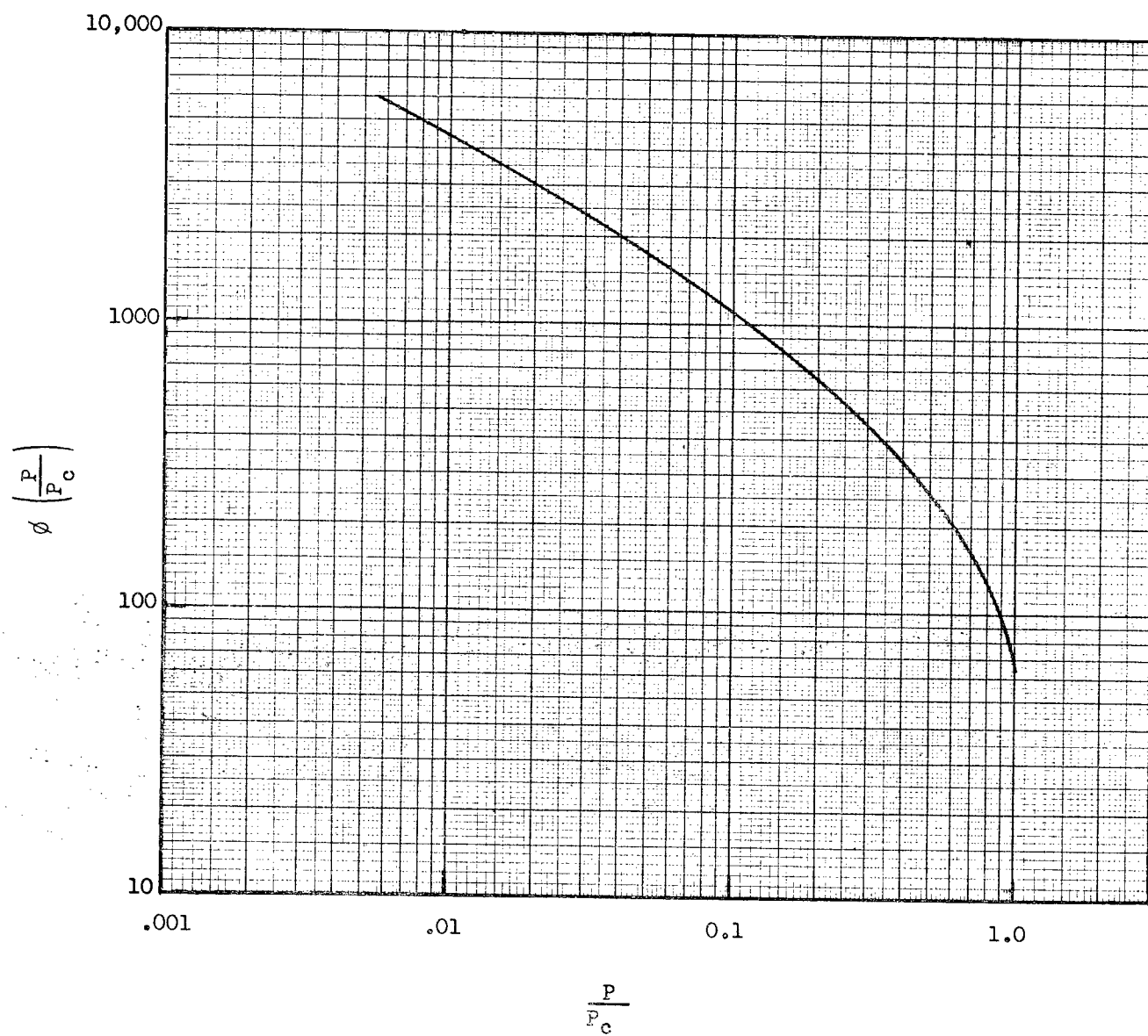


FIG. 11 CORRELATION PARAMETER OF GRIFFITH

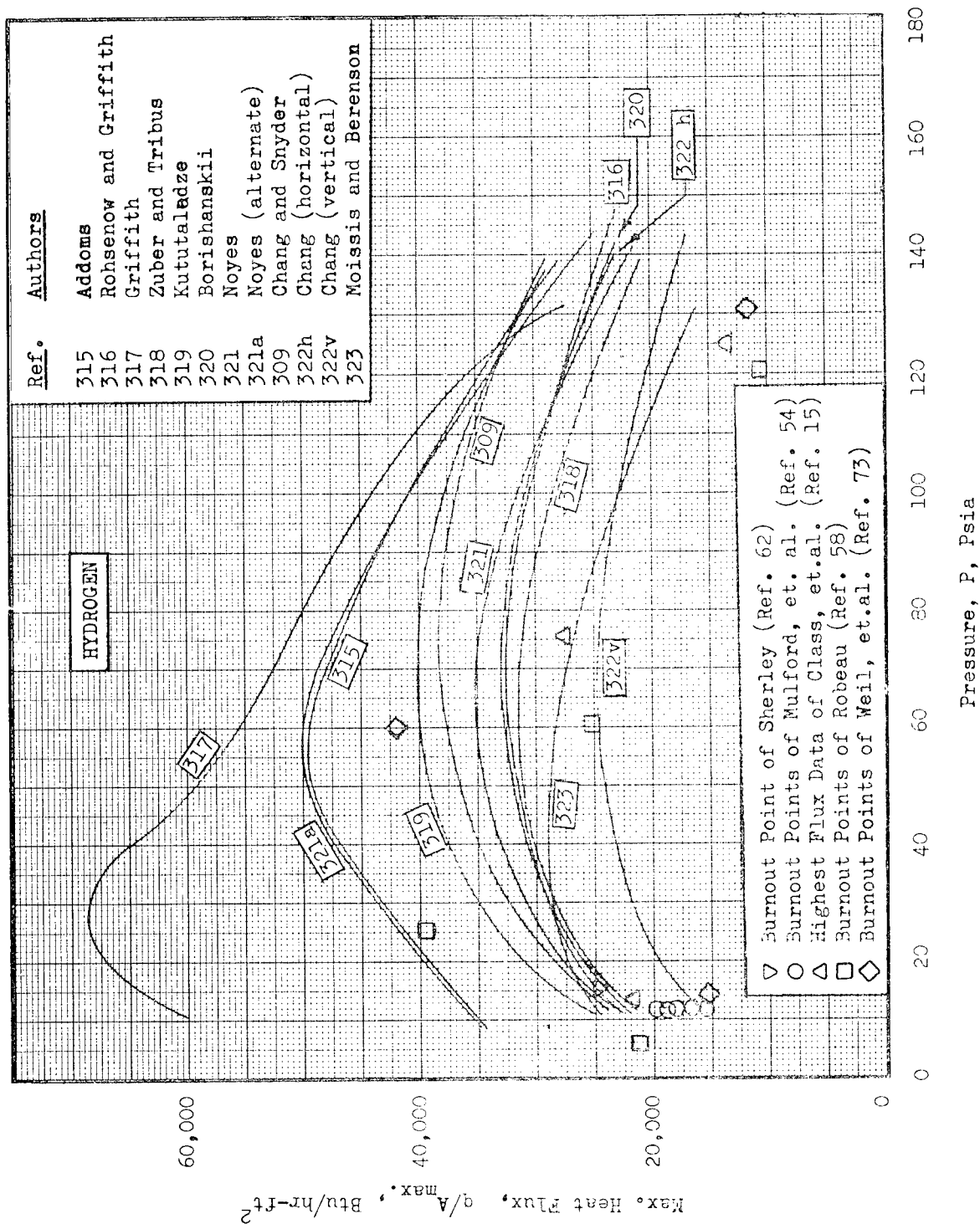


FIG. 12 COMPARISON OF THEORIES FOR POOL NUCLEATE BOILING MAXIMUM HEAT FLUX FOR HYDROGEN

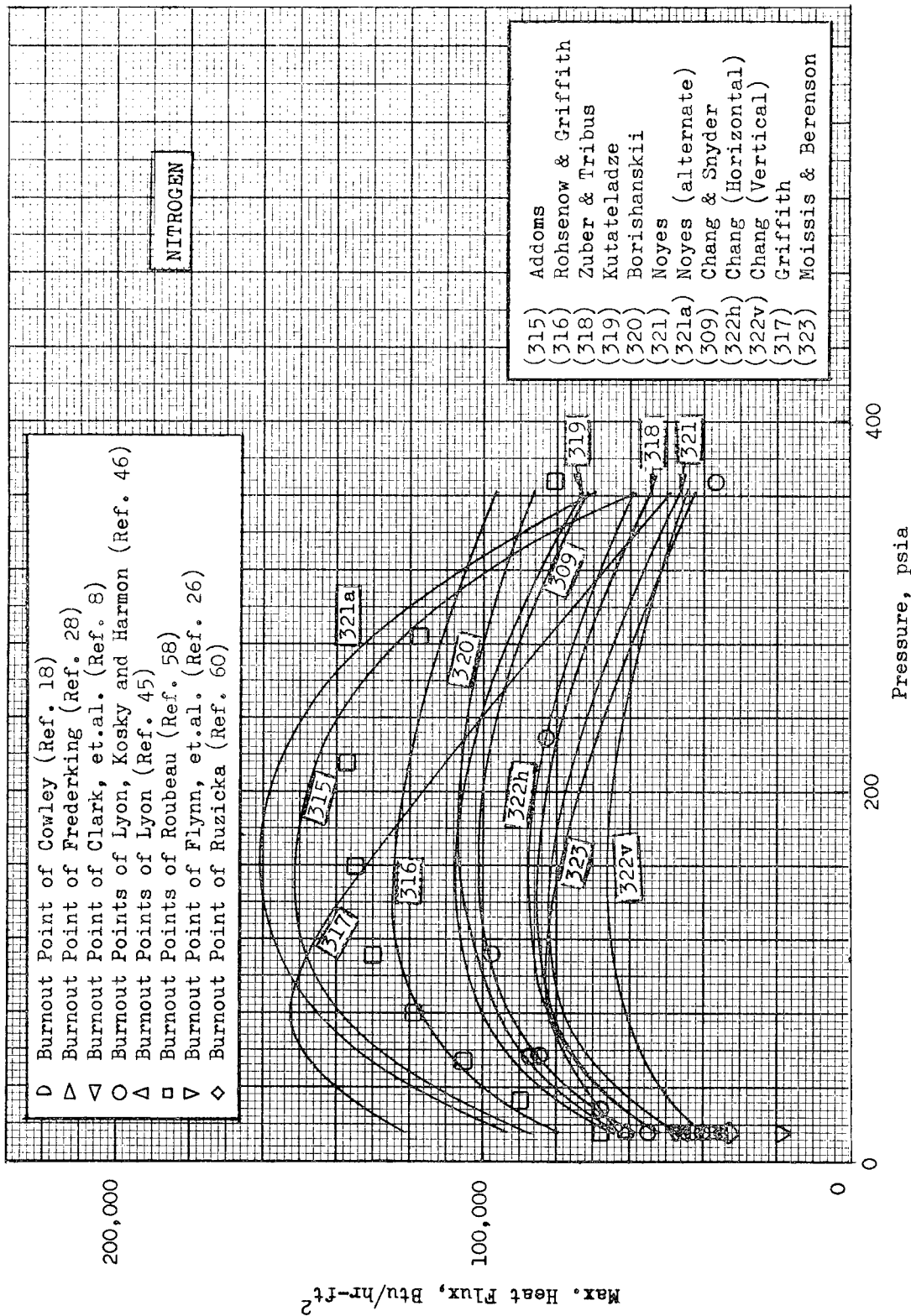


FIG. 13 COMPARISON OF THEORIES FOR POOL NUCLEATE BOILING MAXIMUM HEAT FLUX FOR NITROGEN

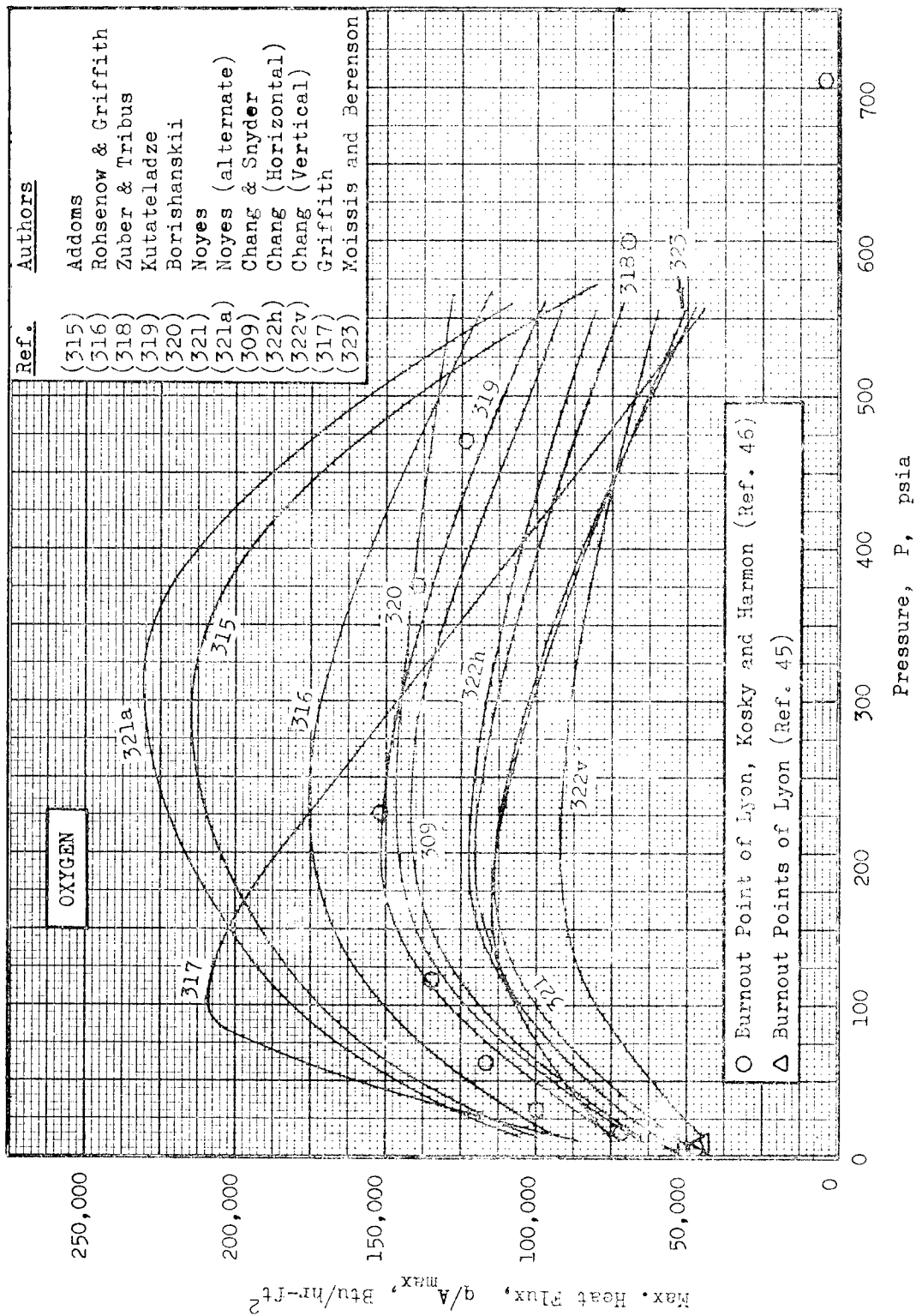


FIG. 14 COMPARISON OF THEORIES FOR POOL NUCLEATE BOILING MAXIMUM HEAT FLUX FOR OXYGEN

POOL FILM BOILING MINIMUM HEAT FLUX

Just as the nucleate boiling regime is limited to a maximum heat flux, the film boiling regime is limited to a minimum heat flux as shown in Fig. 2. Available theories for the pool film boiling minimum heat flux are summarized in Table 8 in terms of the same parameter used for the maximum heat flux, namely:

$$\frac{(q/A)_{\min}}{\lambda (\rho_V)_f} = \Phi_2 \quad (35)$$

All the theories are based on hydrodynamic instability of the liquid-vapor boundary and strictly apply only to boiling above a horizontal flat surface. In all cases, the physical properties are evaluated at the saturation temperature, except $(\rho_V)_f$ which is evaluated at the average vapor film temperature.

Calculations of the minimum heat flux were carried out using the equations in Table 8 for each of the three cryogenic fluids. The results are plotted in Fig. 15, 16, and 17 for H_2 , N_2 , and O_2 , respectively. By using the parameter $(q/A)_{\min} \left[\rho_V / (\rho_V)_f \right]$ as the ordinate rather than just $(q/A)_{\min}$, it was possible to plot the theories in terms of pressure only. At relatively low values of ΔT , these two vapor densities approach each other and the ordinate approaches the value of $(q/A)_{\min}$. At larger ΔT values, the ordinate is somewhat higher than $(q/A)_{\min}$. Experimental data for the pool film boiling minimum heat flux of cryogenics are very meager, as discussed in the next main section.

TABLE 8

SUMMARY OF POOL FILM BOILING MINIMUM
HEAT FLUX THEORIES

$$\frac{(q/A)_{\min}}{\lambda (\rho_V)_f} = \Phi_2 \text{ (consistent units)}$$

| Reference | Φ_2 | Equation No. |
|--|---|--------------|
| Zuber and Tribus (318) | $K_1 \left[\frac{\sigma g g_c (\rho_L - \rho_V)}{(\rho_L + \rho_V)^2} \right]^{1/4}$, $K_1 = 0.099 \text{ to } 0.131$ | 36 |
| Zuber and Tribus (318) (alternate approach) | $K_2 \left[\frac{\sigma g g_c}{\rho_L - \rho_V} \right]^{1/4}$, $K_2 = 0.109 \text{ to } 0.144$ | 37 |
| Zuber (324) | $0.177 \left[\frac{\sigma g g_c (\rho_L - \rho_V)}{(\rho_L + \rho_V)^2} \right]^{1/4}$ | 38 |
| Berenson (325) | $0.09 \left[\frac{\sigma g g_c (\rho_L - \rho_V)}{(\rho_L + \rho_V)^2} \right]^{1/4}$ | 39 |

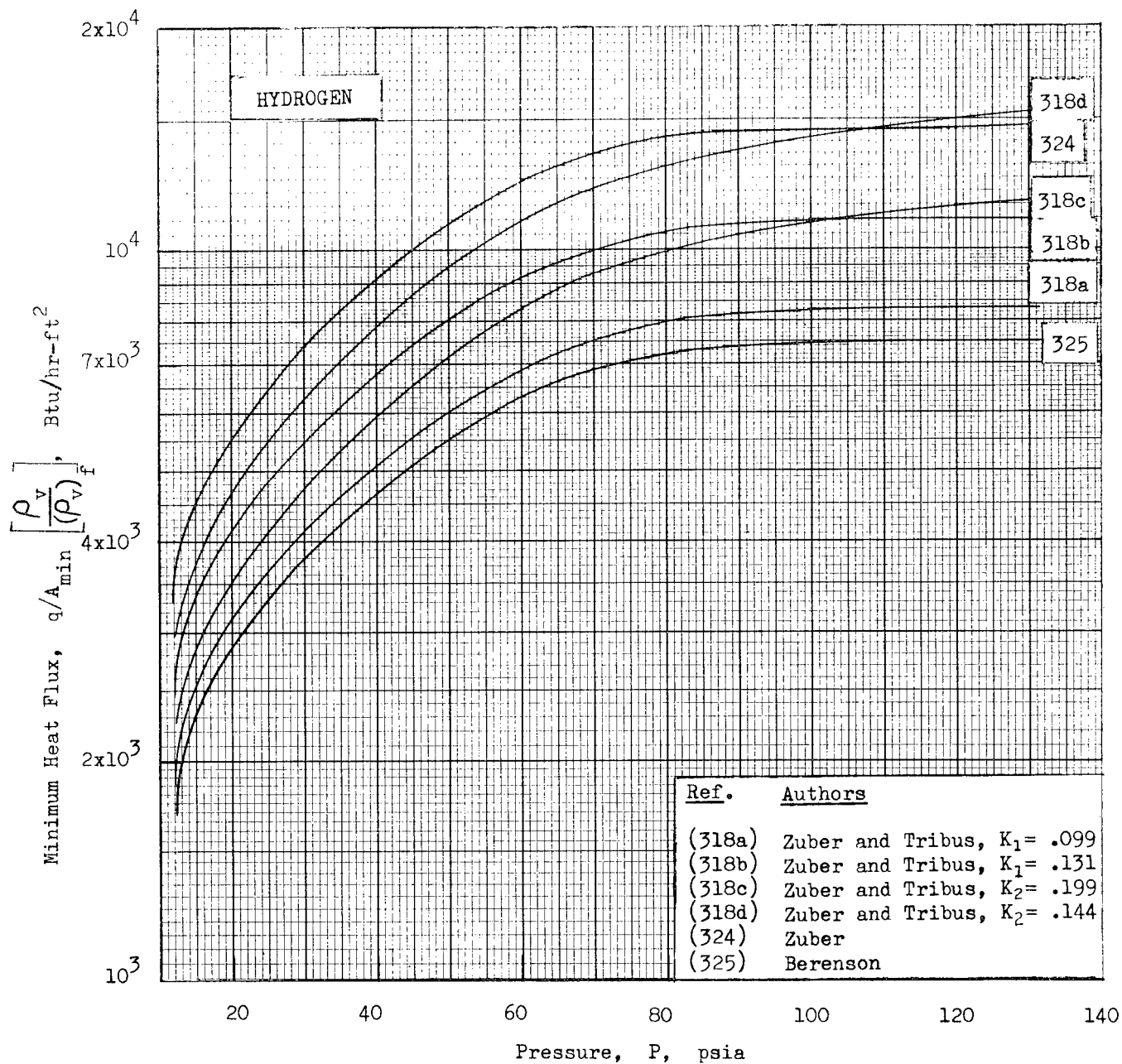


FIG. 15 POOL FILM BOILING MINIMUM HEAT FLUX FOR HYDROGEN

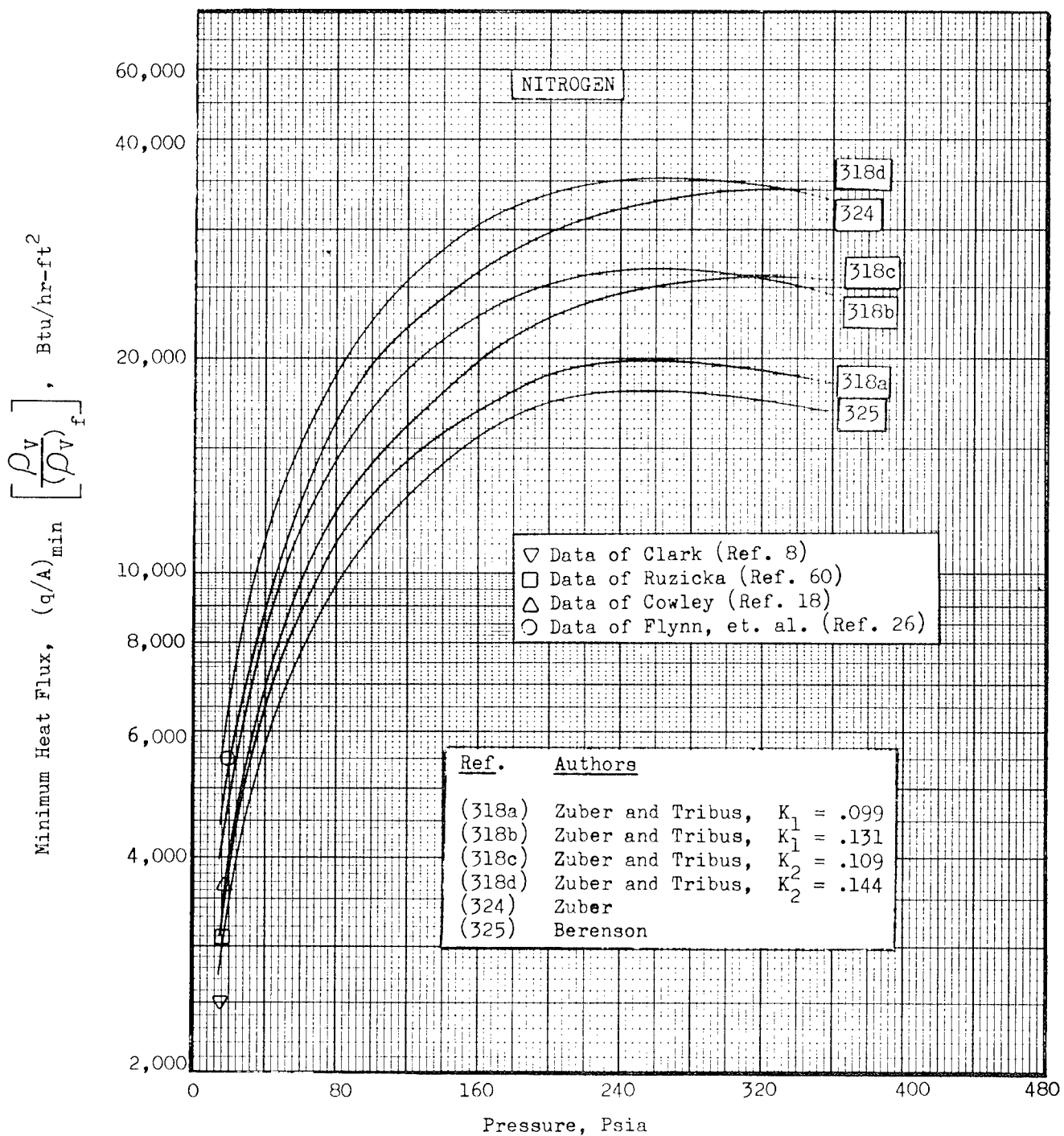


FIG. 16 POOL FILM BOILING MINIMUM HEAT FLUX FOR NITROGEN

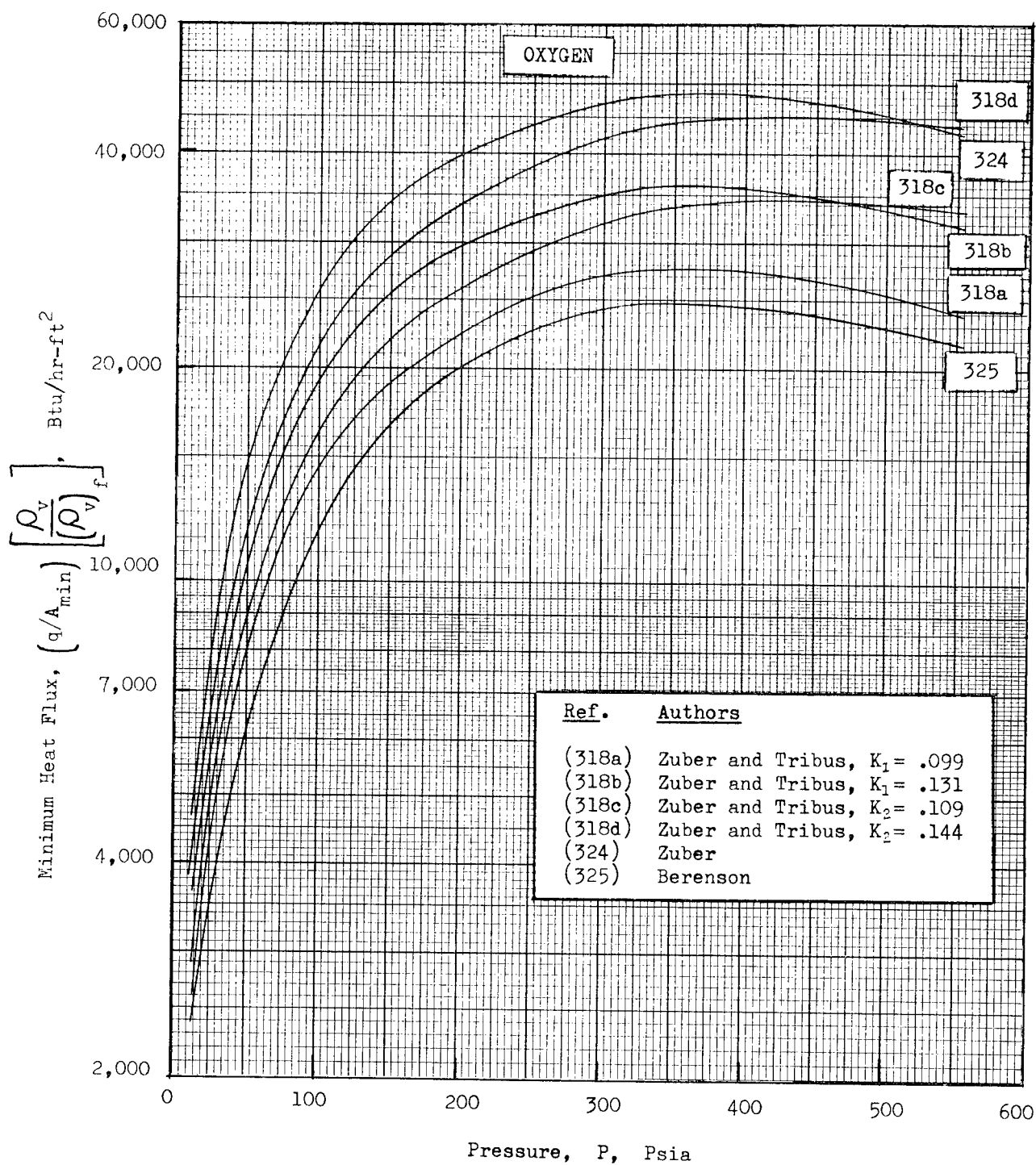


FIG. 17 POOL FILM BOILING MINIMUM HEAT FLUX FOR OXYGEN

POOL STABLE FILM BOILING

The pool stable film boiling regime is important for cryogenic fluids because it can be achieved at surface temperatures within the practical limits of a number of materials. In fact, it is possible to attain higher heat fluxes than the pool nucleate boiling maximum heat flux by operating under conditions of film boiling. This regime is much more amenable to theoretical development than pool nucleate boiling. Since the original theoretical derivations by L. A. Bromley in 1948 (Ref. 5 and 6), based on the similarity to film condensation, a great deal of effort has been expended on improving the theory and extending it to different boiling surface geometries. The theories are best summarized with respect to the geometric configuration. Corrections for the effect of thermal radiation through the vapor film at high temperatures may be important and are discussed at the end of this section. It is important to note that nitrogen was one of the fluids used by Bromley initially to verify his theory.

Long Horizontal Cylinders

Bromley's original equation, assuming laminar flow, was:

$$h_c = C_3 \left[\frac{k_V^3 \rho_V (\rho_L - \rho_V) g \lambda'}{D (T_w - T_s) \mu_V} \right]^{1/4} \quad (40)$$

where: The constant C_3 was found to be bracketed theoretically from 0.512 (stagnant liquid surrounding the tube) to 0.724 (liquid moves completely freely with the vapor). An average experimental value of $C_3 = 0.62$ was determined by Bromley from experimental data.

and:

$$\lambda' = \lambda + 0.5 C_V (T_w - T_s) \quad (41)$$

All vapor properties except in $(\rho_L - \rho_V)$ terms are evaluated at:

$$T_{ave} = \frac{T_w + T_s}{2}$$

Bromley later (Ref. 326) modified Eq. 41 to take into account more properly the superheating of the vapor film:

$$\lambda' = \lambda \left[1 + 0.4 \frac{C_V (T_w - T_s)}{\lambda} \right]^2 \quad (42)$$

Rohsenow (Ref. 327) further modified Eq. 42 to account for crossflow within the film:

$$\lambda' = \lambda \left[1 + 0.675 \frac{C_V (T_w - T_s)}{\lambda} \right] \approx \lambda \left[1 + 0.54 \frac{C_V (T_w - T_s)}{\lambda} \right]^2 \quad (45)$$

More recently, McFadden and Grosh (Ref. 328) determined the effects of variable density and specific heat for the vapor film by numerically solving the boundary layer equations for stable, free convection film boiling. They considered a vertical surface as well as a horizontal cylinder. They found, in general, that compared to the assumption of constant properties, a variable specific heat tends to increase the heat transfer coefficient while a variable density tends to thicken the vapor layer and thereby decrease the heat transfer coefficient. The latter effect was predominant, but in general, only at pressures approaching the critical (about $P_r > 0.9$) was the influence of variable properties

important. Frederking (Ref. 329) also obtained a numerical boundary layer solution for a vertical plate and a horizontal cylinder. His method accounts for the influence of momentum transport at the vapor-liquid interface and covers a wide range of vapor superheat.

An alternate form of Eq. 40 in terms of dimensionless groups as discussed by Frederking (Ref. 330) is:

$$Nu_D = 0.62 \left[Ra_D \left(\frac{\lambda'}{C_V (T_w - T_s)} \right) \right]^{1/4} \quad (44)$$

$$\text{where: } Nu_D = \text{Nusselt number} = \frac{h_c D}{k_V} \quad (45)$$

$$Ra_D = \text{Rayleigh number} = \frac{g D^3 \rho_V (\rho_L - \rho_V) C_V}{k_V \mu_V} \quad (46)$$

In general, Eq. 40 and 44 are accurate only for a restricted range of cylinder diameter. For very small diameters, the vapor film thickness may approach the diameter (this is not allowed for in the theory) and predicted values of h_c may be somewhat lower. For very large diameters, an h_c of zero is predicted which is not consistent with experimental findings. Modifications of Eq. 40 for the effect of diameter over a wide range are discussed by Banchero, et al. (Ref. 3) and Frederking (Ref. 27) in the light of experimental data for horizontal wires and large cylinders. Banchero in particular, on the basis of extensive data for oxygen, recommends that the C_3 constant in Eq. 40 be replaced by the expression:

$$C_3 = a \left(\frac{1}{D} + c \right) D^{1/4} \quad (47)$$

where a and c must be determined from experimental data.

Horizontal Plates (Facing Up)

Based on a wave theory for natural convection, Chang (Ref. 331) developed the following equation which is rearranged in terms of the Rayleigh number:

$$Nu_{L_c} = 0.278 \left[Ra_{L_c} \left(\frac{\lambda}{C_V (T_w - T_s)} \right) \right]^{1/3} \quad (47)$$

where: L_c is substituted for D in Eq. 45 and 46.

It should be noted that the characteristic length, L_c , in Eq. 47 cancels out.

More recently, Berenson (Ref. 332) used the Taylor instability concept to derive the following equation in terms of the Rayleigh number for the region of the minimum:

$$Nu_B = 0.425 \left[Ra_B \left(\frac{\lambda'}{C_V (T_w - T_s)} \right) \right]^{1/4} \quad (48)$$

where:

$$B = \left[\frac{g_c \sigma}{g (\rho_L - \rho_V)} \right]^{1/2} \quad \text{is substituted for D in Eq. 45 and 46.} \quad (49)$$

Vertical Surfaces

Bromley (Ref. 5 and 6) also derived an expression for film boiling from a vertical surface assuming laminar flow. In terms of the average Nusselt number over a vertical length, L, and the Rayleigh number, his expression was:

$$Nu_L = C_4 \left[Ra_L \left(\frac{\lambda'}{C_V (T_w - T_s)} \right) \right]^{1/4} \quad (50)$$

where: L is substituted for D in Eq. 45 and 46.

The constant C_h in Eq. 50 was theoretically determined by Hsu and Westwater (Ref. 42) to be bracketed between 0.667 and 0.943. Bonilla (Ref. 333) suggested an average value of 0.80.

Ellion (Ref. 334) derived an equation similar to Eq. 50 for the case of uniform heat flux. He obtained a constant, C_2 , of 0.716. More recently, a number of laminar boundary layer solutions for vertical surfaces have been developed, including those of McFadden and Grosh (Ref. 328), Cess (Ref. 335), Sparrow and Cess (Ref. 336), Koh (Ref. 337), Koh and Nilson (Ref. 338), and Frederking (Ref. 329). The aim of these more refined analyses has been to account for inertia forces, convective energy transport, interfacial velocity, variable physical properties and interacting radiation and convection effects.

Koh's exact laminar boundary layer analysis for constant properties, in particular, results in a lucid description of the effects of shear stress and vapor velocity at the vapor-liquid interface. He shows that the constant C_h in Eq. 50 of Bromley is actually a function of:

$$\frac{C_V \mu_V}{k_V}, \left[\frac{\rho_V \mu_V}{\rho_L \mu_L} \right]^{1/2} \quad \text{and} \quad \frac{C_V (\Delta T)}{\lambda (Pr)_V}$$

For values of $\left[\rho_V \mu_V / \rho_L \mu_L \right]^{1/2} > 0.001$ and values of $C_V (\Delta T) / \lambda (Pr)_V$, Koh predicts values of h_c considerably higher than those predicted by Eq. 50.

In many practical situations, the above laminar flow analyses for vertical surfaces are not valid. Hsu and Westwater (Ref. 338) observed heat fluxes 100 to 300 percent greater than predicted by Eq. 50. The increase

was caused by the development of turbulent flow above a critical height corresponding to a critical vapor film thickness and film thickness Reynolds number. The critical Reynolds number for transition from viscous to turbulent flow at a height L_0 is given by:

$$Re^* = \frac{y^* u_V^* (\rho_V)_f}{\mu_V} = 100$$

$$\text{where: } y^* = \left[\frac{2 \mu_V^2 Re^*}{g (\rho_V)_f [\rho_L - (\rho_V)_f]} \right]^{1/3} \quad (52)$$

$$\text{and: } L_0 = \frac{\mu_V Re^* \lambda' y^*}{2 k_V (\Delta T)} \quad (53)$$

For $Re^* > 100$, they developed an equation for h_c which accounted for the turbulent flow effects. Bankoff in a written discussion to Ref. 338 presented the following simpler alternate turbulent flow equation for the average heat transfer coefficient:

$$\frac{h_c}{\rho_V c_V \left(\frac{g^2 L \mu_V}{\rho_V} \right)^{1/5}} = 0.29 \left(\frac{\rho_L - \rho_V}{\rho_V} \right)^{2/5} \left[\frac{c_V (\Delta T)}{\lambda} \right]^{1/5} \quad (54)$$

The constant 0.29 in Eq. 54 is actually subject to some variation depending on the nature of the fluid.

Radiation Effects

In his original derivation for a horizontal cylinder, Bromley (Ref. 5 and 6) also included an expression for the transfer of heat from the cylinder wall, through the vapor, to the liquid by thermal radiation. He noted that the coefficient for convection, h_c , was dependent on the effective coefficient for radiation, h_r . For $h_r < h_c$, he developed the following approximate relations:

$$h_{\text{total}} = h_c + (3/4)h_r \quad (55)$$

where:

$$h_r = \frac{\sigma' (T_w^4 - T_s^4)}{\left(\frac{1}{\epsilon_w} + \frac{1}{\alpha_L} - 1 \right) (T_w - T_s)} \quad (56)$$

In the case of N_2 boiling on a 0.350-inch horizontal carbon tube at atmospheric pressure, he found that the radiation contribution became important above a wall temperature of about 500 F. More detailed evaluations of the effect of thermal radiation on film boiling have been presented by Chang (Ref. 331) and Koh and Nilson (Ref. 338).

Theoretical calculations of stable pool film boiling were carried out using the following form which is applicable to the convective contribution for several geometries:

$$\frac{(q/A)_c L_{\text{eq}}^{1/4}}{C_5} = \left[\frac{k_V^3 \rho_V (\rho_V - \rho_L) g \lambda' (\Delta T)^3}{\mu_V} \right]^{1/4}$$

The results are plotted for each of three pressures for each of the three cryogenic fluids in Fig. 18, 19, and 20. Values of λ' were computed from Eq. 43. The curves are applicable to Eq. 40, 48, and 50 where the values of C_5 and L_{eq} are:

| <u>Geometry</u> | <u>Equation</u> | <u>C_5</u> | <u>L_{eq}</u> |
|---------------------------------|-----------------|-------------------------|----------------------------|
| Horizontal Cylinder | 40 | 0.62 | D |
| Horizontal Plate (facing up) | 48 | 0.425 | B (Eq. 49) |
| Vertical Surface | 50 | 0.80 | L |

FORCED CONVECTION SUBCOOLED NUCLEATE BOILING

The previous discussions of boiling theory were restricted to the case of saturated pool boiling. Boiling can also occur in a subcooled liquid if it is brought into contact with a surface with a temperature sufficiently above the saturation temperature. This is sometimes referred to as surface or local boiling because the vapor bubbles formed are subsequently condensed by the subcooled liquid and no net generation of vapor occurs. The case where the subcooled liquid is forced to flow past the heated surface is of great practical interest. This is referred to as forced convection subcooled (or surface) boiling. As with pool boiling, a nucleate regime exists which is limited to a maximum heat flux and transition to film boiling can occur. The use of forced convection permits the attainment of much higher heat fluxes than can be achieved under pool conditions. The nucleate regime is discussed in this section.

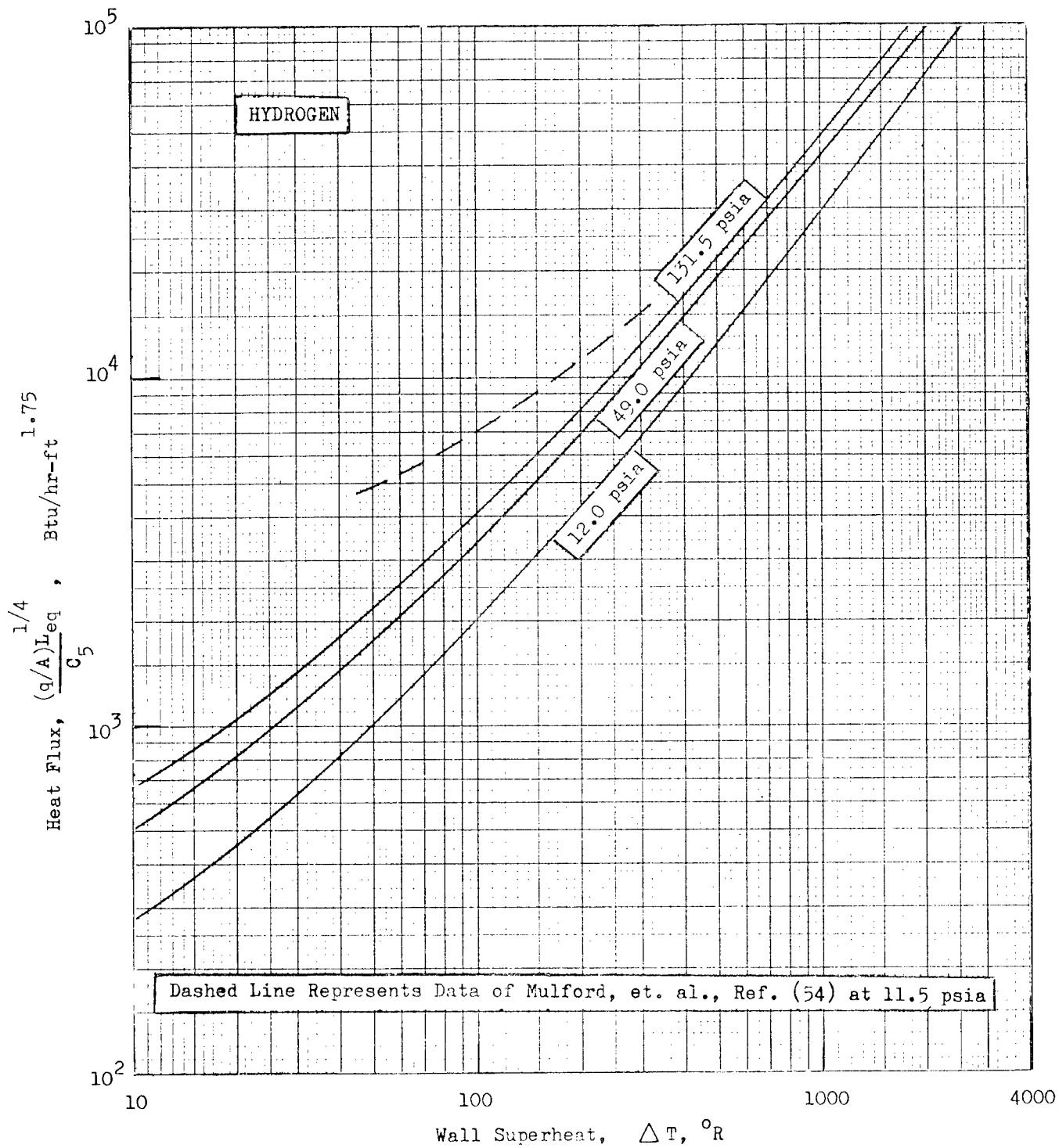


FIG. 18 STABLE POOL FILM BOILING OF HYDROGEN

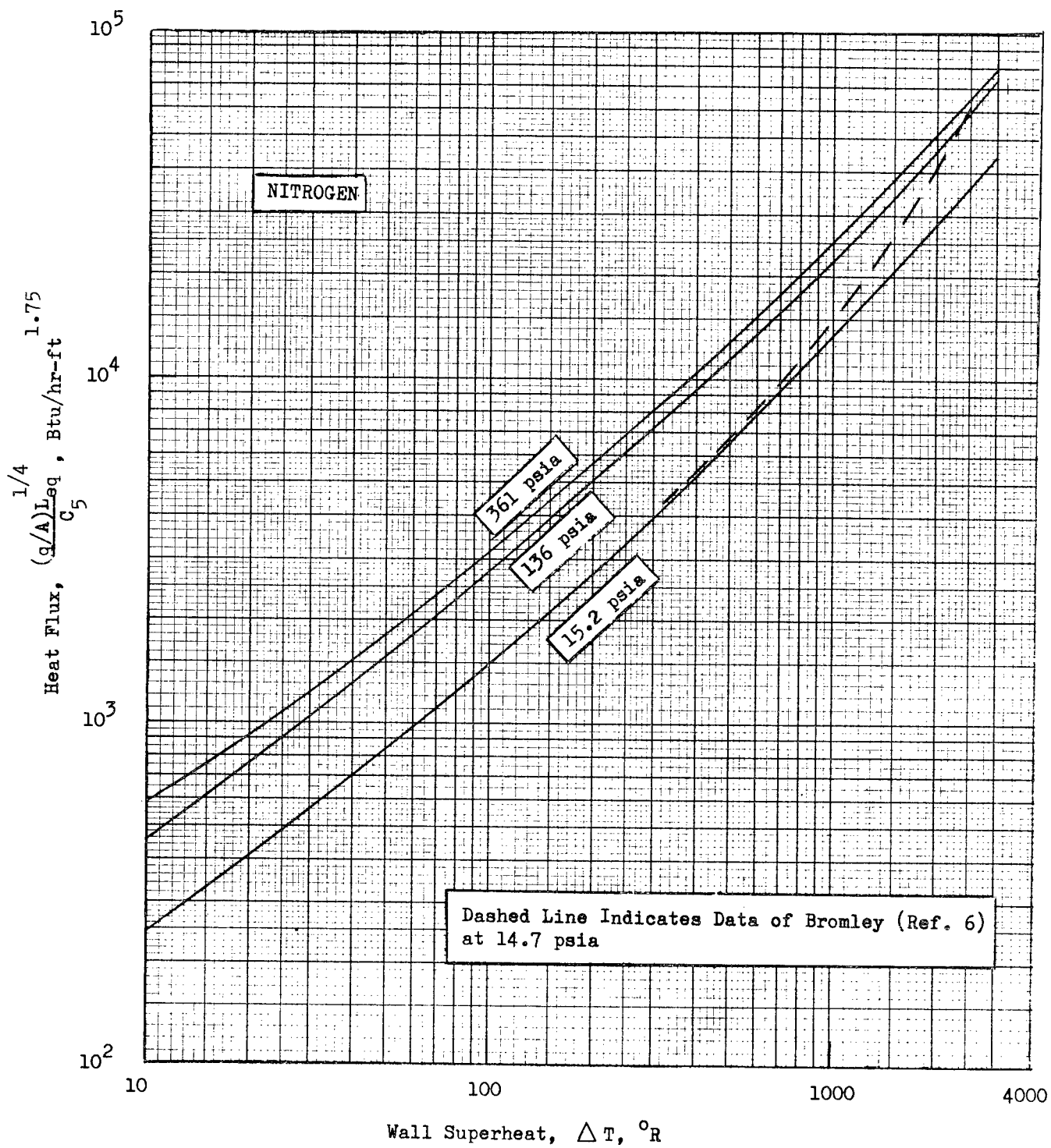


FIG. 19 STABLE POOL FILM BOILING OF NITROGEN

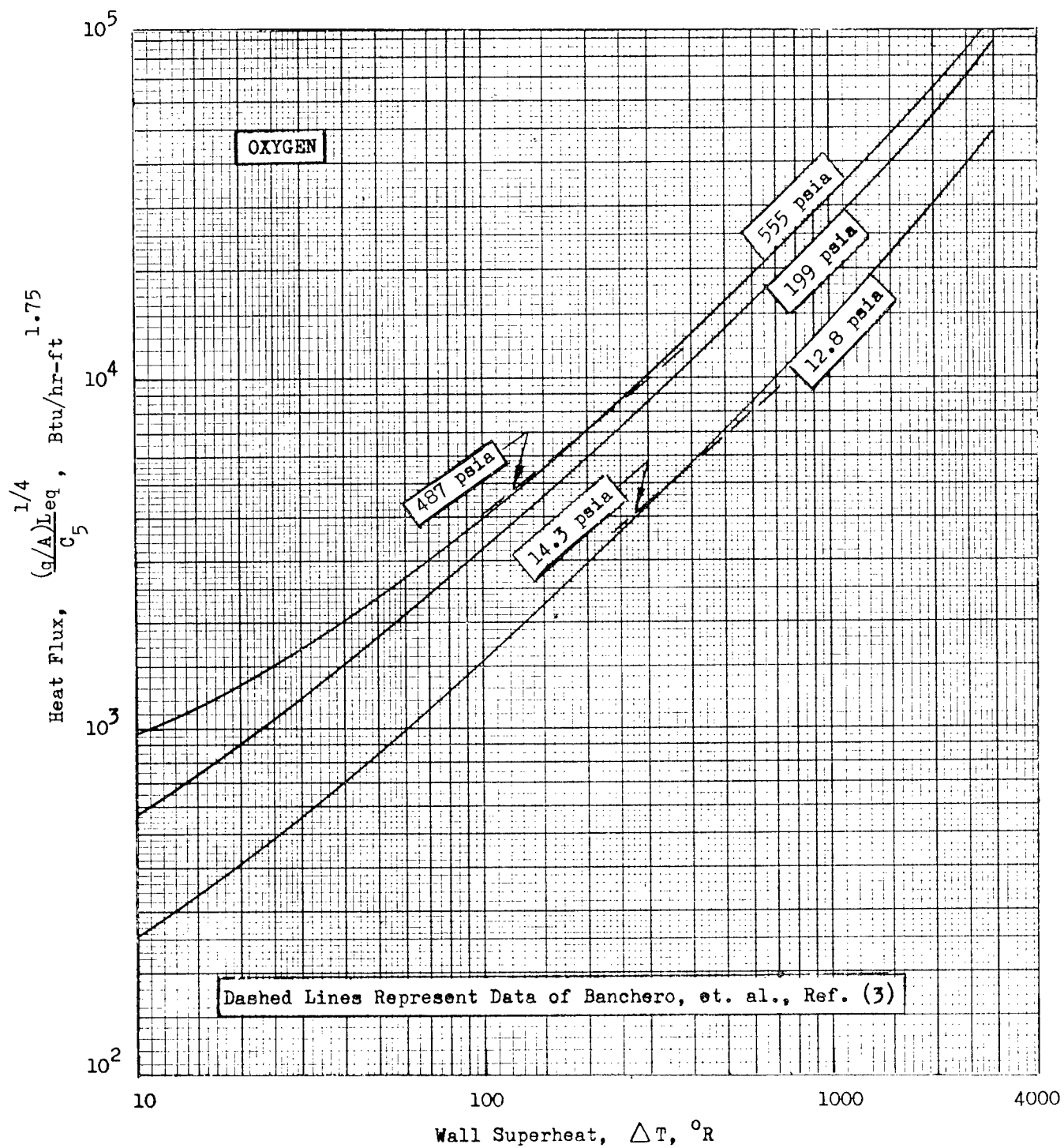


FIG. 20 STABLE POOL FILM BOILING OF OXYGEN

Curves of heat flux vs ΔT are also used to correlate forced convection subcooled nucleate boiling. McAdams (Ref. 202) shows that the proper temperature difference to use is the wall superheat, $\Delta T = T_w - T_s$ rather than the total over-all temperature difference between the wall and the subcooled liquid ($T_w - T_b$). A typical curve for forced convection subcooled nucleate boiling is shown in Fig. 21. As discussed by Bergles and Rohsenow (Ref. 339), three distinct regions exist. At low wall superheat, boiling is essentially absent and the heat transfer is governed by forced convection (Curve AB). At moderate wall superheat, the heat transfer is determined by the combined effects of forced convection and surface boiling (Curve BC). At higher wall superheat, the effect of forced convection seems to disappear and the heat transfer is governed by fully developed nucleate boiling (Curve CD). At some heat flux above the point D, the maximum heat flux occurs. Several methods for predicting the curve of Fig. 21 have been developed.

Rohsenow (Ref. 301) recommended an additive heat flux method based on ordinary forced convection without phase change and pool nucleate boiling as given by the equation:

$$(q/A) = (q/A)_{FC} + (q/A)_B \quad (57)$$

where $(q/A)_B$ is assumed equal to $(q/A)_{PB}$

$$(q/A)_{FC} = h_{FC} (T_w - T_b) \quad (58)$$

For a typical case of turbulent flow inside straight, smooth, circular tubes at moderate temperature differences, the McAdams equation (Ref. 202) gives h_{FC} as:

$$\left(\frac{h_{FC} D}{k_L} \right)_b = 0.023 \left(\frac{DG}{\mu_L} \right)_b^{0.8} \left(\frac{C_L \mu_L}{k_L} \right)_b^{0.4} \quad (59)$$

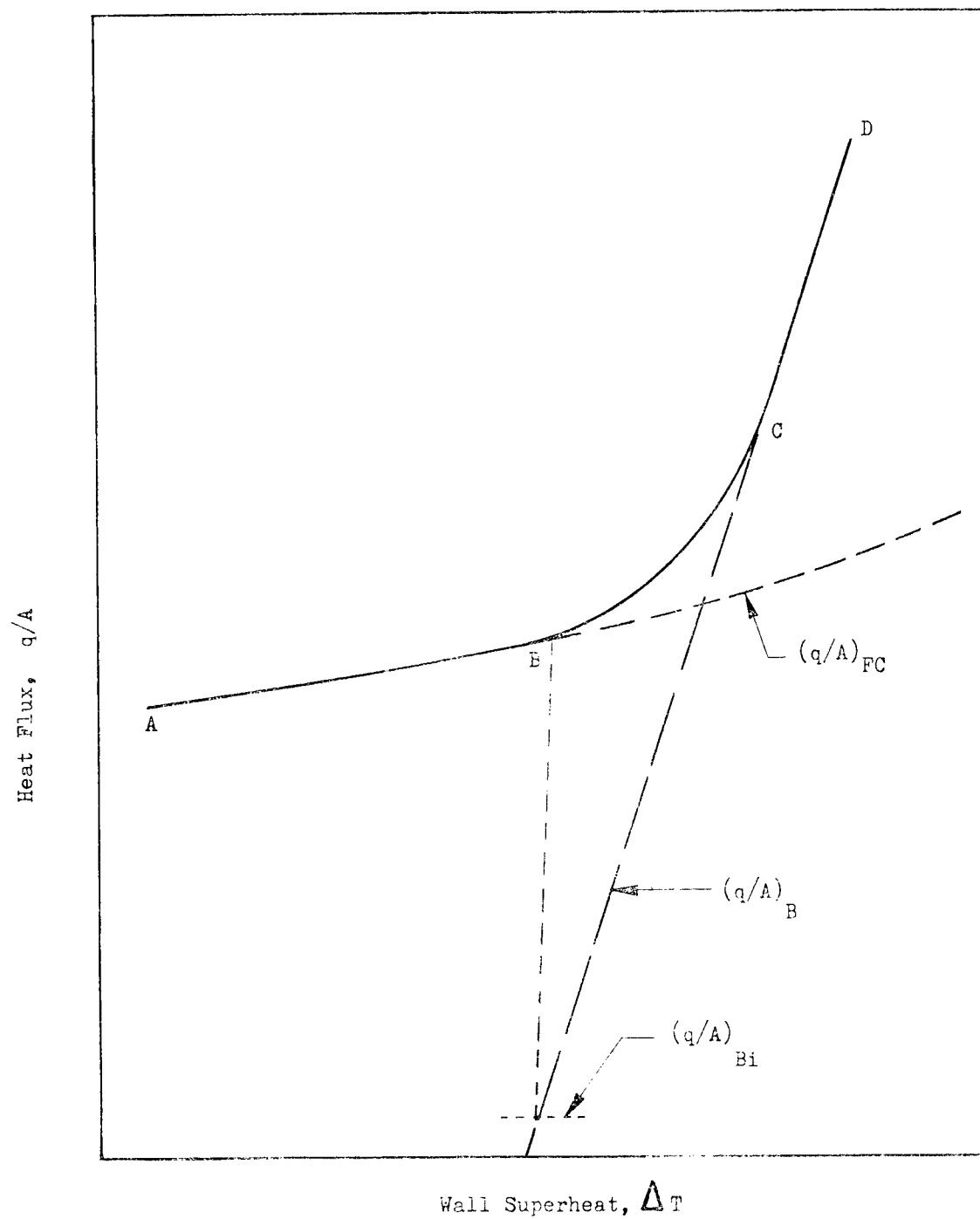


FIG. 21 TYPICAL FORCED CONVECTION SUBCOOLED NUCLEATE BOILING CURVE

The pool nucleate boiling contribution, $(q/A)_{PB}$, is calculated from Rohsenow's theory, Eq. 2. In general, as shown in Fig. 21, $(q/A)_{PB} = (q/A)_B$ is negligible at low ΔT , but becomes dominant at higher ΔT .

Nishikawa and Yamagata (Ref. 310) also recommended Eq. 57; $(q/A)_{PB}$ given by a modified form of their equation as presented in Table 6. For sub-cooled forced convection nucleate boiling, they found it necessary to account for a reduced bubble agitation effect. Accordingly, C_2 in Table 6 was modified to:

$$C_2 = \frac{512}{10} \left[\frac{(\rho_L - \rho_V) k_L T_s g}{M^2 B \rho_V \lambda} \right] \left(\frac{P}{P_{atm}} \right)^2 f \xi \quad (60)$$

Forster and Greif (Ref. 305) disagreed with the additive method given by Eq. 57. They recommended simply using their Eq. 5 in Table 5 for pool nucleate boiling as long as $(q/A)_{PB}$ is at least about 1.4 times $(q/A)_{FC}$ for a given $(T_w - T_s)$. They gave no method for obtaining the BC portion of the curve in Fig. 21. As stated by Zuber and Fried (Ref. 302), Kutateladze (Ref. 303) and Michenko (Ref. 307) also recommended just calculating (q/A) on the basis of pool nucleate boiling equations alone.

More recently, Kutateladze (Ref. 341) presented the following expression for the entire boiling curve:

$$q/A = (q/A)_{FC} \left\{ 1 + \left[\frac{(q/A)_{PB}}{(q/A)_{FC}} \right]^2 \right\}^{1/2} \quad (61)$$

From this equation it is seen that:

When $(q/A)_{PB}/(q/A)_{FC} = 0.1$, $q/A = 1.005 (q/A)_{FC}$

When $(q/A)_{PB}/(q/A)_{FC} = 10$, $q/A = 1.005 (q/A)_{PB}$

When $(q/A)_{PB} = (q/A)_{FC}$, $q/A = 1.414 (q/A)_{PB}$

This theory permits the prediction of the entire boiling curve ABCD in Fig. 21. One possible method for turbulent flow in straight, smooth, circular tubes would be to use Eq. 61 in conjunction with Eq. 4 and 59. Equations for $(q/A)_{FC}$ with other configurations are discussed by McAdams (Ref. 202).

Levy (Ref. 306) extended his method for pool nucleate boiling given in Table 6 to subcooled forced convection nucleate boiling by including the sensible heat effect giving:

$$C_2 = \left[\frac{\lambda + C_L (T_s - T_b)}{\lambda} \right] \varphi (\rho_V \lambda) \quad (62)$$

Presumably, the resulting expression for $(q/A)_{PB}$ would have to be coupled with a suitable equation for $(q/A)_{FC}$.

The most recent attempt at developing a theory for the entire boiling curve in Fig. 21 was by Bergles and Rohsenow (Ref. 339). They suggested a modification of Kutateladze's expression (Eq. 61) to a more proper incipient boiling region in the vicinity of point B in Fig. 21. Their recommended equation was:

$$q/A = (q/A)_{FC} \left\{ 1 + \left[\frac{(q/A)_B}{(q/A)_{FC}} \left(1 - \frac{(q/A)_{Bi}}{(q/A)_B} \right) \right]^2 \right\}^{1/2} \quad (63)$$

The term $(q/A)_{Bi}$ as shown in Fig. 21 is the boiling contribution to the total heat at incipient boiling. Bergles and Rohsenow showed that the $(q/A)_B$ contribution as obtained under flow conditions may not be the same as $(q/A)_{PB}$ for just pool boiling on the identical surface.

In summary, the preferred type expression for forced convection subcooled nucleate boiling includes contributions due both to ordinary forced convection without boiling and to the boiling effect. As is discussed in the next main section, little experimental data on cryogenics exists for this type of boiling.

FORCED CONVECTION SUBCOOLED NUCLEATE BOILING MAXIMUM HEAT FLUX

Forced convection nucleate boiling is also limited to a maximum heat flux and corresponding maximum ΔT . For subcooled conditions, a number of theories for estimating this maximum have been proposed. Some of these theories have been applied to noncryogenic bulk boiling under limited conditions.

Griffith (Ref. 317) extended his pool boiling theory (Eq. 27) to subcooled liquids with forced convection inside tubes by multiplying the factor Φ_1 in Table 7 by the following empirical expression. This expression corrects for both subcooling and forced convection.

$$F = 1 + 0.0144 \left[\frac{\rho_L c_L (T_s - T_b)}{\rho_V \lambda} \right] + 10^{-6} (Re_L) + 0.5 \times 10^{-3} \left[\frac{Re_L \rho_L c_L (T_s - T_b)}{\rho_V \lambda} \right]^{0.5} \quad (64)$$

$$\text{where } (Re_L) = \left(\frac{DG}{\mu_L} \right)$$

He correlated noncryogenic data with Eq. 64 for qualities from 0 to 70 percent.

Zuber and Tribus (Ref. 318) extended their pool boiling theory to subcooled liquids and, in a preliminary fashion, to forced convection flow conditions at low quality by an additive procedure to give the following equation.

$$(q/A)_{\max} = \frac{\pi}{24} \rho_V \left[\lambda + c_L (T_s - T_b) \right] \left[\frac{\sigma g_c (\rho_L - \rho_V)}{\rho_V^2} \right]^{1/4} \left[\frac{\rho_L}{\rho_L + \rho_V} \right]^{1/2} + \sqrt{\frac{2\pi f}{\alpha_L}} k_L (T_s - T_b) + \sqrt{\frac{2\pi V}{\lambda_o \alpha_L}} k_L (T_s - T_b) \quad (65)$$

where:

$$f = \frac{1}{2\pi} \left[\frac{g (\rho_L - \rho_V)}{g_c \sigma} \right]^{1/2} \left[\frac{\sigma g_c (\rho_L - \rho_V)}{\rho_V^2} \right]^{1/4} \left[\frac{\rho_L}{\rho_L + \rho_V} \right]^{1/2} \quad (66)$$

$$\lambda_o = 2\pi \left[\frac{\sigma g_c}{g (\rho_L - \rho_V)} \right]^{1/2} \quad (67)$$

Kutateladze (Ref. 342) proposed the following expression for flow in tubes to include the effects of subcooling and forced convection, presumably for low-quality conditions:

$$(q/A)_{\max} \left[\frac{\rho_V^2}{\sigma g_c (\rho_L - \rho_V)} \right]^{1/4} = 0.085 \left[V \left(\frac{\rho_L - \rho_V}{\sigma g_c} \right)^{1/4} \right]^{1/2} \left[1 + 0.057 \left(\frac{\rho_L}{\rho_V} \right)^{0.5} \frac{c_L (T_s - T_b)}{\lambda} \right] \quad (68)$$

where:

$$D > \left[\frac{\sigma g_c}{g (\rho_L - \rho_V)} \right]^{1/2}$$

Gambill (Ref. 345) proposed an additive method similar to Griffith, and Zuber and Tribus where he combined a Kutateladze-type expression for the boiling contribution and a McAdams-type expression for the forced convection contribution to obtain the following equation for low-quality conditions:

$$(q/A)_{\max} = \kappa \lambda \rho_V \left[\frac{\sigma g_c g (\rho_L - \rho_V)}{\rho_V^2} \right]^{1/4} \left[1 + \left(\frac{\rho_L}{\rho_V} \right)^{0.923} \frac{c_L (T_s - T_b)}{25 \lambda} \right] + \kappa' \left(\frac{k_L}{D} \right) \text{Re}^m \text{Pr}^n (T_w - T_b) \quad (69)$$

Typically: $\kappa = \frac{\pi}{24}$

$$\kappa' = 0.023$$

$$m = 0.8$$

$$n = 0.4$$

Gambill conducted an extensive comparison of Eq. 69 with available experimental data for the nucleate boiling maximum heat flux with flowing, subcooled, wetting liquids in the absence of net vaporization. No cryogenic data were included. For flow through tubes, he obtained an average deviation of about 19 percent with a maximum deviation of about 80 percent.

As with ordinary fluids, it would be expected that the forced convection subcooled nucleate boiling maximum heat flux for a given configuration-fluid combination would depend on the pressure, degree of subcooling, and flow velocity as typically given by Gambill's equation. The flow velocity effect, in particular, is important in permitting the absorption

of high heat fluxes. A graph for estimating the contribution of forced convection to nucleate boiling, including the maximum condition, is given in Fig. 22, where the generalized heat transfer coefficient based on Eq. 59 is plotted as a function of liquid bulk temperature for all three cryogenic fluids. That is:

$$\frac{h_{FC} D^{0.2}}{V^{0.8}} = 0.023 \left(\frac{k_L^{0.6} \rho_L^{0.8} C_L^{0.4}}{\mu_L^{0.4}} \right) = \phi(T_b) \quad (70)$$

where all properties are evaluated at the bulk temperature.

The meager cryogenic data available for the maximum heat flux are discussed in the next main section.

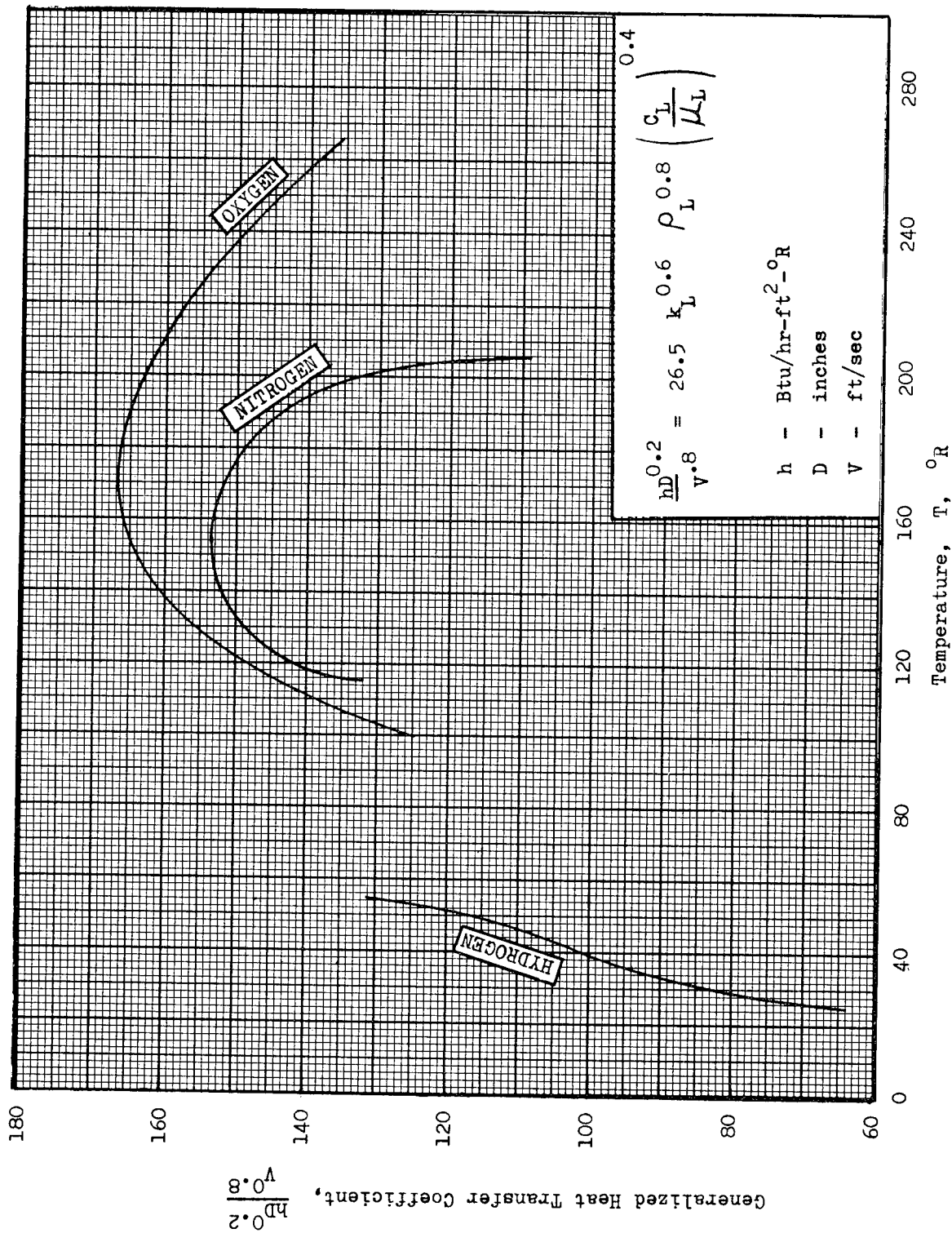


FIG. 22 GENERALIZED FORCED CONVECTION NON-BOILING HEAT TRANSFER COEFFICIENT AT SATURATED CONDITIONS

FORCED CONVECTION SATURATED BOILING

In the two previous sections, the discussion was limited to conditions of no net vaporization. If the fluid is initially saturated or if sufficient heat transfer to the bulk fluid takes place to bring it to the saturation point, then a net change of phase takes place. This may be referred to as saturated or bulk boiling.

Some effort has been devoted to the problem of bulk boiling. Unfortunately however, no general understanding has yet been obtained. In addition to dependence upon numerous variables through different possible modes of boiling (nucleate, transition, and film) the pattern of the two-phase flow profoundly affects the heat transfer rate. Chen (Ref. 346) has illustrated the flow patterns possible as heat transfer with net vaporization takes place. These flow patterns, as shown in Fig. 23, include conditions of nucleate boiling, slug flow, annular and mist flow, and liquid deficiency at the wall.

The qualitative effects of fluid quality upon the heat transfer coefficient have been discussed in considerable detail by Zuber and Fried (Ref. 302) and Collier (Ref. 347) who divide the bulk boiling phenomena into three distinct regions of boiling. Region 1 is the region of nucleate boiling in which the vapor is formed at the heating surface in the form of bubbles that grow, detach, and become dispersed in the liquid, or recondensed, depending upon the bulk conditions of the fluid. It is believed that in this region the heat transfer is governed by the mechanisms of nucleate boiling. Consequently, the equations for heat transfer in this region are similar to those for pool nucleate boiling with an additional contribution included to account for bulk velocity and its effect upon bubble motion as discussed above and given by equations such as Eq. 61 and 62.

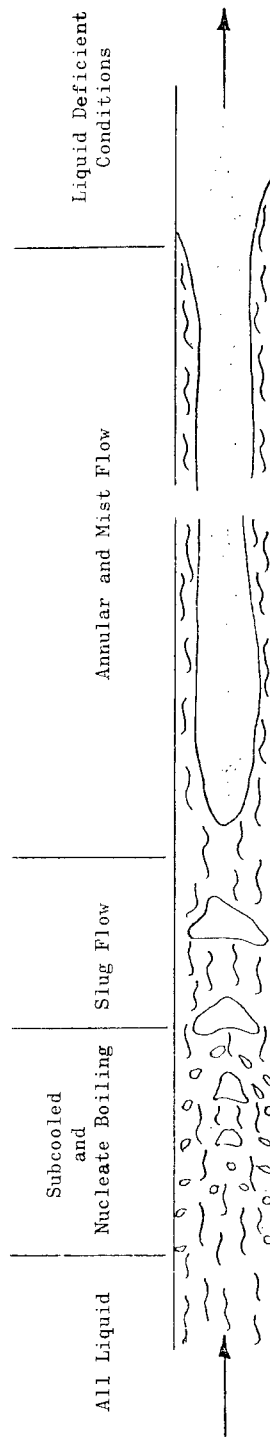


Figure 23. Flow Regimes Along Boiler

Region 2 is the forced convection region in which the slug and annular and mist regimes occur with net vaporization. Here the heat transfer coefficient increases with quality. As the quality increases along the duct, the increased velocity of the two-phase mixture may suppress the nucleate boiling process. Beyond this point, heat transfer becomes governed solely by the forced convection process. The actual flow pattern of the two-phase mixture is not exactly known. One school of thought is that only a liquid film is in contact with the surface (Ref. 348). Another is that the liquid is continuously being deposited upon and re-entrained from the heating surface (Ref. 349).

Region 3 is the liquid deficient region, in which the heat transfer coefficient decreases with increasing quality. In this region, a liquid film no longer wets the surface. Heat transfer is no longer due to a highly conducting liquid film, but rather to a poorly conducting gas. As a consequence, the heat transfer coefficient decreases sharply.

An excellent discussion of recent attempts to correlate cryogenic bulk boiling is given by Zuber and Fried (Ref. 302) and is not repeated here.

In a very recent paper, Chen (Ref. 346) made a major contribution to bulk boiling theory. He distinguished between the various flow regimes for convective flow of saturated fluids: (1) subcooled nucleate boiling, (2) slug flow, (3) annular or annular-mist flow, and (4) liquid deficient conditions as discussed above and shown in Fig. 23. For vertical, axial, stable flow at heat fluxes below the critical, he developed the following additive relation for the (no slug) annular or annular-mist flow regime which extends from about 1- to 70-percent quality. The relation is based upon the McAdams forced convection relation

(Eq. 59) corrected for the presence of vapor by the Martinelli two-phase parameter (X_{tt}) and the Forster-Zuber pool boiling expression (Eq. 4) corrected for suppression of bubble growth due to flow. Thus:

$$q/A = \left[(h_{FC}) F + h_{F-Z} S \right] \Delta T \quad (71)$$

where

h_{FC} is given by Eq. 59

h_{F-Z} is given by the following rearrangement of Eq. 4

$$h_{F-Z} = 0.00122 \frac{k_L^{0.79} c_L^{0.45} \rho_L^{0.49} g_c^{0.25} (\Delta T)^{0.24} (\Delta P)^{0.75}}{\sigma^{0.5} \mu_L^{0.29} \lambda^{0.24} \rho_V^{0.24}} \quad (72)$$

F is a two-phase correction as a function of X_{tt} given in Fig. 24. It accounts for an increase in convective turbulence due to the presence of vapor.

X_{tt} = Martinelli two-phase parameter

$$= (z/x)^{0.9} (\rho_V/\rho_L)^{0.5} (\mu_L/\mu_V)^{0.9} \quad (73)$$

S is a suppression factor as a function of $Re_L^{1.25}$ given in Fig. 25.

It accounts for the suppression of bubble growth due to flow.

$$Re_L = \frac{D G (1 - x)}{\mu_L} \quad (74)$$

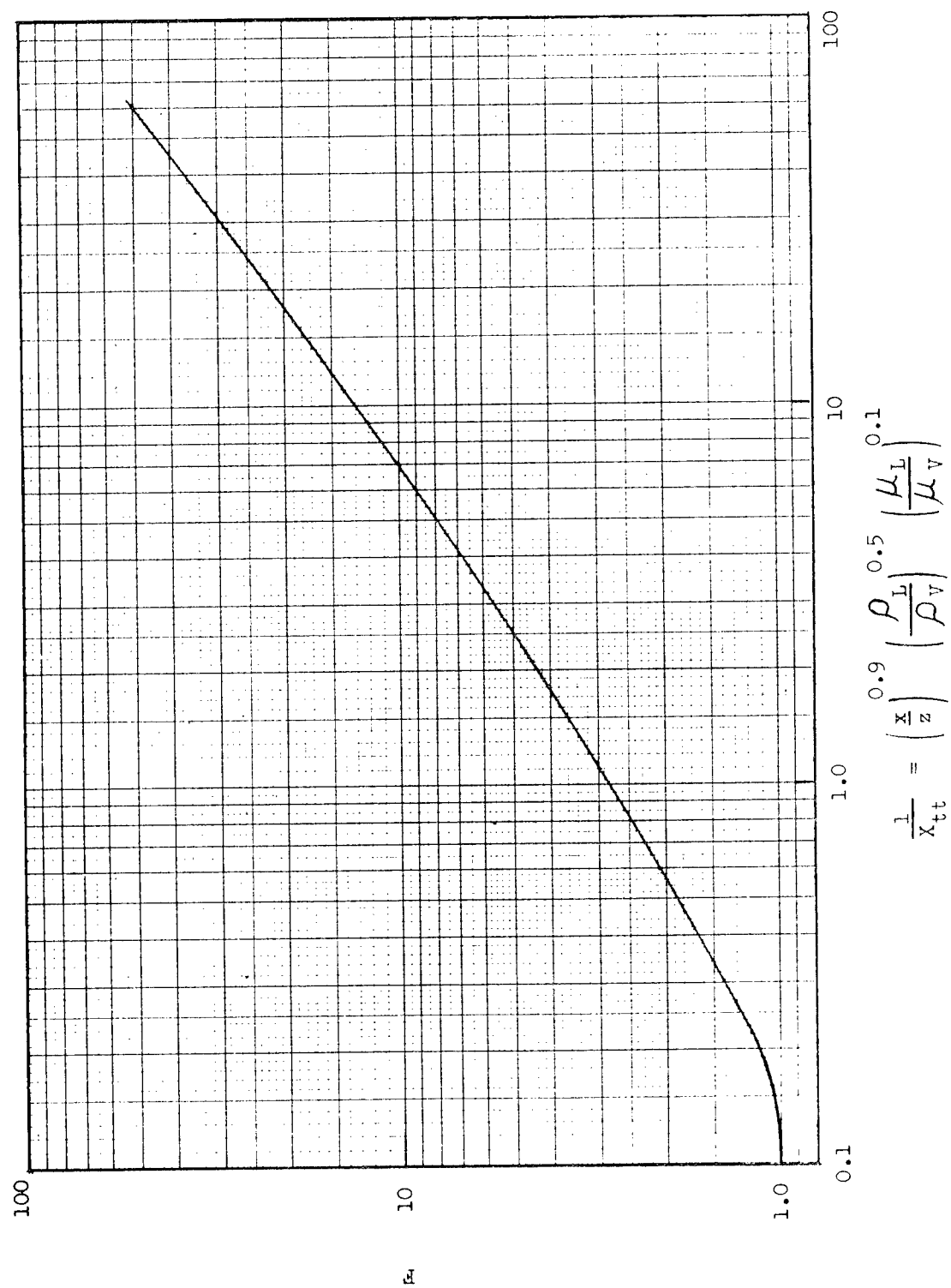
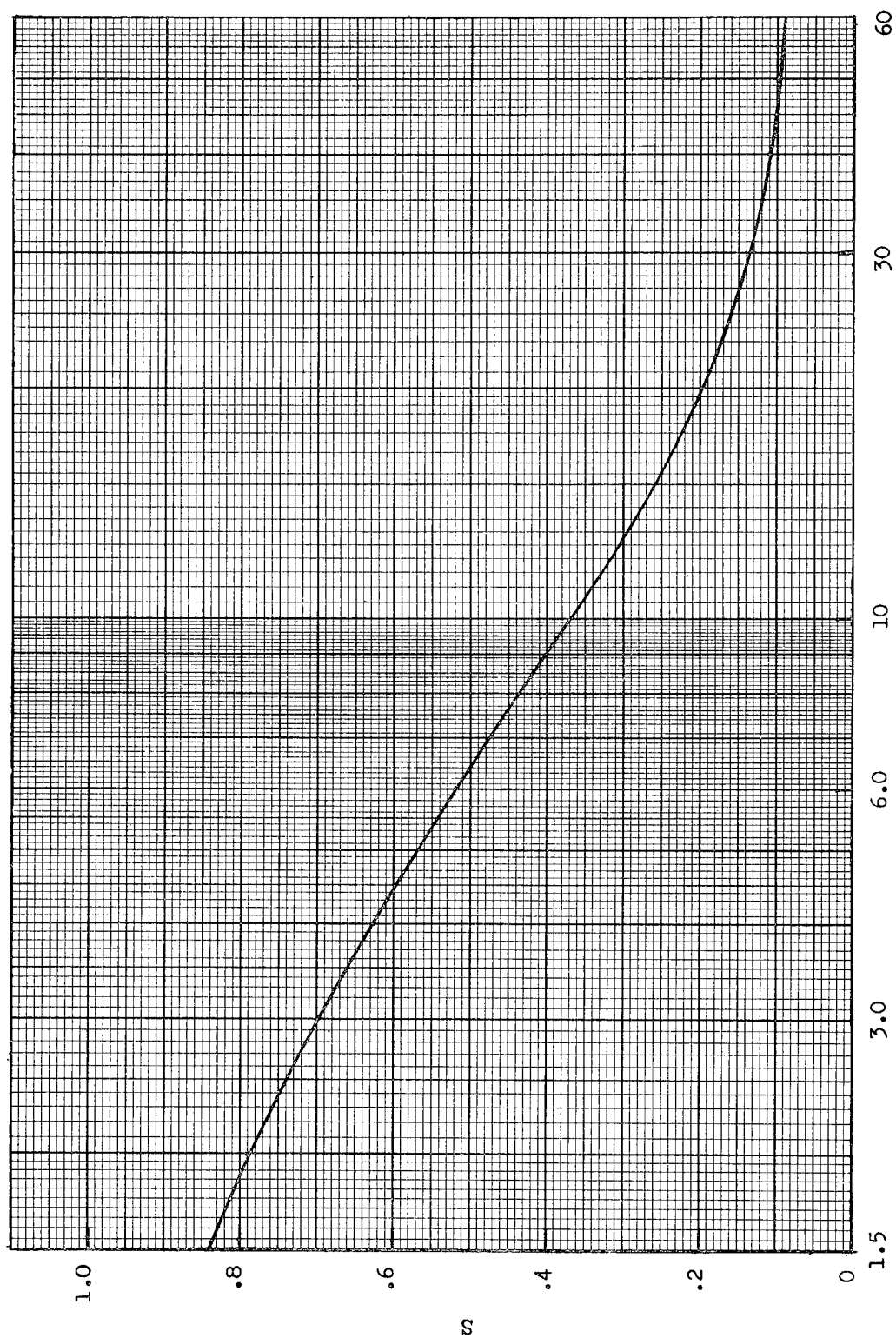


FIG. 24 REYNOLDS NUMBER FACTOR, F , OF CHEN



$(Re_L)(F)^{1.25} \times 10^{-4}$

FIG. 25 SUPPRESSION FACTOR, S , OF CHEN

Chen tested Eq. 71 against existing data for water, methanol, cyclohexane, pentane, benzene, and heptane and obtained a remarkable correlation with an average deviation of only ± 11 percent for a quality range of 1 to 71 percent. More theoretical development is required to extend Chen's theory to other flow regimes and geometric configurations.

Also of great interest in forced convection saturated boiling is the maximum heat flux. No generally applicable equations have yet been developed. The effects of the stream quality and the transition from the forced convection region to the liquid deficient regime add additional complications. An initial theoretical study of this problem has recently been presented by Chang (Ref. 322).

FORCED CONVECTION FILM BOILING

General theoretical equations for forced convection film boiling both under subcooled and saturated flow conditions have not yet been developed. A few theories for specific geometries have been presented.

Bromley et al. (Ref. 350) presented the following equations for saturated forced convection film boiling:

$$\text{For } \frac{U'}{\sqrt{g D}} < 1.0$$

$$h = 0.62 \left[\frac{k_V^2 (\rho_L - \rho_V) \rho_V g \lambda' C_L}{D (\Delta T) Pr_V} \right]^{1/4} + \frac{3}{4} h_r \quad (75)$$

For $\frac{U'}{\sqrt{g D}} > 2.0$

$$h = 2.7 \left[\frac{U' k_V \rho_V \lambda'}{D (\Delta T)} \right]^{1/2} + \frac{7}{8} h_r \quad (76)$$

where

λ' is given by Eq. 42

and values for

$$1.0 \leq \frac{U'}{\sqrt{g D}} \leq 2.0$$

may be estimated from empirical plots in Ref. 350.

Motte and Bromley (Ref. 351) later presented the following relation for subcooled film boiling:

$$\begin{aligned} h & \left[\frac{D (\Delta T)}{U' k_V \rho_V \lambda'} \right]^{1/2} - \frac{7.29}{h} \left[\frac{U' k_V \rho_V \lambda'}{D (\Delta T)} \right]^{1/2} \\ & = C (\Delta T_s) C_L \rho_i \left[\frac{U'' L}{\Delta T k_V \rho_V \lambda} \right]^{1/2} (U'' L / \mu_L)^{-0} \end{aligned} \quad (77)$$

where

C = constant

U' = incident velocity of liquid on tube

U'' = velocity of liquid in flow passage where level of turbulence is determined

Equations 75 to 77 are specific for the case of upward flow of the fluid outside of a horizontal heated tube, and have been used to obtain correlations with data from fluids such as n-heptane, carbon tetrachloride, and ethyl alcohol. These equations should not be considered as exact relations, and application to cryogenics has yet to be proved.

Cess and Sparrow (Ref. 352) obtained a numerical solution to the problem of saturated laminar film boiling with two-phase flow over a flat plate by a boundary layer analysis. A closed-form solution which approximates the exact numerical solution to about 1 percent is as follows:

$$\begin{aligned} \frac{Nu}{\sqrt{Re}} \left(\frac{\mu_V}{\mu_L} \right) \left[1 + \sqrt{\pi} \left(\frac{Nu}{\sqrt{Re}} \right) \left(\frac{\mu_V}{\mu_L} \right) \right]^{1/2} \\ = 0.5 \left[\frac{(\rho \mu)_L}{(\rho \mu)_V} \frac{C_V (\Delta T)}{\lambda (Pr)_V} \right]^{-1/2} \end{aligned} \quad (78)$$

No experimental data were presented for comparison, and the assumptions necessary for the solution limit the applicability. Cess and Sparrow (Ref. 353) also extended the above case to subcooled conditions but only obtained numerical solutions.

EXPERIMENTAL DATA

In the previous section the various theoretical correlations for predicting boiling heat transfer were reviewed. In most cases, specific theoretical calculations for the three cryogenic fluids of interest were carried out and graphical results were presented. In this section, the available experimental cryogenic boiling data from the 74 references listed in the Experimental Data Bibliography are discussed and compared with the theoretical correlations.

POOL BOILING

Experimental data for pool boiling of H_2 , N_2 , and O_2 are presented in Fig. 26, 27, and 28, respectively, as heat flux vs ΔT . The numbers in parentheses are the Bibliography reference numbers. The operating pressures are also stated. For a given reference, additional labeling of the curves is given where more than one geometric configuration was tested. Both nucleate and stable film boiling data are included. In some cases, the lower end of the nucleate boiling curves correspond to the natural convection region. Observed values of the pool nucleate boiling maximum heat flux are indicated by a circle symbol at the upper terminus of the corresponding nucleate boiling curve. Observed values of the pool film boiling minimum heat flux, where available, are indicated by a square symbol at the lower terminus of the corresponding film boiling curve. In general, the curves plotted in Fig. 26, 27, and 28 are the respective authors' correlating lines for their own data. Data covering unusual conditions such as greased or roughened surfaces and zero-gravity are not plotted in these figures but are discussed in the Conclusions section below.

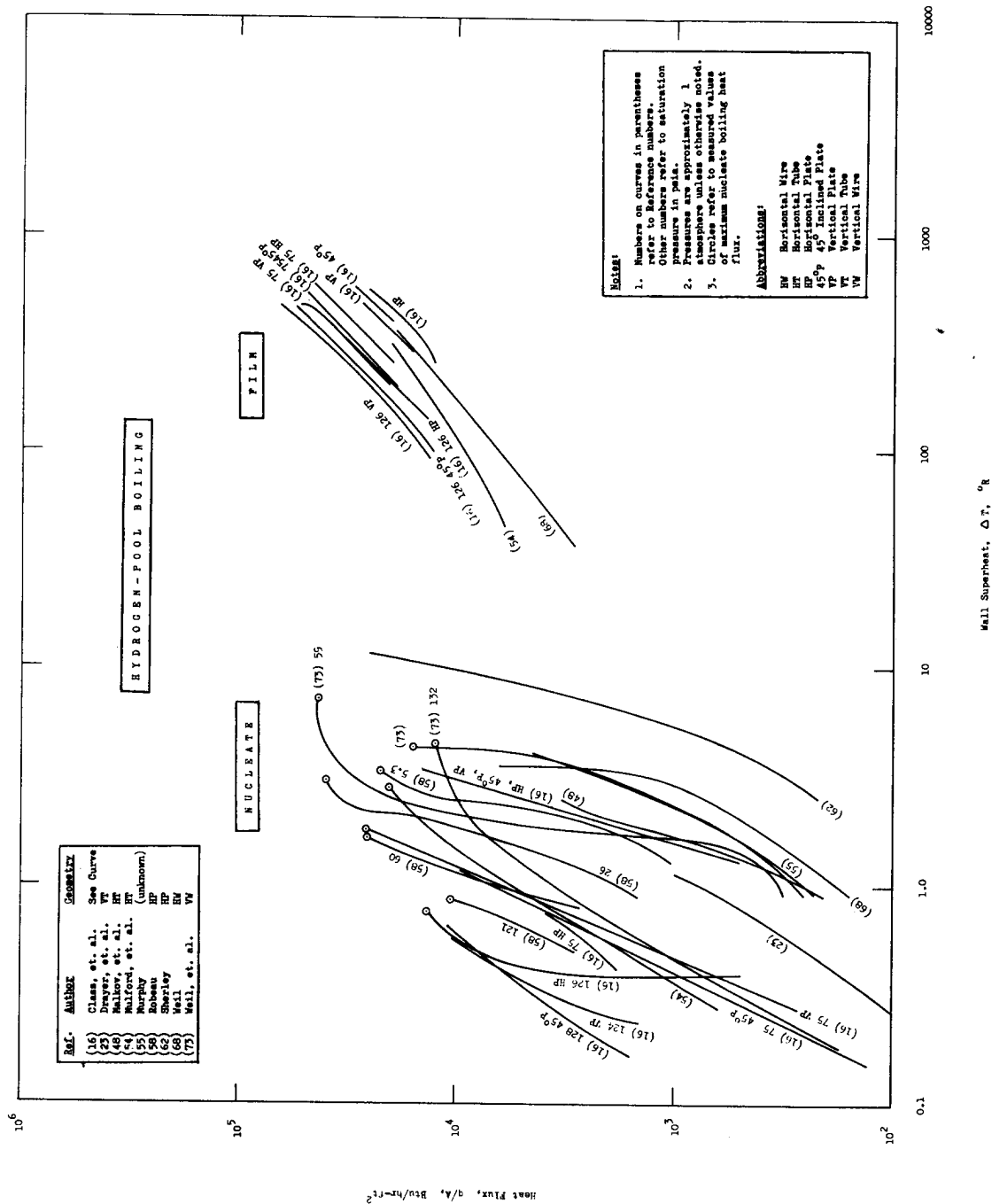


Figure 26. Experimental Pool Boiling Data for Hydrogen

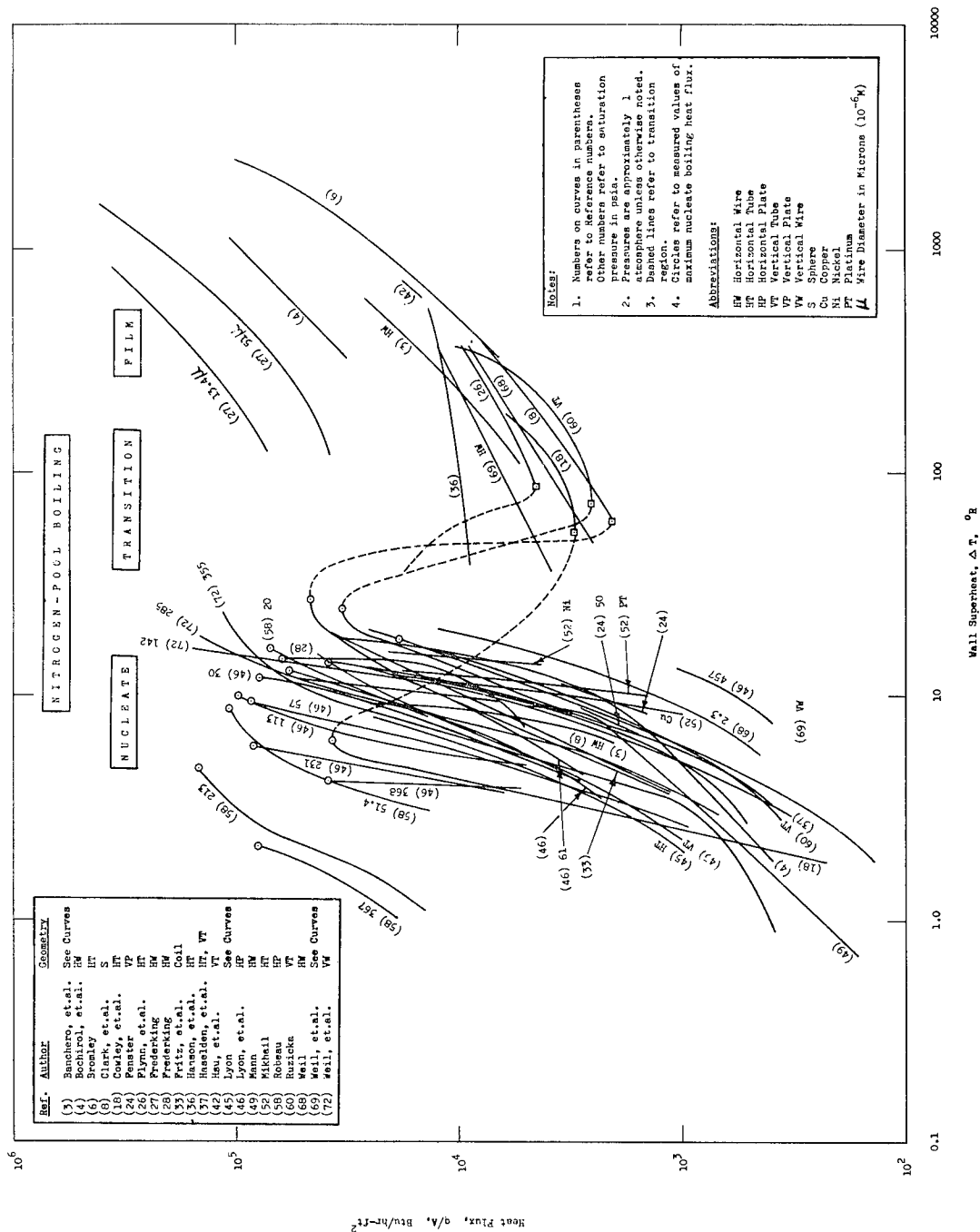


Figure 27. Experimental Pool Boiling Data for Nitrogen

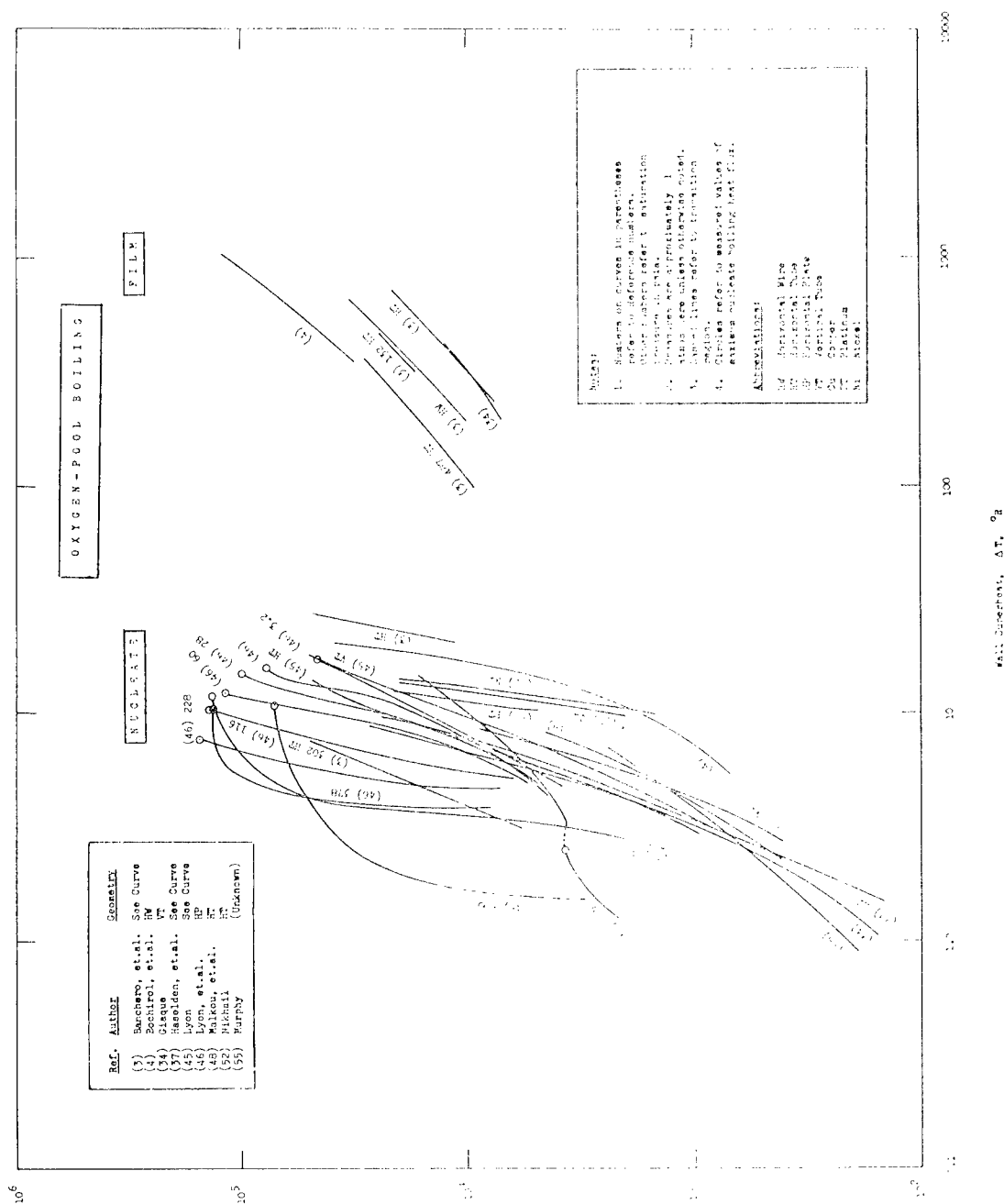


Figure 28. Experimental Pool Boiling Data for Oxygen

Hydrogen

The experimental data for hydrogen, as plotted in Fig. 26, cover the following references: 1, 15, 16, 22, 23, 48, 54, 55, 56, 58, 62, 68, 70, and 73.

As shown, the nucleate boiling data of various investigators for a variety of geometric shapes at a pressure of about 14.7 psia (11.5 to 14.7) cover a considerable span of ΔT . For example, a heat flux of 1000 Btu/hr-sq ft was obtained at a ΔT of about 0.5 R by Mulford, et al. (Ref. 54) for a horizontal cylinder, and at a ΔT of about 5.0 R by Sherley (Ref. 62) for a horizontal flat plate. This span is plotted as dashed lines for comparison to the theoretical predictions in Fig. 4. The span encompasses all the theoretical predictions except that of Nishikawa and Yamagata, which appears to be in poor agreement with the other theories. From the data of Class, et al. (Ref. 16) at 12.0 psia, the effect of surface orientation is negligible. However, surface orientation is seen to assume some importance at higher pressures. The data of Class, et al. (Ref. 16), Roubeau (Ref. 58), and Weil, et al. (Ref. 73) indicate that for a given ΔT , the effect of increasing pressure is to increase the heat flux as long as the maximum is not approached. This is in agreement with the trend of theoretical prediction shown in Fig. 7 where the Forster and Zuber equation is plotted for three different pressures.

The data for the maximum heat flux as shown in Fig. 26 cover a range from about 10,000 to 43,000 Btu/hr-sq ft depending mainly on pressure. These data are compared to theoretical predictions in Fig. 12. The data appear to scatter. At the highest pressures, the data all fall somewhat below all the theories.

The experimental results for stable film boiling of hydrogen as shown in Fig. 26 include several geometric shapes including wires, cylinders, and plates. The plate data cover a range of pressure. As predicted theoretically in Fig. 18, the film boiling heat flux shown in Fig. 26 does increase somewhat with increasing pressure. The data of Mulford, et al. (Ref. 54) for a horizontal cylinder are included as a dashed line in Fig. 18 for comparison to Bromley's theory. Under Mulford's conditions, the radiation effect was negligible. Somewhat higher experimental values were obtained than were predicted theoretically. Class, et al. (Ref. 16) reported a similar difference when comparing their data with Bromley's theory. In general, for a plate, the data of Class, et al. (Ref. 16) show that the effect of going from a horizontal to a vertical orientation is to increase the heat flux for a given ΔT . No experimental pool film boiling minimum heat flux values are available for comparison to theory.

Nitrogen

The experimental data for pool boiling of nitrogen as plotted in Fig. 27 cover the following references: 2, 3, 4, 5, 6, 7, 8, 9, 10, 11, 12, 13, 14, 18, 24, 25, 26, 27, 28, 29, 30, 31, 32, 36, 37, 41, 42, 45, 46, 47, 49, 50, 51, 52, 58, 60, 61, 68, 69, 71, and 72.

As is evident from the above list and from a comparison of Fig. 26, 27, and 28, the pool boiling of nitrogen has been studied more extensively than either hydrogen or oxygen.

Compared to hydrogen, the nucleate boiling data of various investigators for nitrogen at essentially 14.7 psia cover a much narrower span on the log ΔT scale. At a heat flux of 1000 Btu/hr-sq ft, the ΔT for nitrogen

is greater than for hydrogen. It varies from a value of about 2.5 R from the data of Cowley (Ref. 18) for a horizontal cylinder, to a value of about 6 R from the data of Ruzicka (Ref. 60) for a vertical cylinder. This span is plotted as dashed lines for comparison to the theoretical predictions in Fig. 5. The span encompasses all the theoretical correlations with the exception of the equations of Kutateladze, Chang and Snyder, and Nishikawa and Yamagata. Based on the data of Lyon (Ref. 45), the heat flux for a given ΔT is somewhat higher for a horizontal surface compared to a vertical surface. The data of Lyon, et al. (Ref. 46), Roubeau (Ref. 58), and Weil, et al. (Ref. 72) indicate that, in general, the effect of increasing pressure is to increase the heat flux for a given ΔT . As with the other cryogenics, this is in agreement with the trend of the theoretical prediction as shown in Fig. 8 for nitrogen where the Forster and Zuber equation is plotted for three different pressures.

The experimental values for the maximum heat flux over a wide range of pressure are compared to theoretical predictions in Fig. 13. The data at a pressure of about 14.7 psia vary over a very wide range from about 18,500 Btu/hr-sq ft from the data of Flynn, et al. (Ref. 26) for a horizontal cylinder, to 61,000 Btu/hr-sq ft from the data of Frederking (Ref. 28) for a horizontal wire. In addition, over the entire range of pressure, the data of Roubeau (Ref. 58) for a horizontal plate differ markedly from the data of Lyon, et al. (Ref. 46) for the same geometrical condition.

Four data points for the minimum heat flux at atmospheric pressure are compared to theoretical predictions in Fig. 16. Again, a considerable spread in the data is evident. For the most part, however, the data are in the range of the theories.

The experimental data for stable film boiling of nitrogen as shown in Fig. 27, dramatically illustrate the large effect of cylinder diameter in going from the 0.350-inch-diameter cylinder of Bromley (Ref. 6) to the 13.4-micron-diameter wire of Frederking (Ref. 27). The atmospheric pressure data of Bromley are compared with theory in Fig. 19. Excellent agreement is obtained for $\Delta T < 1000$ R. At higher ΔT values, the data deviate because of the rapidly increasing contribution of radiation to the over-all heat transfer.

Oxygen

The pool boiling experimental data for oxygen as plotted in Fig. 28 cover the following references: 2, 3, 4, 34, 37, 45, 46, 47, 48, 52, and 59.

Compared to the hydrogen data shown in Fig. 26, the nucleate boiling data of various investigators for oxygen at a pressure of about 14.7 psia cover a considerably narrower span on the log ΔT scale. At a heat flux of 1000 Btu/hr-sq ft, the ΔT for oxygen is greater than for hydrogen and just slightly greater than for nitrogen, as predicted by all theories. It varies from a value of about 3 R from the data of Lyon (Ref. 45) for a horizontal cylinder, to a value of about 7 R from the data of Bochirol, et al. (Ref. 4) for a horizontal wire. This span is plotted as dashed lines for comparison to the theoretical predictions in Fig. 6. As with nitrogen, the span encompasses all the theoretical correlations with the exception of the equations of Kutateladze, Chang and Snyder, and Nishikawa and Yamagata. Based on the data of Lyon (Ref. 45) and Haselten, et al. (Ref. 37), the heat flux for a given ΔT is somewhat higher for a horizontal surface compared to a vertical surface. The data of Lyon, et al. (Ref. 46) indicate that, in general, the effect of

increasing pressure is to increase the heat flux for a given ΔT . As with the other cryogenics, this is in agreement with the trend of the theoretical prediction as shown in Fig. 9 for oxygen where the Forster and Zuber equation is plotted for three different pressures.

The experimental data of Lyon, et al. (Ref. 45 and 46) for the maximum heat flux over a wide range of pressure, are compared to theoretical predictions in Fig. 14. The data cover a range of about 45,000 to 150,000 Btu/hr-sq ft. These values are considerably higher than for hydrogen and somewhat higher than for nitrogen. As with hydrogen and nitrogen at high pressures, a sharper decrease in maximum heat flux is experienced than is predicted.

The experimental results for stable film boiling of oxygen as shown in Fig. 28 include data on wires and cylinders. As previously discussed, the film boiling heat flux increases somewhat with increasing pressure as shown by the horizontal cylinder data of Banchero, et al. (Ref. 3). The data for the two extreme pressures are shown as dashed lines in Fig. 20 for comparison to Bromley's theory. Again, the radiation contribution is negligible over the range of the experimental data. The agreement is quite good. As discussed above, however, a diameter correction is required to correlate wire data. No experimental data for the minimum heat flux are available.

SUBCOOLED FORCED CONVECTION BOILING

The available experimental data for subcooled forced convection boiling are presented in Fig. 29. The heat flux is plotted against $(T_w - T_b)$ rather than $\Delta T = T_w - T_s$, because in general, T_b was more well defined in the experiments than T_s . As discussed above, however, the use of ΔT is preferred for generalized correlation.

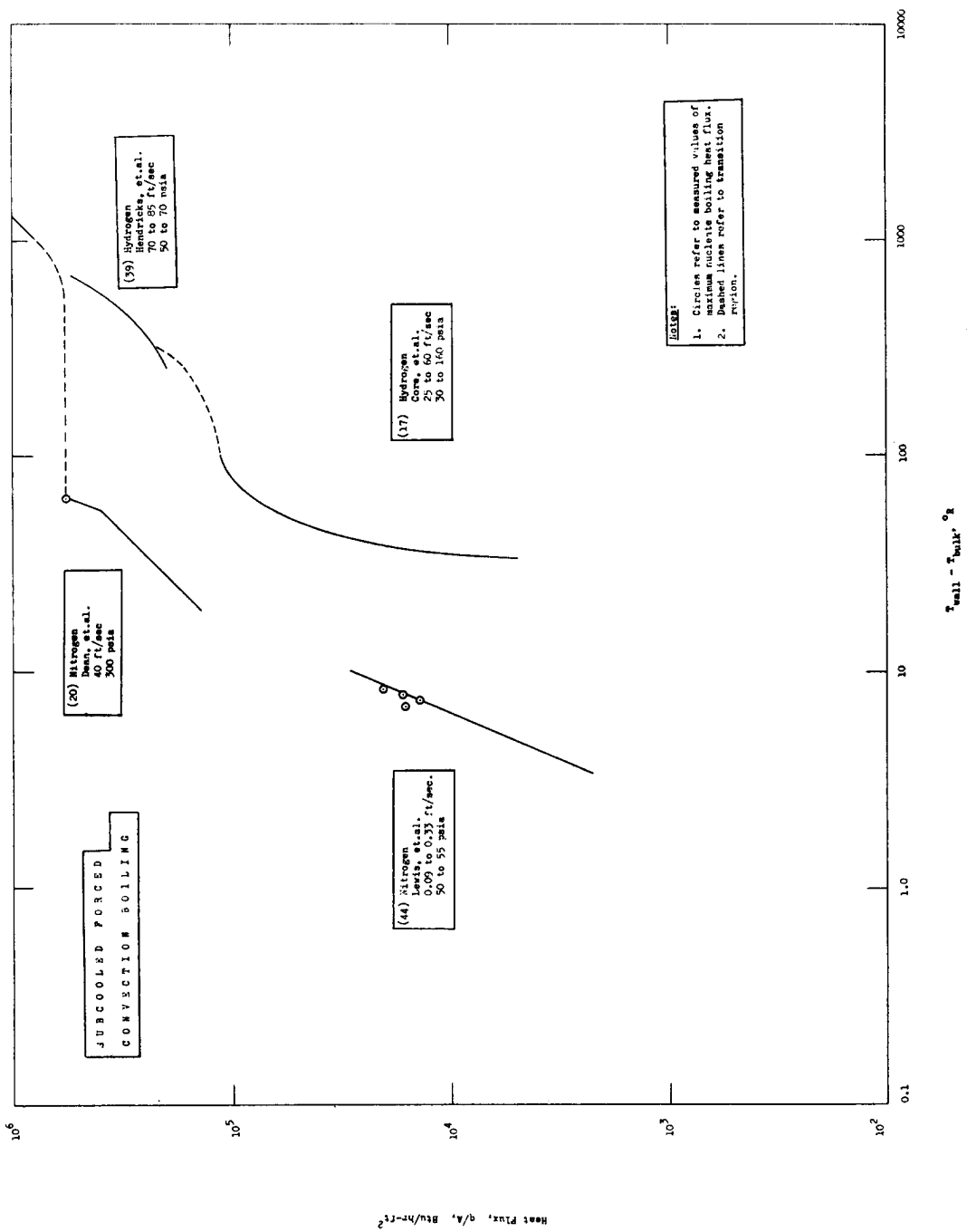


Figure 29. Experimental Subcooled Forced Convection Boiling Data

Data for both hydrogen and nitrogen are included. No oxygen data are available. The data cover the following references: 17, 20, 21, 39, and 44. References 17, 39, and 44 also included bulk boiling data which are discussed in the next section. The numbers in parentheses refer to the Bibliography reference numbers. Other pertinent data such as velocity range, pressure range, geometry, and orientation are also included in Fig. 29. Although the experimental information is quite meager, the nonboiling, nucleate boiling, transition, and film boiling regions are all included to at least some extent. In addition, some observed values of the forced convection subcooled nucleate boiling maximum heat flux are indicated by circles at or near the upper terminus of the corresponding nucleate boiling curve.

In most cases, the curves plotted in Fig. 29 are the authors' correlating lines for their own data. With the exception of Ref. 20 and 21, saturated forced convection data were also obtained in the respective studies, but the curves shown in Fig. 29 represent subcooled data only. The saturated or bulk boiling data are discussed in the next section.

The data of Lewis, et al. (Ref. 44) as shown in Fig. 29 are for the nucleate boiling of nitrogen flowing upward inside a vertical circular tube having an inside diameter of 0.555 inch. The degree of subcooling was less than 5 R and both the pressures and flow velocities were relatively low. At these conditions, the contribution of forced convection to the total heat flux as given in Eq. 58, 59, and 61, and as estimated from Fig. 22 (assuming turbulent flow), is less than 1000 Btu/hr-sq ft. This is much less than the lowest heat flux shown for the Lewis data. Thus, the forced convection process is strongly dominated by nucleate boiling. As would be expected, therefore, the Lewis heat flux curve

for N_2 shown in Fig. 29 agrees closely with the low pressure pool boiling curves for nitrogen shown in Fig. 27. Several values of Lewis' are also shown in Fig. 29 for the maximum nucleate boiling heat flux. Again, for the low velocities studied, the forced convection contribution to the maximum heat flux as given by Eq. 69 is relatively small. Comparison of these maximum heat flux points with similar pool boiling data in Fig. 27 shows fairly good agreement; the Lewis values appearing to be generally somewhat low. Lewis, et al. also obtained some hydrogen data, but did not consider the temperature measurements to be of sufficient accuracy to warrant any correlation.

The data of Dean, et al. (Ref. 20 and 21) as shown in Fig. 29 are for nitrogen flowing through a vertical annulus with an equivalent diameter $(D_o - D_i)$ of 0.138 inch. The data cover the entire region from nonboiling to film boiling. The degree of subcooling was of the order of 50 to 60 F at a pressure of 300 psia and a relatively high flow velocity of 40 ft/sec. For the nucleate boiling region at these conditions, the contribution of forced convection to the heat flux may be estimated from Fig. 22 by using the equivalent diameter and modifying the ordinate as recommended for an annulus by Wiegand as given in McAdams (Ref. 202). Thus, the ordinate in Fig. 22 becomes:

$$\frac{h D^{0.2}}{V^{0.8}} \left(\frac{D_i}{D_o} \right)^{0.45}$$

where in this case, $D_i = 0.01568$ ft and $D_o = 0.02717$ ft. A value of $(q/A)_{FC}$ of the order of 350,000 is accordingly estimated for $T_w - T_b = 60$ R. This is of the order of the experimental nonboiling and nucleate boiling results of Dean as shown in Fig. 29. At this relatively high velocity, the contribution of forced convection to the total heat flux

is very significant. The nucleate boiling contribution to the total heat flux is difficult to estimate because of experimental uncertainty as to the $T_w - T_s$ values. However, for a pressure of 300 psia, the maximum pool nucleate boiling heat flux for nitrogen as estimated from Fig. 13 is of the order of 100,000 Btu/hr-sq ft. The contribution due to subcooling is estimated from Eq. 69 to be about 15,000 Btu/hr-sq ft. Thus, the total estimated heat flux in the region of the maximum is about 465,000 Btu/hr-sq ft. This is in fairly good agreement with the data. The results of Dean also extend into the film boiling region where no suitable theoretical correlation is available for comparison. Compared to the pool film boiling data of Fig. 27, however, it is evident that a significant effect of forced convection exists. In summary, comparison of the forced convection results of Dean, et al. in Fig. 29 with pool boiling results in Fig. 27 shows that, as predicted by theory, the application of forced convection in conjunction with the boiling process permits the attainment of much higher heat fluxes than are possible with pool boiling only.

The data of Core, et al. (Ref. 17) as shown in Fig. 29 are for hydrogen flowing through a vertical circular tube with an inside diameter of 0.1675 inch. The data cover a region from nucleate to film boiling. The degree of subcooling was as high as approximately 15 F. The pressure was varied from about 30 to 160 psia and the velocity from about 25 to 60 ft/sec. At Core's operating conditions, the contribution of forced convection to the heat flux is estimated from Fig. 22 to vary from about 50,000 to 200,000 Btu/hr-sq ft over the range of pressure, velocity, and $T_w - T_b$ studied. In general, as seen in Fig. 29, this range of heat flux values appears to be higher than measured by Core, et al. for the nucleate boiling region. The apparent failure of Eq. 70 and Fig. 22 in this case

to satisfactorily predict $(q/A)_{FC}$ may be due to the well-known difficulty of making estimations for liquids in the vicinity of the critical temperature, especially when the wall temperature is above the critical, as was the case here. In this region, physical properties can change drastically and the choice of the bulk temperature to evaluate physical properties is very uncertain. Again, it is difficult to estimate the nucleate boiling contribution to the heat flux, but the maximum values for pool boiling as seen in Fig. 12 and 26 vary from about 15,000 to 40,000 Btu/hr-sq ft, depending on the pressure. These values are in the lower range of Core's data. Thus, it appears probable that both nucleate boiling and forced convection were contributing to the over-all heat flux.

The data of Hendricks, et al. (Ref. 39) as shown in Fig. 29 are for hydrogen flowing through a vertical circular tube with an inside diameter of 0.313 inch. The subcooled data cover only the film boiling region. The degree of subcooling was less than about 5 F. The pressure was varied from about 50 to 70 psia and the velocity from about 70 to 85 ft/sec. Compared to the pool film boiling data shown in Fig. 26, much higher heat fluxes were obtained by Hendricks with forced convection for a given temperature difference. The data of Core in the film boiling region are in approximate agreement with that of Hendricks.

SATURATED FORCED CONVECTION BOILING

Experimental data for the saturated forced convection boiling of hydrogen, nitrogen, and oxygen are covered in the following references: 17, 35, 39, 43, 44, 53, 57, 63, 66, 67, and 74. As discussed above, this area of cryogenic boiling is considerably more complicated than the areas of pool boiling or subcooled forced convection boiling. Compared to the

latter, at least two additional variables must be considered in saturated forced convection boiling. These are quality of the flowing stream and type of flow regime. Because of the large number of parameters involved, and the general lack of sufficient study of each variable independently, the data are not plotted as heat flux vs temperature here. Instead, the ranges of parameters covered in the various investigations are summarized in Table 9 and the findings are discussed.

Core, et al. (Ref. 17) obtained data for hydrogen at relatively high velocities over a wide range of pressure and quality. Their data covered a wide range of boiling conditions. Data in the nucleate regime were obtained at surprisingly high values of $T_w - T_b$ (50 to 100 R). Heat fluxes as high as 3,100,000 Btu/hr-sq ft were achieved in the film boiling region.

Hendricks, et al. (Ref. 35 and 39) also obtained data for hydrogen at relatively high velocities over a wide range of pressure and quality. However, they covered only the film boiling region. Heat fluxes as high as 520,000 Btu/hr-sq ft were obtained.

Jones, et al. (Ref. 43) studied heat transfer to saturated nitrogen at relatively low velocities in a very long 0.43-inch-ID horizontal circular tube. They determined the critical quality corresponding to the point at which the heat transfer coefficient drops off sharply due, presumably to transition to the liquid deficient region shown in Fig. 23 and discussed above. Heat fluxes to about 4500 Btu/hr-sq ft were measured. The critical quality varied from 80 to 99 percent, depending on heat flux and flowrate.

TABLE 9

SATURATED FORCED CONVECTION BOILING EXPERIMENTS

| Ref. No. | Authors | Fluid(s) | Inlet Pressure, psia | Inlet Velocity, ft/sec | Exit Quality, Weight Percent Vapor | Type of Boiling |
|----------|--------------------|--------------------------|----------------------|-----------------------------|------------------------------------|--------------------------------------|
| 17 | Core, et al. | Hydrogen | 28 to 184 | 20 to 60 | 0 to 100 | Nucleate, Transition, and Film |
| 35, 39 | Hendricks, et al. | Hydrogen | 27 to 72 | 40 to 84 | 9 to 90 | Film |
| 43 | Jones, et al. | Nitrogen | 15 to 20 | 0.22 to 0.76 | 77 to 99 | Maximum Nucleate |
| 44, 66 | Lewis, et al. | { Hydrogen { Nitrogen | 30 to 74 47 to 56 | 0.20 to 1.2 0.09 to 0.33 | 0 to 100 0 to 100 | Nucleate, Maximum Nucleate, and Film |
| 53 | Monroe, et al. | { Nitrogen { Oxygen | 15 15 | 0.24 0.17 | - - - | Transition |
| 57 | Richards, et al. | { Hydrogen { Nitrogen | 15 to 25 15 to 25 | 3.6 to 37 1.1 to 6.2 | 5 to 30 10 to 26 | Maximum Nucleate |
| 63 | Sydoriak, et al. | { Hydrogen { Nitrogen | - - - | - - - | 46 to 52 23 to 38 | Maximum Nucleate |
| 67, 74 | Wright and Walters | Hydrogen | 20 to 40 | 20 to 55 | 2.4 to, 23 | Nucleate and Film |

Lewis, et al. (Ref. 44 and 66) conducted tests with both hydrogen and nitrogen at relatively low velocities. They also concentrated on determining the critical quality and corresponding maximum heat flux, but over a somewhat wider range of variables than Jones, et al. With hydrogen, they achieved maximum nucleate boiling heat fluxes up to 25,000 Btu/hr-sq ft over a wide range of critical quality. With nitrogen, maximum nucleate boiling heat fluxes to 26,000 Btu/hr-sq ft were achieved over a wide range of quality. Data in the film boiling region downstream of the transition point were obtained at heat fluxes up to 40,000 Btu/hr-sq ft with both cryogenic fluids.

The data presented by Monroe, et al. (Ref. 53) cover only the transition region for oxygen and nitrogen flowing in a vertical tube with an inside diameter of 0.5 inch at very low velocity and low pressure. The data of Richards, et al. (Ref. 57) and Sydoriak, et al. (Ref. 63) present data for the maximum nucleate boiling heat flux of nitrogen and hydrogen for flow through vertical annuli at moderate velocities to relatively high velocities. Critical heat fluxes up to about 38,000 Btu/hr-sq ft were achieved.

The data of Wright and Walters (Ref. 67 and 74) are for hydrogen flowing in a horizontal tube with an inside diameter of 0.25 inch. A moderate pressure range was covered at relatively high velocities. Only low exit quality values were obtained. Under these limited conditions, a satisfactory correlation of the data was obtained for both the nucleate and film boiling regions. The use of relatively high velocities resulted in heat fluxes as high as 123,000 Btu/hr-sq ft for the film boiling region.

CONCLUSIONS

Based on the experimental information contained in the literature surveyed during this study, and the comparisons made with theoretical predictions, as discussed in the previous section, the following conclusions may be drawn concerning heat transfer to boiling hydrogen, nitrogen, and oxygen.

POOL NUCLEATE BOILING

Data at Atmospheric Pressure

A considerable quantity of pool nucleate boiling experimental data has been obtained for all three cryogenic fluids at atmospheric pressure. In general, as with other fluids, the heat flux increases rapidly with increasing ΔT . The data cannot be correlated by a single line, but cover a relatively wide range of ΔT for a given heat flux. The spread is attributed primarily to effects of surface condition, and surface geometry and orientation. In general, hydrogen boils at much lower values of ΔT than nitrogen or oxygen. Nitrogen may boil at slightly lower values of ΔT than oxygen. This is consistent with the trends predicted by theory.

Surface Roughness and Orientation

Based on the experimental data of Ref. 15, 45, and 52 covering all three cryogenic fluids, a profound effect of surface roughness on pool nucleate boiling exists. In general, when a smooth or polished surface is roughened, the required ΔT for a given nucleate boiling heat flux is reduced.

Because of the large effect of surface roughness, detailed comparisons and firm conclusions for different geometrical shapes are not possible. The experimental data of Ref. 49 and 60 for nitrogen do indicate little effect of diameter for tubes and wires on the nucleate boiling heat flux, except at low heat flux values where natural convection may be predominant. The effect of surface orientation is somewhat uncertain. The data of Ref. 15 for H_2 indicate a negligible effect on the ΔT for a plate in going from a vertical to a horizontal orientation. On the other hand, the data of Ref. 37 and 45 for nitrogen and oxygen indicate that, in general, the required ΔT for a given nucleate boiling heat flux with a cylinder is decreased in going from a vertical to a horizontal orientation.

Comparison of Theories With Data

In general, the pool nucleate boiling theories summarized in Tables 5 and 6 do not consider the nature, geometry, or orientation of the heater surface. Comparison of the theories with data at atmospheric pressure indicates that the correlations of Rohsenow, Forster and Zuber, Forster and Greif, Levy, Michenko, and Laboutzov fall within the spread of the experimental data.

Increasing Pressure

For a given fluid-heater combination, sufficient experimental data are available to show that the effect of increasing pressure is to decrease the required ΔT for a given pool nucleate boiling heat flux. This is in agreement with the trends predicted by the pool nucleate boiling theories such as that of Forster and Zuber.

Effect of Gravity

As shown both by the experimental data of Sherley (Ref. 62) for hydrogen and Clark, et al. (Ref. 8) for nitrogen, the effect of both very low and high gravity on the nucleate boiling heat flux is practically negligible. As explained by Clark, this is probably due to the relatively high bubble Froude numbers (ratio of inertial to gravitational force) for cryogenic fluids.

Greased or Coated Surface

The experimental data of Ref. 15 and 45 show that the required ΔT may be increased significantly for a given nucleate boiling heat flux if the surface is greased or coated with a glossy film. This is most pronounced for a horizontal orientation of the surface.

POOL NUCLEATE BOILING MAXIMUM HEAT FLUX

Effect of Pressure

Some experimental data on the pool nucleate boiling maximum heat flux are available for all three cryogenic fluids over a wide range of pressure. In general, as with other fluids, the maximum heat flux curve goes through a peak value at a pressure somewhat less than 50 percent of the critical pressure. For a given fluid, the data cannot be correlated by a single line, but instead cover a range of maximum heat flux for a given pressure. No satisfactory explanation exists for the spread of the data. In general, at a given reduced pressure, P/P_c , the maximum

heat flux of hydrogen is considerably lower than for nitrogen and oxygen. Somewhat higher maximum heat fluxes can be achieved with oxygen as compared to nitrogen. This is consistent with the trends predicted by theory.

Surface Roughness and Orientation

Based on the experimental data of Ref. 15, 45, and 54 covering all three cryogenic fluids, the effect of surface roughness on the maximum heat flux is small or negligible. If the surface is greased, however, the data of Ref. 15 for hydrogen show that the maximum heat flux can be increased by from 50- to 100-percent, depending on surface orientation. The data of Ref. 45 for nitrogen and oxygen also show some increase in the maximum heat flux when the surface is coated with a glossy film. The data of Ref. 45 further show that a higher maximum heat flux can be achieved with a vertical surface than with a horizontal surface. This is in disagreement with the opposite prediction of the equations of Chang (Ref. 322).

Comparison of Theories With Data

In general, the pool nucleate boiling maximum heat flux theories summarized in Table 7 do not consider the geometry or orientation of the heater surface. Comparison of the theories with experimental data as shown in Fig. 12, 13, and 14 shows that the equations of Rohsenow and Griffith, Zuber and Tribus, Kutateladze, Borishanskii, Noyes, Chang and Snyder, and Moissis and Berenson fall within, or in the near vicinity of the data scatter, except at high pressures.

Effect of Gravity

As shown by the experimental data of Sherley (Ref. 62) for hydrogen and Clark, et al. (Ref. 8) for nitrogen, the maximum heat flux is reduced by about 50-percent in going from standard gravity to near-zero gravity.

POOL FILM BOILING MINIMUM HEAT FLUX

Few experimental data are available for the pool film boiling minimum heat flux. Only nitrogen at atmospheric pressure has been studied to any extent and the results appear to vary widely, depending on surface geometry and orientation. The data do fall roughly within the theoretical predictions. Based on the data of Lyon, et al. (Ref. 46), it is interesting to note that as the critical pressure is approached, the transition region between nucleate and film boiling seems to disappear leaving only an inflection point in the q/A vs ΔT curve in place of the maximum and minimum heat flux values. Near the critical pressure, stable film boiling can occur at very low values of ΔT .

STABLE POOL FILM BOILING

Data at Atmospheric Pressure

A fair quantity of stable pool film boiling experimental data have been obtained for all three cryogenic fluids at atmospheric pressure. In general, as with other fluids, the heat flux increases with increasing ΔT until the surface fails. At high surface temperatures, the effect of the radiation contribution may become important. In general, for a given ΔT , somewhat higher heat fluxes can be achieved with hydrogen than with nitrogen or oxygen. This is consistent with the trends predicted by theory.

Surface Roughness and Orientation

Based on the experimental data of Ref. 15, and as predicted theoretically, there is no effect of surface roughness or a greased surface on pool film boiling. The experimental data of Ref. 15 and 42 show that a horizontal surface requires a higher ΔT to sustain a given heat flux than a vertical surface. For horizontal cylinders or wires, the data of Ref. 3 and 27 indicate an increasingly larger effect of diameter at values less than 0.1 inch than predicted by the theory of Bromley as discussed in the Boiling Theory section above. Frederking (Ref. 27), in particular, has achieved heat fluxes of almost 1 Btu/sec-sq in. with very fine wires.

Effect of Pressure

With proper corrections for small diameter, height and/or radiation, the pool film boiling theories provide a relatively adequate means of predicting pool film boiling heat flux. The effect of pressure as shown by the experimental data of Ref. 3 is to increase the heat flux; this is in good agreement with the theory.

Effect of Gravity

The data of Ref. 8 show that near-zero gravity conditions cause a considerable reduction in film boiling heat flux for a given ΔT , as predicted by theory.

SUBCOOLED FORCED CONVECTION BOILING

Compared to that available for pool boiling, only a very limited amount of data are available for subcooled forced convection boiling. No known data for oxygen even exist. Therefore, few conclusions can be drawn. In general, the results available do show that forced convection can be used to achieve much higher heat fluxes than are possible with pool boiling. This is true not only in the nucleate, but also in the film boiling region. Theoretical methods such as Eq. 61, 63, and 69 show promise for allowing approximate predictions of the nucleate boiling region.

SATURATED FORCED CONVECTION BOILING

This type of boiling is considerably more complex than the other types discussed above. Again, only a limited amount of experimental data are available. Oxygen has only been studied in the transition region. The results show that at relatively low heat fluxes, a nucleate-type boiling is obtained until a critical heat flux and a corresponding critical quality are reached. Beyond this point, a film boiling-type region exists which may or may not correspond to a liquid deficient condition, depending on the quality and flow velocity of the flowing stream. As with subcooled conditions, very high heat fluxes can be attained with saturated forced convection boiling.

RECOMMENDATIONS

On the basis of the results of the literature survey presented above, the following recommendations are made for additional analytical and experimental studies that are required to provide an adequate knowledge of heat transfer to boiling cryogenics.

1. One of the most important variables in pool nucleate boiling is the nature of the surface. Additional experiments with all three cryogenic fluids are required with surfaces of known distribution and geometry of bubble nucleation sites. The data should be compared to theories such as that of Lienhard (Ref. 313).
2. Additional data on the maximum pool nucleate boiling heat flux for all three fluids over a wide range of pressure, geometry, and orientation are required to determine the reasons for the apparent disagreement among the meager data thus far available. This discrepancy has also been discussed recently by Squire (Ref. 207).
3. Experimental data on the pool film boiling minimum heat flux are practically nonexistent and are needed for all three fluids over a wide range of pressure and conditions of geometry and orientation for adequate comparison with available theory.
4. Subcooled forced convection boiling studies are greatly needed. They should be conducted with all three cryogenic fluids over a wide range of conditions of pressure, velocity, and heat flux in both straight and curved tubes. Data covering the entire region from nonboiling through nucleate, transition, and to

stable film boiling should be obtained. Supplementary pool boiling measurements should be made with the same materials to provide basic information to test the adequacy of available theories in the nucleate boiling region. The importance of this has recently been shown by Bergles and Rohsenow (Ref. 339). These studies can be conveniently made in electrically heated tubes with a pressurized flow system. The concurrent development of a theory for the subcooled film boiling region is necessary.

5. The need for more detailed and comprehensive experimental and analytical studies of saturated forced convection boiling with all three cryogenic fluids cannot be overemphasized. Data should be obtained in the same manner and over the same ranges of variables as discussed in Item 4 above. Local axial conditions must be carefully determined. Both partial and complete vaporization of the fluids should be examined. Chen's theory (Ref. 346) should be tested to determine its adequacy for cryogenic fluids up to the critical quality. Data in the liquid deficient region should be compared to ordinary forced convection, nonboiling correlations.

NOMENCLATURE

| | | |
|------------|---|--|
| a_g | = | ratio of local to sea-level gravitational acceleration |
| C | = | specific heat at constant pressure |
| D | = | diameter |
| f | = | frequency |
| f_g | = | heating surface condition factor |
| F | = | Reynolds number factor of Chen |
| g | = | acceleration due to gravity |
| g_c | = | constant = 32.17 lbm-ft/lbf-sec ² |
| G | = | mass velocity |
| G^* | = | characteristic mass velocity for pool boiling |
| h | = | heat transfer coefficient |
| J | = | mechanical equivalent of heat = 778.2 ft-lbf/Btu |
| k | = | thermal conductivity |
| L^* | = | characteristic length for boiling |
| L_o | = | transition height |
| Nu | = | Nusselt number |
| P | = | pressure |
| ΔP | = | pressure difference corresponding to ΔT |
| Pr | = | Prandtl number |
| q/A | = | heat flux |
| Ra | = | Rayleigh number |

Re = Reynolds number
 S = suppression factor of Chen
 St = Stanton number
 T = temperature
 ΔT = wall superheat = $T_w - T_s$
 u, U = velocity
 V = velocity
 x = weight fraction vapor (quality)
 X_{tt} = Martinelli two-phase parameter
 y = height
 z = weight fraction liquid

Greek Letters:

α = thermal diffusivity
 α' = absorptivity
 β = coefficient of volumetric expansion
 Δ = difference
 ϵ = emissivity
 λ = heat of vaporization
 μ = viscosity
 π = constant = 3.1416
 ρ = density
 σ = surface tension
 σ' = Stefan-Boltzmann constant

Subscripts:

| | | |
|----------------|---|-------------------|
| atm | = | atmospheric |
| b | = | bulk condition |
| B | = | boiling |
| Bi | = | incipient boiling |
| c | = | convection |
| f | = | film condition |
| FC | = | forced convection |
| L | = | liquid |
| PB | = | pool boiling |
| r | = | radiation |
| s | = | saturation |
| s _L | = | saturated liquid |
| V | = | vapor |
| w | = | wall condition |

EXPERIMENTAL DATA BIBLIOGRAPHY

(Refer to Table 1 for Coding Scheme)

- *1. Aerophysics Group
 "June-August Progress Report for the Combined Laboratory and
 KC-135 Aircraft Zero-G Test Program
 Convair-Astronautics Report No. AE61-0871, 5 September 1961
 H₂: A1-B1-C1-D3-E2 X
 H₂: A4-B1-C1-D3-E2

- *2. Banchemo, J. T., Barker, G. E., and Boll, R. H.
 "Stable-Film Boiling of Liquid Oxygen Outside Single Horizontal
 Tubes and Wires"
 Chem. Eng. Progr. Symposium Ser. 51, No. 17, 21-31 (1955)
 O₂: A3-B1-C7, C8-E3 X

- *3. Banchemo, J. T., Barker, G. E., and Boll, R. H.
 "Heat Transfer Characteristics of Boiling Oxygen, Fluorine, and
 Hydrazine," Part A
 University of Michigan Engineering Research Institute, Project M834,
 November 1951
 O₂: A1-B1-C7, C8-E3
 O₂: A3-B1-C7, C8, C9-E3 XXX
 N₂: A1-B1-C8-E3
 N₂: A3-B1-C8, C9-E3

- *4. Bochirol, L., Bonjour, E. and Weil, L.
 "Improvement of Heat Transfer by the Application of an Electric
 Field to Boiling Liquified Gases"
 International Inst. of Refrigeration,
 Commission I, Eindhoven, The Netherlands,
 28-30 June 1960, Annexe 1960-1, p. 251-256
 N₂: A1-B1-C8-D5-E2
 O₂: A1-B1-C8-D5-E2 X
 N₂: A3-B1-C8-D5-E2
 O₂: A3-B1-C8-D5-E2

*Refer to Table 2 for other reference reporting the same study.

- *5. Bromley, L. A.
 "Heat Transfer in Stable Film Boiling"
 PhD Thesis, University of California, Berkeley, 1948
 N₂: A3-B1-C7-E3 XXX

- *6. Bromley, L. A.
 "Heat Transfer in Stable Film Boiling"
 Chem. Eng. Prog. 46, 221-227 (1950) XX
 N₂: A3-B1-C7-E2, E4

- *7. Bromley, L. A.
 Document 2750, American Documentation Institute
 N₂: A3-B1-C7-E1 X

- *8. Clark, J. A., and Merte, H.
 "Boiling Heat Transfer to a Cryogenic Fluid in Both Low and High Gravity Fields"
 Paper presented at the XIth International Congress of Refrigeration, August 27 to September 4, 1963, in Munich, Germany
 N₂: A1-B1-C11-D3-E2
 N₂: A2-B1-C11-D3-E2 XX
 N₂: A3-B1-C11-D3-E2
 N₂: A4-B1-C11-D3-E2

- *9. Clark, J. A., and Merte, H.
 "Nucleate, Transition, and Film Boiling Heat Transfer at Zero Gravity"
 Paper presented at Second Symposium on Physical and Biological Phenomena under Zero-G Conditions, January 18, 1963
 N₂: A1-B1-C11-D3-E2
 N₂: A2-B1-C11-D3-E2 XXX
 N₂: A3-B1-C11-D3-E2
 N₂: A4-B1-C11-D3-E2

*Refer to Table 2 for other references reporting the same study.

- *10. Clark, J. A., et al.
"Pressurization of Liquid Oxygen Containers"
University of Michigan, Mich. Rept. No. 04268-2-P
Progress Report No. 2, January to August 1961
N₂: A1-B1-C11-D3-E2
N₂: A2-B1-C11-D3-E2 XXX
N₂: A3-B1-C11-D3-E2
N₂: A4-B1-C11-D3-E2
- *11. Clark, J. A., et al.
"Pressurization of Liquid Oxygen Containers"
University of Michigan, Mich. Rept. No. 04268-3-P
Progress Report No. 3, August to November 1961
N₂: A1-B1-C11-D3-E2
N₂: A2-B1-C11-D3-E2 X
N₂: A3-B1-C11-D3-E2
N₂: A4-B1-C11-D3-E2
- *12. Clark, J. A., et al.
"Pressurization of Liquid Oxygen Containers"
University of Michigan, Mich. Rept. No. 04268-4-P
Progress Report No. 4, December 1961 to July 1962
N₂: A1-B1-C11-D3-E2, E4
N₂: A2-B1-C11-D3-E2, E4 X
N₂: A4-B1-C11-D3-E2, E4
- *13. Clark, J. A., et al.
"Pressurization of Liquid Oxygen Containers"
University of Michigan, Mich. Rept. No. 04268-5-P
Progress Report No. 5, August to November 1962
N₂: A1-B1-C11-D3-E2
N₂: A2-B1-C11-D3-E2 X
N₂: A3-B1-C11-D3-E2
N₂: A4-B1-C11-D3-E2

19. Dean, J. W.
"An Experimental Investigation of the Thermal Characteristics
of Condensing and Boiling Nitrogen Films"
M. S. Thesis, University of Colorado, 1958
N₂: A1-B4-C5b-E3 XX
- *20. Dean, L. E. and Thompson, L. M.
"Heat Transfer Characteristics of Liquid Nitrogen"
Bell Aircraft Corp., Rept. No. 56-982-035, 1955
N₂: A1-B2-C4b-E3
N₂: A2-B2-C4b-E3 XX
N₂: A3-B2-C4b-E3
N₂: A4-B2-C4b-E3
- *21. Dean, L. E., and Thompson, L. M.
"Study of Heat Transfer to Liquid Nitrogen"
ASME Paper 56-SA-4, June 1956
N₂: A1-B2-C4B-E2 X
N₂: A3-B2-C4B-E2
- *22. Drayer, D. E.
"An Experimental Investigation of the Heat Transfer Coefficients
for Boiling and Condensing Hydrogen Films"
PhD Thesis, Chemical Engineering, University of Colorado, 1961
H₂: A1-B1-C5-E3 XXX
- *23. Drayer, D. E., and Timmerhaus, K. D.
"An Experimental Investigation of the Individual Boiling and
Condensing Heat Transfer Coefficients for Hydrogen"
Advances in Cryogenic Eng. 7, 401-412(1962)
H₂: A1-B1-C5-E3 XX
- *24. Fenster, S. K.
"The Transient Thermal Response of a Step Pressurized Boiling
Nitrogen System"
PhD Thesis, Mechanical Engineering, University of Michigan, 1959
N₂: A1-B1-C3-E2 XXX

*Refer to Table 2 for other references reporting the same study.

- *25. Fenster, S. K., Van Wylen, G. J., and Clark, J. A.
 "Transient Phenomena Associated with the Pressurization of
 Liquid Nitrogen Boiling at Constant Heat Flux"
 Advances in Cryogenic Engr. 5, 226-234 (1959)
 N₂: A1-B1-C3-E2 X
26. Flynn, T. M., Draper, J. W., and Roos, J. J.
 "The Nucleate and Film Boiling Curve of Liquid Nitrogen at
 One Atmosphere"
 Advances in Cryogenic Engineering, 7, 539-545 (1961)
 N₂: A1-B1-C7-E2
 N₂: A2-B1-C7-E2 XX
 N₂: A3-B1-C7-E2
 N₂: A4-B1-C7-E2
- *27. Frederking, T.
 "Film Boiling of Helium I and Other Liquefied Gases on Single
 Wires"
 AIChE Journal 5, 403-406 (1959)
 N₂: A3-B1-C8-E2 X
- *28. Frederking, T.
 "Heat Transfer in the Evaporation of Liquid Helium and Nitrogen"
 Forsch. Gebiete Ingenieurw, 27, 17-30 (1961)
 N₂: A1-B1-C7, C8-E2 XX
 N₂: A4-B1-C7, C8-E2
- *29. Frederking, T.
 "Film Boiling Heat Transfer in Liquid Helium and Nitrogen"
 Forsch. Gebiete Ingenieurw, 27, 58-61 (1961)
 N₂: A3-B1-C7, C8-E2 X
- *30. Frederking, T.
 Personal Communication, 30 September 1963
 (Tabulated data for Ref. 29)
 N₂: A3-B1-C8-E1 X

*Refer to Table 2 for other references reporting the same study.

- *31. Frederking, T.
Document 5972, American Documentation Institute, Washington, D.C.
N₂: A3-B1-C8-E1 X
- *32. Frederking, T., and Grassman, P.
"Film Boiling of Liquefied Gases, Especially of Liquid Helium I."
International Institute of Refrigeration Problems of Low
Temperature Physics and Thermodynamics
Proc. of the Meeting of Commission of the International
Institute of Refrigeration
Delft, 1958, Pergamon Press, N. Y., p 317-322
N₂: A3-B1-C8-E2 X
33. Fritz, J. J. and Johnston, H. L.
"Design and Operation of Liquid Nitrogen-Cooled Solenoid Magnets"
Rev. Scientific Instruments, 21, 416-420 (1950)
N₂: A1-B1-C5-E1 X
- *34. Giaque, W. F., Stout, J. W., Barleau, R. E., and Egan, C. J.
"Cascade Oxygen System"
National Defense Research Committee
Office of Scientific Research and Development
OSRD 491, Serial No. 201
Report Mar. 1, 1942, Division B.
DDC Document AT1 204778
O₂: A1-B1-C5-E2 XX
O₂: A3-B1-C5-E2
- *35. Graham, R. W., Hendricks, R. C., Hsu, Y. Y., and Friedman, R.
"Experimental Heat Transfer and Pressure Drop of Film Boiling
Liquid Hydrogen Flowing Through a Heated Tube"
Advances in Cryogenic Eng. 6, 517-524 (1960)
H₂: A3-B3-C4a-E2 XX
H₂: A3-B2-C4a-E2
36. Hanson, W. B. and Richards, R. J.
"Heat Transfer to Liquefied Gases"
National Bureau of Standards, Boulder, Colorado
Lab Note 56-1, 1956
N₂: A3-B1-C7-E2 X

*Refer to Table 2 for other references reporting the same study.

37. Haselden, G. G., and Peters, J. I.
"Heat Transfer to Boiling Liquid Oxygen and Liquid Nitrogen"
Trans. Inst. Chem. Eng. (London) 27, 201-208 (1949)
N₂: A1-B1-C5, C7-E3 XXX
O₂: A1-B1-C5, C7-E3
38. Haselden, G. G. and Prosad, S.
"Heat Transfer from Condensing Oxygen and Nitrogen Vapours"
Trans. Inst. Chem. Eng. (London) 27, 195-200 (1949)
N₂: A1-B4-C4b-E3 XXX
O₂: A1-B4-C4b-E3
- *39. Hendricks, R. C., Graham, R. W., Hsu, Y. Y., and Friedman, R.
"Experimental Heat Transfer and Pressure Drop of Liquid
Hydrogen Flowing Through a Heated Tube"
National Aeronautics and Space Administration - Lewis
NASA TN-D-765, May 1961
H₂: A3-B2-C4a-E3
H₂: A3-B3-C4a-E3 XX
- *40. Hendricks, R. C., Graham, R. W., Hsu, Y. Y., and Mederios, A.
"Correlation of Hydrogen Heat Transfer in Boiling and
Supercritical Pressure States"
J. Am. Rocket Soc. 32, 244-52 (1962)
H₂: A3-B3-C4a-E2, E4 X
- *41. Hsu, Y. Y.
"Film Boiling on Vertical Surfaces"
PhD Thesis, Chemical Engineering, University of Illinois, 1958
N₂: A3-B1-C5-E3 XXX
- *42. Hsu, Y. Y., and Westwater, J. M.
"Film Boiling from Vertical Tubes"
AIChE Journal 4, 58-62 (1958)
N₂: A3-B1-C5-E2, E4 X

*Refer to Table 2 for other references reporting the same study.

43. Jones, J. H. and Altman, M.
"Two Phase Flow and Heat Transfer for Boiling Liquid Nitrogen
in Horizontal Tubes"
AIChE Preprint No. 52 presented at the ASME-AIChE Heat Transfer
Conference, Boston, Mass., August 11-14, 1963
N₂: A1-B3-C6a-E3 X
- *44. Lewis, J. P., Goodykoontz, J. H., and Kline, J. F.
"Boiling Heat Transfer to Liquid Hydrogen and Nitrogen in
Forced Flow"
National Aeronautics and Space Administration
Rept. No. NASA-TND-1314, September 1962
H₂: A1-B2-C4a-E3
H₂: A1-B3-C4a-E3
H₂: A3-B3-C4a-E3
H₂: A4-B3-C4a-E3 XXX
N₂: A1-B2-C4a-E3
N₂: A1-B3-C4a-E3
N₂: A3-B3-C4a-E3
N₂: A4-B3-C4a-E3
45. Lyon, D. N.
"Peak Nucleate Boiling Heat Fluxes and Nucleate Boiling Heat
Transfer Coefficients for Liquid N₂, Liquid O₂ and Their Mixtures
in Pool Boiling at Atmospheric Pressure"
Low Temperature Laboratory Dept., Depts. of Chemistry and
Chemical Engineering, University of California, Berkeley, Calif.,
1963
N₂: A1-B1-C5-D1-E2
N₂: A1-B1-C7-D1-E2
N₂: A4-B1-C5-D1-E1
N₂: A4-B1-C7-D1-E1 XXX
O₂: A1-B1-C5-D1-E2
O₂: A1-B1-C7-D1-E2
O₂: A4-B1-C5-D1-E1
O₂: A4-B1-C7-D1-E1

*Refer to Table 2 for other references reporting the same study.

- *50. Merte, H. and Clark, J. A.
 "Boiling Heat Transfer with Cryogenic Fluids at Standard, Fractional, and Near-Zero Gravity"
 Paper No. 63-HT-28 presented at the ASME-AIChE Heat Transfer Conference, Boston, Mass., August 11-14, 1963
 N_2 : A1-B1-C11-D3-E2
 N_2 : A3-B1-C11-D3-E2 XX
 N_2 : A2-B1-C11-D3-E2
 N_2 : A4-B1-C11-D3-E2
- *51. Merte, H. and Clark, J. A.
 "Boiling Heat Transfer Data for Liquid Nitrogen at Standard and Near-Zero Gravity"
 Advances in Cryogenic Engineering, 7, 546-550 (1962)
 N_2 : A1-B1-C11-D3-E2
 N_2 : A2-B1-C11-D3-E2 XX
 N_2 : A3-B1-C11-D3-E2
 N_2 : A4-B1-C11-D3-E2
52. Mikhail, N. R.
 "Studies in Heat Transfer to Boiling Liquids at Low Temperatures"
 PhD Thesis, Dept. of Chem. Eng., Imperial College of Science and Technology, London, 1952
 N_2 : A1-B1-C7-D1-E3 XXX
 O_2 : A1-B1-C7-D1-E3
53. Monroe, A. G., Bristow, A. S., and Newell, J. E.
 "Heat Transfer to Boiling Liquids at Low Temperatures and Elevated Pressures"
 J. Appl. Chem. 2, 613-624 (1952)
 O_2 : A2-B3-C4a-E2 XX
 N_2 : A2-B3-C4a-E2

*Refer to Table 2 for other references reporting the same study.

- *62. Sherley, J. E.
 "Nucleate Boiling Heat-Transfer Data for Liquid Hydrogen at
 Standard and Zero Gravity"
 Advances in Cryogenic Engineering, 8, 495-500 (1963)
 H_2 : A1-B1-C1-D3-E2, E4 XX
 H_2 : A4-B1-C1-D3-E2
63. Sydoriak, S. G., and Roberts, T. R.
 "A Study of Boiling in Short Narrow Channels and Its Application
 to Design of Magnets Cooled by Liquid H_2 and N_2 "
 J. Appl. Phys. 28, 143-148 (1957)
 N_2 : A1-B4-C4b-E2
 N_2 : A1-B3-C4b-E2 XX
 H_2 : A1-B4-C4b-E2
 H_2 : A1-B3-C4b-E2
64. Timmerhaus, K. D., Drayer, D. E., and Dean, J. W.
 "An Experimental Investigation of Over-All Heat Transfer Coefficients
 for Condensing and Boiling Hydrogen Films"
 International Developments in Heat Transfer Published by
 ASME, 2, 270-278 (1961)
 (Over-all coefficients only reported)
65. Vichnes, I. P. and Elukin, N. K.
 "Heat Transfer During the Boiling of Liquids in Tubes"
 Inzh. Fiz. Zh., Akad. Nauk. Belorussk. SSR 3, 74-80 (1960)
 O_2 : A -B1-C4a, E2 X
 N_2 : A -B1-C4a, E2
- *66. von Glahn, U. H. and Lewis, J. P.
 "Nucleate-and Film-Boiling Studies with Liquid Hydrogen"
 Advances in Cryogenic Engr. 2, 262-269 (1959)
 N_2 : A3-B3-C4a-E2
 N_2 : A4-B3-C4a-E2 XX
 H_2 : A3-B3-C4a-E2
 H_2 : A4-B3-C4a-E2

*Refer to Table 2 for other references reporting the same study.

- *67. Walters, H. H.
 "Single Tube Heat Transfer Tests with Liquid Hydrogen"
 Advances in Cryogenic Engineering, 6, 509-516 (1960)
 H_2 : A1-B3-C6a-E2 XX
 H_2 : A3-B3-C6a-E2
68. Weil, L.
 "Heat Transfer Coefficients of Boiling Liquefied Gases"
 Proc. 8th International Congress of Refrigeration, London,
 29 August to 11 September 1951
 Commission I, p. 181-186
 N_2 : A1-B1-C8-E2
 H_2 : A1-B1-C8-E2 X
 N_2 : A3-B1-C8-E2
 H_2 : A3-B1-C8-E2
69. Weil, Louis, and Lacaze, Albert
 "Coefficients of Thermal Exchange in Boiling Nitrogen"
 Compt. rend. 230, 186-188 (1950)
 N_2 : A1-B1-C5, C9-D1-E2 X
 N_2 : A3-B1-C5, C9-D1-E2
70. Weil, Louis, and Lacaze, Albert
 "Heat Exchanged in Boiling Hydrogen Under Atmospheric Pressure"
 J. phys. radium 12, 890 (1951)
 H_2 : A1-B1-C8-E2 X
 H_2 : A3-B1-C8-E2
71. Weil, L., and Lacaze, A.
 "Variation With Pressure of the Coefficient of Exchange in
 Boiling Nitrogen"
 Soci  te Fran  oise de Physique
 Proces-Verbaux et Resumes des Communications. No. 9,
 45S - 46S (1951)
 N_2 : A1-B1-C9-E2 X

*Refer to Table 2 for other references reporting the same study.

72. Weil, L., and Lacaze, A.
"Heat Exchange in Liquid Nitrogen Boiling Under Different Pressures"
Bull. inst. intern. froid., Annexe 1955-2, 85-88 (1954)
N₂: A1-B1-C9-E2 X
73. Weil, L., and Lacaze, A.
"Measurements of Heat Exchange in Liquid Hydrogen Boiling Under Pressure"
9th Intern. Inst. on Refrigeration, Proceedings Comm. I and II, Paris, 1955, Paper I 13, p. 1-024 to 1-027
H₂: A1-B1-C9-E2 X
- *74. Wright, C. C. and Walters, H. H.
"Single Tube Heat Transfer Tests, Gaseous and Liquid Hydrogen"
AiResearch Mfg. Co., Rept. November 1958 to June 1959
WADC TR 59-423, AD 228875, August 1959
H₂: A1-B3-C6a-E3 XXX
H₂: A3-B3-C6a-E3

*Refer to Table 2 for other references reporting the same study.

SUBJECT CROSS REFERENCES

(Numbers Refer to Experimental Data Bibliography)

BOILING REGIMES AND FLOW CONDITIONS

Hydrogen Pool Nucleate Boiling:

1, 15, 16, 22, 23, 48, 54, 55, 56, 58, 62, 64, 68, 70, 73

Nitrogen Pool Nucleate Boiling:

3, 4, 8, 9, 10, 11, 12, 13, 14, 18, 24, 25, 26, 28, 33, 37, 45,
46, 47, 49, 50, 51, 52, 58, 60, 61, 65, 68, 69, 71, 72

Oxygen Pool Nucleate Boiling:

3, 4, 34, 37, 45, 46, 47, 48, 52, 55, 59, 65

Hydrogen Subcooled Forced Convection Nucleate Boiling:

17, 44

Nitrogen Subcooled Forced Convection Nucleate Boiling:

20, 21, 44

Hydrogen Saturated Forced Convection Nucleate Boiling:

17, 44, 57, 63, 67, 74

Nitrogen Saturated Forced Convection Nucleate Boiling:

43, 44, 57, 63

Hydrogen Maximum Pool Nucleate Boiling Heat Flux:

1, 15, 54, 56, 58, 62

Nitrogen Maximum Pool Nucleate Boiling Heat Flux:

8, 9, 10, 11, 12, 13, 14, 18, 26, 28, 45, 46, 47, 50, 51, 54, 58,
60, 61

Oxygen Maximum Pool Nucleate Boiling Heat Flux:

45, 46, 47

Hydrogen Maximum Forced Convection Nucleate Boiling Heat Flux:

44, 66

Nitrogen Maximum Forced Convection Nucleate Boiling Heat Flux:

20, 44, 66

Hydrogen Transition Boiling:

17

Nitrogen Transition Boiling:

8, 9, 10, 11, 12, 13, 14, 18, 20, 26, 50, 51, 53, 60, 61

Oxygen Transition Boiling:

53

Hydrogen Pool Film Boiling:

15, 16, 54, 68, 70

Nitrogen Pool Film Boiling:

3, 4, 5, 6, 7, 8, 9, 10, 11, 13, 14, 18, 26, 27, 29, 30, 31, 32,
36, 41, 42, 46, 47, 50, 51, 60, 61, 68, 69

Oxygen Pool Film Boiling:

2, 3, 4, 34, 46, 47

Hydrogen Forced Convection Subcooled Film Boiling:

17, 35, 39

Nitrogen Forced Convection Subcooled Film Boiling:

20, 21

Hydrogen Forced Convection Saturated Film Boiling:

17, 35, 39, 40, 44, 66, 67, 74

Nitrogen Forced Convection Saturated Film Boiling:

44, 66

GEOMETRY CONDITIONS

Hydrogen Boiling above Horizontal Plates:

1, 15, 16, 56, 58, 62

Nitrogen Boiling above Horizontal Plates:

46, 47, 58

Oxygen Boiling above Horizontal Plates:

46, 47

Hydrogen Boiling on Vertical Plates:

15, 16

Nitrogen Boiling on Vertical Plates

24, 25

Hydrogen Boiling Inside Vertical Tubes:
17, 35, 39, 40, 44, 57, 63, 66

Nitrogen Boiling Inside Vertical Tubes:
20, 21, 38, 44, 53, 57, 63, 65, 66

Oxygen Boiling Inside Vertical Tubes:
38, 53, 65

Hydrogen Boiling Outside Vertical Tubes:
22, 23, 64

Nitrogen Boiling Outside Vertical Tubes:
19, 33, 37, 41, 42, 45, 60, 61, 69

Oxygen Boiling Outside Vertical Tubes:
34, 37, 45

Hydrogen Boiling Inside Horizontal Tubes:
67, 74

Nitrogen Boiling Inside Horizontal Tubes:
43

Hydrogen Boiling Outside Horizontal Tubes:
48, 54

Nitrogen Boiling Outside Horizontal Tubes:
5, 6, 7, 18, 26, 28, 29, 36, 37, 45, 52, 54

Oxygen Boiling Outside Horizontal Tubes:
2, 3, 37, 45, 48, 52

Hydrogen Boiling on Horizontal Wires:
68, 70

Nitrogen Boiling on Horizontal Wires:
3, 4, 27, 28, 29, 30, 31, 32, 49, 68

Oxygen Boiling on Horizontal Wires:
2, 3, 4

Hydrogen Boiling on Vertical Wires:
73

Nitrogen Boiling on Vertical Wires:

3, 60, 61, 69, 71, 72

Oxygen Boiling on Vertical Wires:

3

Hydrogen Boiling on Inclined Plates:

15, 16

Hydrogen Boiling, Miscellaneous Geometry:

55

Nitrogen Boiling, Miscellaneous Geometry:

8, 9, 10, 11, 12, 13, 14, 50, 51

Oxygen Boiling, Miscellaneous Geometry:

55

OTHER CONDITIONS

Hydrogen Boiling, Heater Surface Effects:

15, 16, 48, 54

Nitrogen Boiling, Heater Surface Effects:

18, 45, 52, 69

Oxygen Boiling, Heater Surface Effects:

45, 52

Hydrogen Boiling, G-field Effect:

1, 56, 62

Nitrogen Boiling, G-field Effect:

8, 9, 10, 11, 12, 13, 14, 50, 51

Nitrogen Boiling, Electric Field Effect:

4

Oxygen Boiling, Electric Field Effect:

4

Hydrogen Boiling, Natural Circulation Effect:
57, 63

Nitrogen Boiling, Natural Circulation Effect:
19, 38, 57, 63

Oxygen Boiling, Natural Circulation Effect:
38

PHYSICAL PROPERTY REFERENCES

101. Roder, H. M., and Goodwin, R. D. "Provisional Thermodynamic Functions for Para-Hydrogen," NBS Technical Note 130, December 1961
102. Moses, R. A., Tkachenko, E. A., and Brown, F. J., "Para-Hydrogen P-V-T Relationships, and Specific Heats, Specific Heat Ratios, Acoustic Velocity and Bulk Modulus of Para-Hydrogen," Rocketdyne Memo PR 4114-1003, 10 January 1964.
103. Shaffer, A., and Rousseau, J., "Thermodynamic Properties of 20.4° K Equilibrium Hydrogen," ASD Technical Report 61-360, October 1961
104. Johnson, V. J., "A Compendium of the Properties of Materials at Low Temperature (Phase 1)," WADD Technical Report 60-56, Part 1, December 1961
105. "The Thermodynamic Properties of Nitrogen From 64 to 300° K between 0.1 and 300 Atmospheres," NBS Technical Note 129, January 1962.
106. "Liquid Propellants Handbook, Volume I," Battelle Memorial Institute, October 1958
107. Stewart, R. B., Hust, J. G., and Mc Carty, R. D., Interim Thermodynamic Properties for Gaseous and Liquid Oxygen at Temperatures from 55 to 300° K and Pressures to 300 atm." NBS Report 7922 October 1, 1963
108. Miller and Sullivan, U. S. Bur. Mines Tech. Paper 424 (1928), (Perry, 3rd Ed., p 273)
109. Hougen, O. A., and Watson, K. M., Chemical Process Principles, Part Two, Thermodynamics, John Wiley and Sons, New York, 1948, pp 511-512

110. Abas-Zade, A. K., "The Law of Heat Conductance of Liquids and Vapors," Zhur. Eksptl. i Teoret Fiz. 25, 60 (1952)
111. Starrett, D., "Sources of Data on Hydrogen Properties", Rocketdyne Memo NL-61-548, 30 November 1961
112. Stiel, L. S., and Thodos, G., "The Viscosity of Hydrogen in the Gaseous and Liquid States for Temperatures up to 5000 K, "Ind. Eng. Chem. Fundamentals, 2, No. 3, 233-237 (August 1963)
113. "Tables of Thermal Properties of Gases," U. S. Dept. Comm., NBS Circular 564, Nov. 1, 1955
114. Brebach, W. J., and Thodos, G., "Viscosity-Reduced State Correlation for Diatomic Gases," Ind. Eng. Chem., 50, 1095-1100 (1950)
115. Schaefer, C. A., and Thodos, G., "Reduced Thermal Conductivity Correlation," Ind. Eng. Chem., 50, 1585-1588 (1958)
116. Schaefer, C. A., and Thodos, G., "Thermal Conductivity of Diatomic Gases: Liquid and Gaseous States," AIChE Journal, 5, 3, 367-372 (1959)
117. Stewart, R. B., Germann, F.E.E., and Mc Carty, R. D., "The Surface Tension of Hydrogen," U. S. Dept. Comm., NBS Report 7616, October 1, 1962
118. Guggenheim, E. A., "The Principle of Corresponding States," J. Chem. Phys. 13, 253-261 (1945)
119. Roder, H. M., Diller, D. E., Weber, L. A. and Goodwin, R. D., "The Orthobaric Density of Para-Hydrogen, Derived Heats of Vaporization, and Critical Constants," Cryogenics, 3, 1, 16-22, March 1963
120. Hougen, O. A., and Watson, K. M., Chemical Process Principles, Part One, Material and Energy Balances, John Wiley and Sons, New York, 1947, pp 233-234.

GENERAL REFERENCES

201. Richards, R. J., Steward, W. G., and Jacobs, R. B., "A Survey of the Literature on Heat Transfer from Solid Surfaces to Cryogenic Fluids", NBS Tech. Note No. 122, October 1961
202. McAdams, W. H., "Heat Transmission," 3rd edition, McGraw-Hill Book Company, Inc., New York (1954)
203. Jakob, M., "Heat Transfer", Volume 1, John Wiley and Sons, Inc., New York (1949)
204. Grober, H., Erk, S., and Grigull, V., "Fundamentals of Heat Transfer", McGraw-Hill Book Company, Inc., New York (1961)
205. Rohsenow, W. M., "Heat Transfer With Boiling", Chapter in the book "Modern Developments in Heat Transfer", Ibele, W., editor, Academic Press, Inc., New York (1963)
206. Westwater, J. W., "Boiling of Liquids", Chapters in the book "Advances in Chemical Engineering, Volumes I and II, Drew, T. B. and Hooper, J. W., editors, Academic Press, Inc., New York (1956 and 1958)
207. Squire, W., "A Discrepancy in the Published Results on Heat Transfer to Cryogenic Fluids," Int. J. Heat Mass Transfer, 3, 347 (1961)

THEORY REFERENCES

301. Rohsenow, W. M. "A Method of Correlating Heat-Transfer Data for Surface Boiling of Liquids" Trans. ASME, 74, 969-976 (1952)
302. Zuber, N. and Fried, E. "Two-Phase Flow and Boiling Heat Transfer to Cryogenic Liquids" ARS Journal, 32, 1332-1341 (1962)
303. Kutateladze, S. S. "Heat Transfer During Condensation and Boiling" (Mashgiz, Moscow, 1949, 1952), AEC Translation 3770 Tech. Info. Service, Oak Ridge, Tenn.
304. Forster, H. K. and Zuber, N. "Bubble Dynamics and Boiling Heat Transfer" AIChE Journal, 1, 532-535 (1955)
305. Forster, H. K., and Greif, R. "Heat Transfer to a Boiling Liquid - Mechanisms and Correlations" Trans. ASME, Journal of Heat Transfer, 81, 43-53 (1959)
306. Levy, S. "Generalized Correlation of Boiling Heat Transfer" Trans. ASME, J. Heat Transfer, 81, 37-42 (1959)
307. Michenko, N. "On the Problem of Heat Transfer in Nucleate Boiling" Energomashinostroenie, No. 6, 17-21 (1960)
308. Labountzov, D. A. "Generalized Correlation for Nucleate Boiling" Teploenergetika, 7, No. 5, 76-80 (1960)
309. Chang, Y. P., and Snyder, N. W. "Heat Transfer in Saturated Boiling" Heat Transfer - Storrs, Chem. Eng. Symposium Series 56, No. 30, 25-38 (1960)
310. Nishikawa, K., and Yamagata, K. "On the Correlation of Nucleate Boiling Heat Transfer" Int. J. Heat Mass Transfer, 1, 219-235 (1960)
311. Kurihara, H. M. and Myers, J. E., "The Effects of Superheat and Surface Roughness on Boiling Coefficients," AIChE Journal, 6, 83-91 (1960)
312. Tien, C. L., "A Hydrodynamic Model for Nucleate Pool Boiling", Int. J. Heat Mass Transfer, 5, 533-540 (1962)
313. Lienhard, J. H., "A Semi-Rational Nucleate Boiling Heat Flux Correlation", Int. J. Heat Mass Transfer, 6, 215-219 (1963)

314. McFadden, P. W. and Grassman, P., "The Relation between Bubble Frequency and Diameter During Pool Nucleate Boiling," Int. J. Heat Mass Transfer, 5, 169-173 (1962)
315. Addoms, J. N. ScD Thesis in Chemical Engineering, MIT, 1948
316. Rohsenow, W. M. and Griffith, P. "Correlation of Maximum-Heat-Flux Data for Boiling of Saturated Liquids" Chem. Eng. Progress Symposium Series, No. 18, 52, 47-49 (1956)
317. Griffith, P. "The Correlation of Nucleate Boiling Burnout Data" Paper 57-HT-21, ASME-AIChE Heat Transfer Conference, Pennsylvania, August 11-15, 1957
318. Zuber, N. and Tribus, M. "Further Remarks on the Stability of Boiling" UCLA Report 58-5, January 1958
319. Kutateladze, S. S. "A Hydrodynamic Theory of Changes in the Boiling Process under Free Convection Conditions" Izv. Akad. Nauk. SSSR, Otd. Tekh. Nauk., No. 4, 529-536 (1951)
320. Borishanskii, V. M. "An Equation Generalizing Experimental Data on the Cessation of Bubble Boiling in a Large Volume of Liquid" Zhurn. Tekh. Fiz., 25, 252 (1956)
321. Noyes, R. C. "An Experimental Study of Sodium Pool Boiling Heat Transfer" J. Heat Transfer, May 1963, pp 125-131
322. Chang, Y. P. "Some Possible Critical Conditions in Nucleate Boiling" J. Heat Transfer, May 1963, pp 89-100
323. Moissis, R. and Bereson, P. J., "On the Hydrodynamic Transition in Nucleate Boiling", Journal of Heat Transfer, August 1963, pp 221-229
324. Zuber, N., "Hydrodynamic Aspects of Boiling Heat Transfer", Atomic Energy Commission Report No. AECU-4439, Physics and Mathematics, June 1959
325. Berenson, P. J., "Transition Boiling Heat Transfer from a Horizontal Surface," MIT Heat Transfer Laboratory Technical Report No. 17, Cambridge, Mass., March 1, 1960.
326. Bromley, L. A. "Effect of Heat Capacity of Condensate" Ind. Eng. Chem., 44, 2966-2969 (1952)

- 327. Rohsenow, W. M., "Heat Transfer and Temperature Distribution in Laminar-Film Condensation", Trans. ASME, 78, 1645-1648 (1956)
- 328. McFadden, P. W., and Grosh, R. J., "An Analysis of Laminar Film Boiling With Variable Properties" Int. J. Heat Mass Transfer, 1, 325-335 (1961)
- 329. Frederking, T. H. K., "Laminar Two-Phase Boundary Layers in Natural Convection Film Boiling", J. Applied Math and Physics, 14, 207-218 (1963)
- 330. Frederking, T. H. K., "Stability of Film Boiling Two-Phase Flow in Cryogenic Systems" Univ. of Calif., Dept. of Engineering, Los Angeles, Report on NASA Grant NSG 237-62
- 331. Chang, Y. P., "Wave Theory of Heat Transfer in Film Boiling" J. Heat Transfer, pp 1-12 (February 1959)
- 332. Berenson, P. J., "Film-Boiling Heat Transfer from a Horizontal Surface", J. Heat Transfer, pp 351-358 (August 1961)
- 333. Bonilla, C. F., Nuclear Engineering, p 518 (1957)
- 334. Ellion, M. E., "A Study of the Mechanism of Boiling Heat Transfer" JPL Memo No. 20-88 (March 1954)
- 335. Cess, R. D., "Analysis of Laminar Film Boiling from a Vertical Flat Plate", Res. Rept. 405 FF 340-R2-X, Westinghouse Research Laboratory, Pittsburgh, Pa (March 1959)
- 336. Sparrow, E. M., and Cess, R. D., "The Effect of Subcooled Liquid on Laminar Film Boiling", J. Heat Transfer, 84, 149-156 (1962)
- 337. Koh, J. C. Y., "Analysis of Film Boiling on Vertical Surfaces", J. Heat Transfer, 84, 55 (1962)

338. Hsu, Y. Y., and Westwater, J. W., "Approximate Theory for Film Boiling on Vertical Surfaces" Chem. Eng. Progress Symposium Series, No. 30, 56, 15-24 (1960).
339. Bergles, A. E., and Rohsenow, W. M., "The Determination of Forced-Convection Surface-Boiling Heat Transfer", ASME Paper No. 63-HT-22 presented at the ASME-AIChE Heat Transfer Conference, Boston, Mass., August 11-14, 1963
340. Rohsenow, W. M., "Heat Transfer With Evaporation", Chapter in the publication, "Heat Transfer, A Symposium, 1952", Eng. Research Inst., University of Michigan Press, pp 101-149 (1953)
341. Kutateladze, S. S., "Boiling Heat Transfer", Int. J. Heat Mass Transfer, 4, 31-45 (1961)
342. Kutateladze, S. S., "Critical Heat Flux to Flowing, Wetting, Subcooled Liquids", Energetika, No. 2, 229-239 (1959).
345. Gambill, W. R., "Generalized Prediction of Burnout Heat Flux for Flowing, Subcooled, Wetting Liquids", Chem. Eng. Progress Symposium Series, No. 41, 59, 71-87 (1963)
346. Chen, J. C., "A Correlation for Boiling Heat Transfer to Saturated Fluids in Convective Flow", ASME Paper No. 63-HT-34, Presented at ASME-AIChE Heat Transfer Conference, Boston, Mass., August 11-14, 1963
347. Collier, J. G., "A Review of Two-Phase Heat Transfer," Report AERE CE/R 2496, Atomic Energy Research Establishment, Harwell, England, 1958.
348. Schrock, V. E. and L. M. Grossman: "Forced Convection Boiling Studies," Report 73308-UCX 2182, University of California, Berkeley, 1959.

349. Bennett, J. A. R., J. G. Collier, J. R. C. Pratt, and J. D. Thornton: "Heat Transfer to Two-Phase Gas-Liquid Systems, Part I, Steam-Water Mixture," AERE Report R3159, Atomic Energy Research Establishment, Harwell, England, 1959.
350. Bromley, L. A., LeRoy, N. P., and Robbers, J. A. Heat Transfer in Forced Convection Film Boiling Ind. Eng. Chem., 45, 2639 (1953).
351. Motte, E. I., and Bromley, L. A., "Film Boiling of Flowing Subcooled Liquids" Ind. Eng. Chem. 49, 1921 (1957).
352. Cess, R. D., and Sparrow, E. M., "Film Boiling in a Forced-Convection Boundary-Layer Flow" Trans. ASME, J. Ht. Trans., 371 (1961).
353. Cess, R. D., and Sparrow, E. M., "Subcooled Forced Convection Film Boiling on a Flat Plate" Trans. ASME, J. Ht. Trans. 377 (1961).

APPENDIX A

PHYSICAL PROPERTY GRAPHS

Figures A-1 through A-18 are a graphical presentation of physical properties.

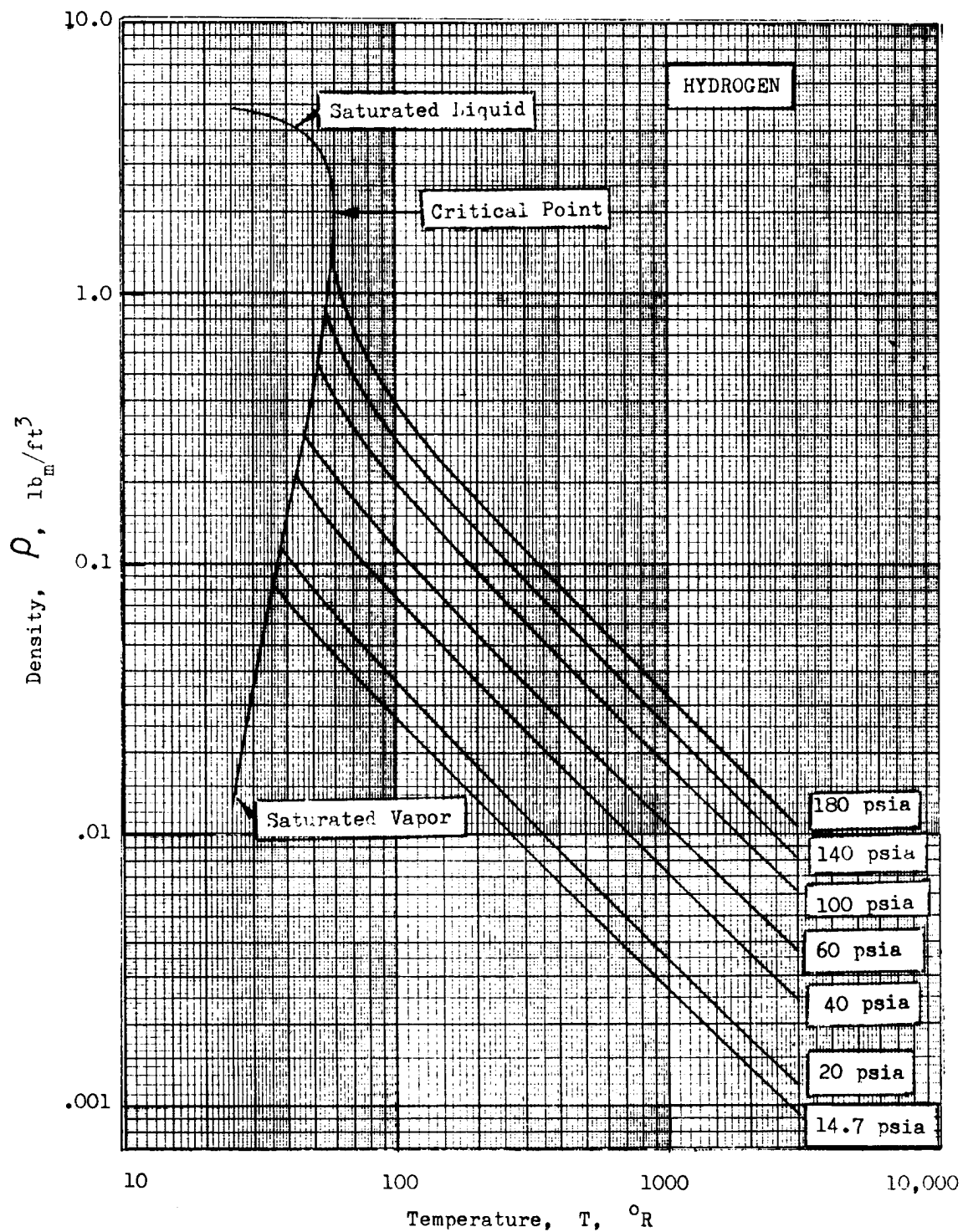


FIG. A-1 DENSITY OF PARA-HYDROGEN

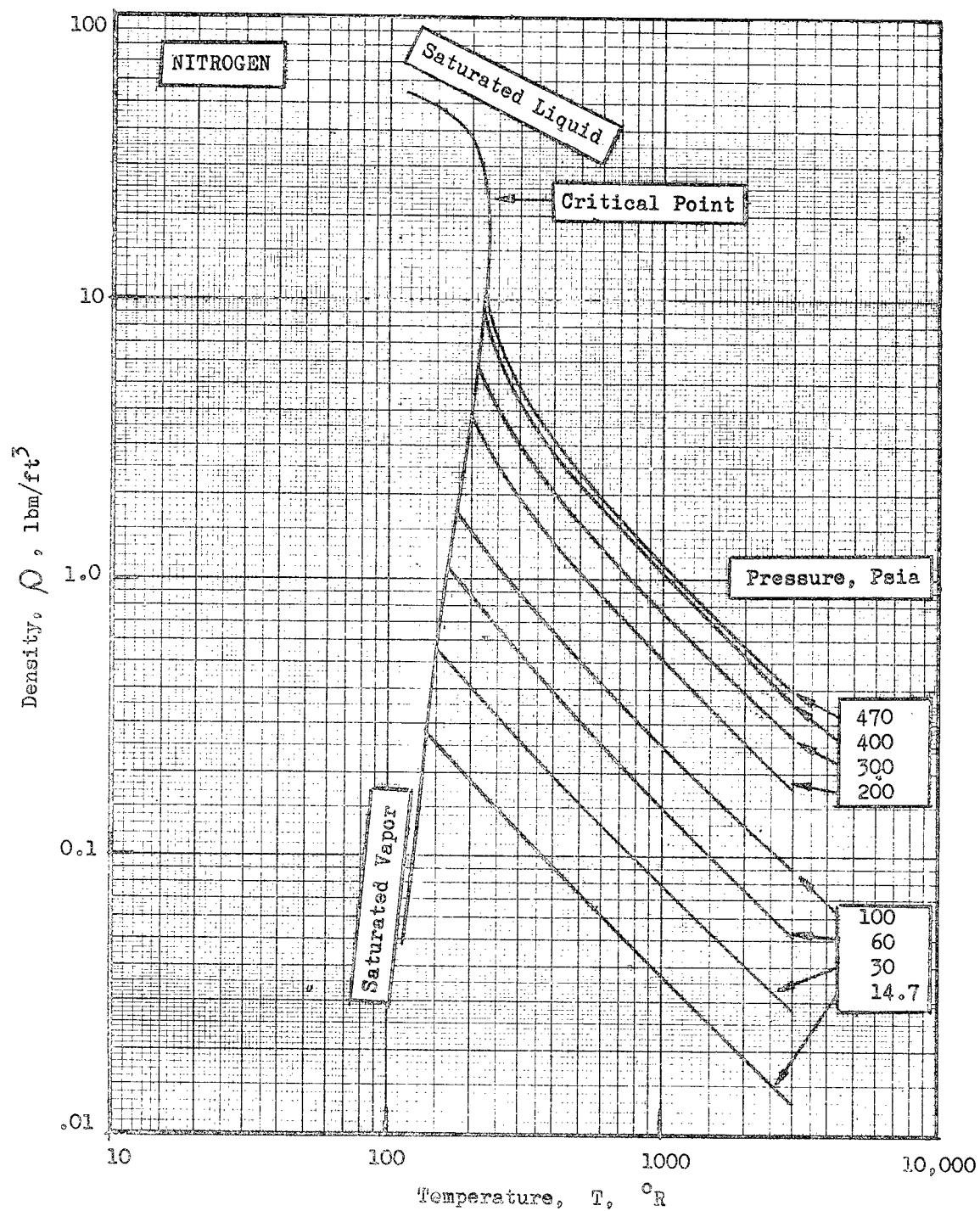


FIG. A-2 DENSITY OF NITROGEN

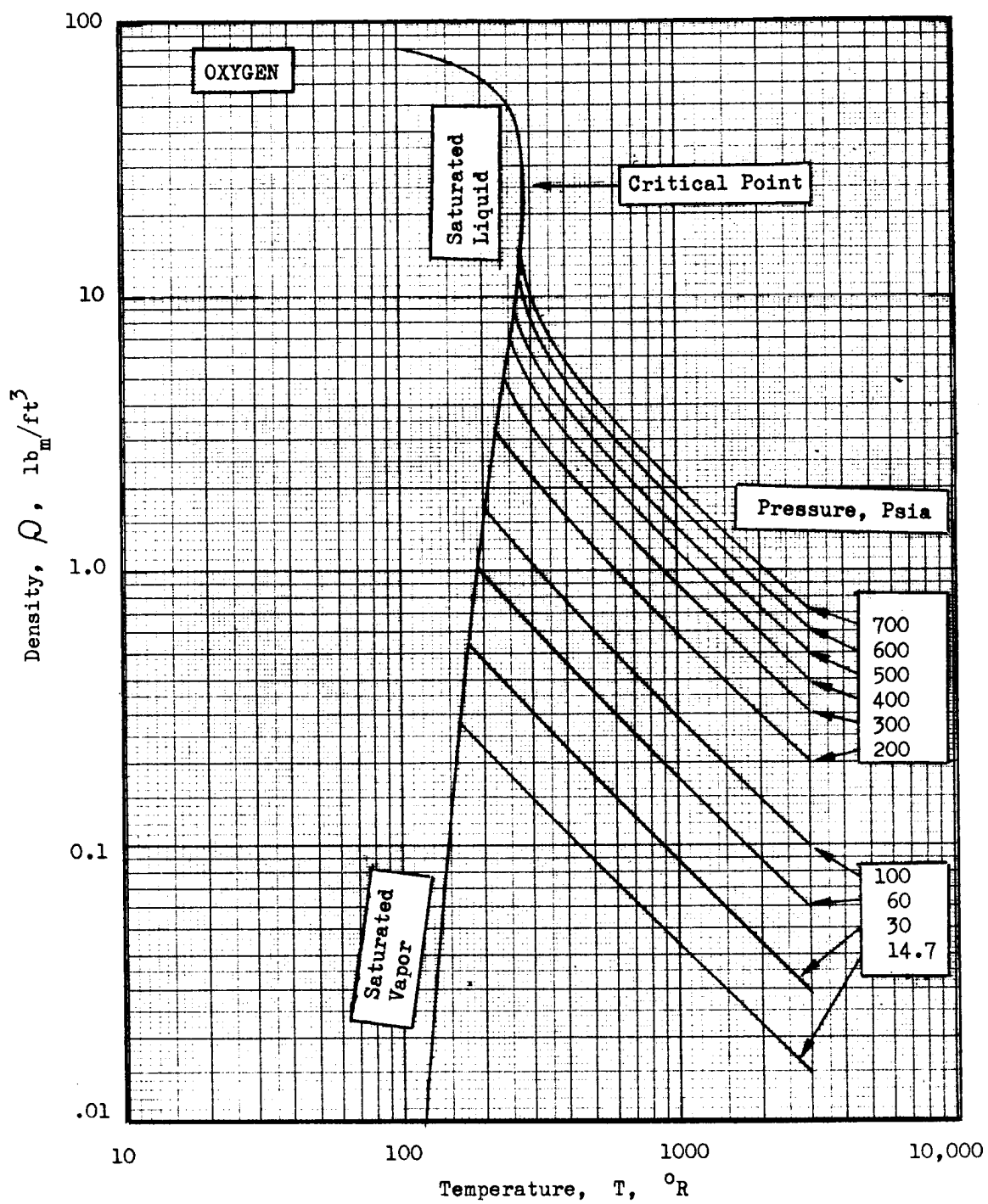


FIG. A-3 DENSITY OF OXYGEN

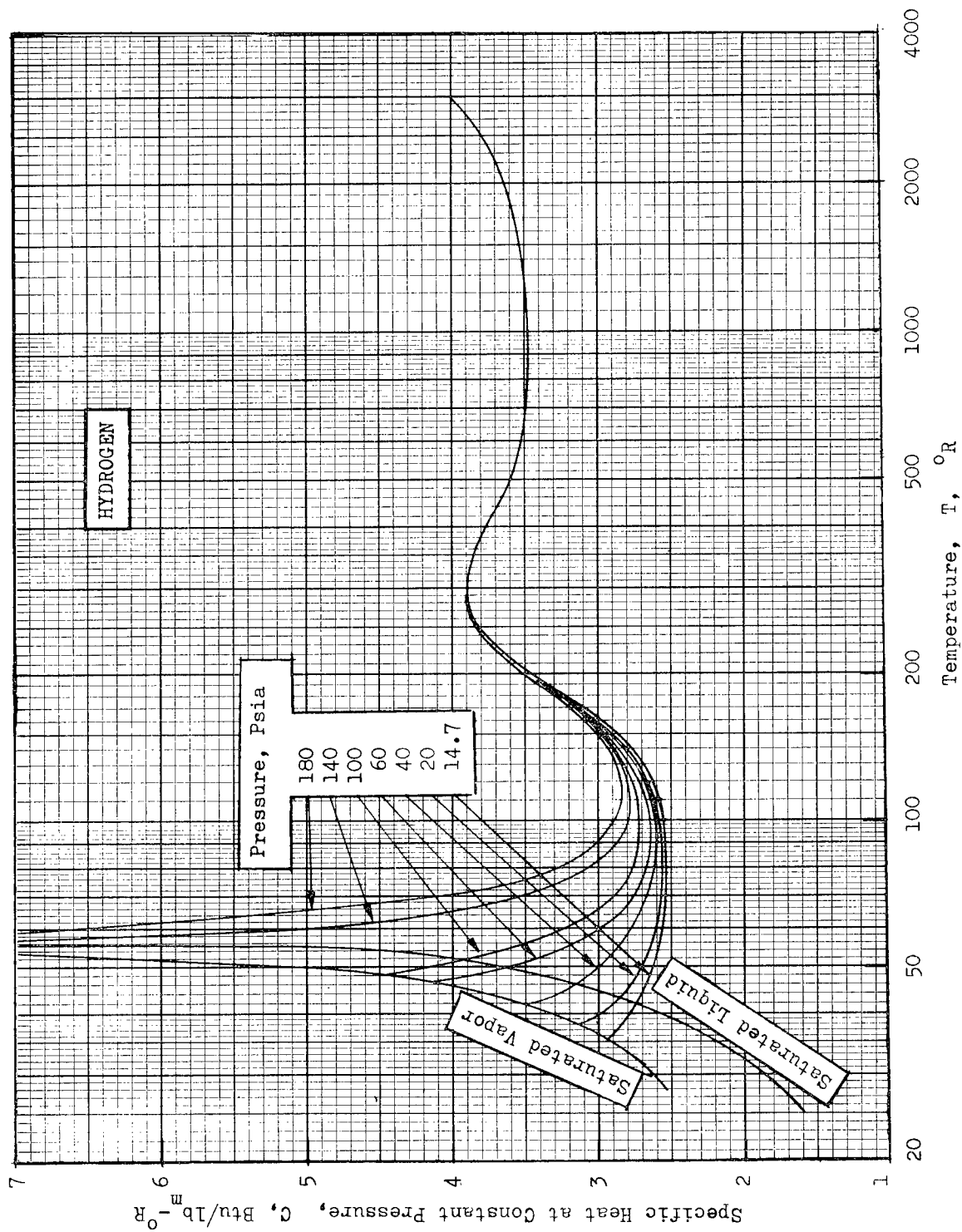


FIG. A-4 SPECIFIC HEAT AT CONSTANT PRESSURE OF PARA-HYDROGEN

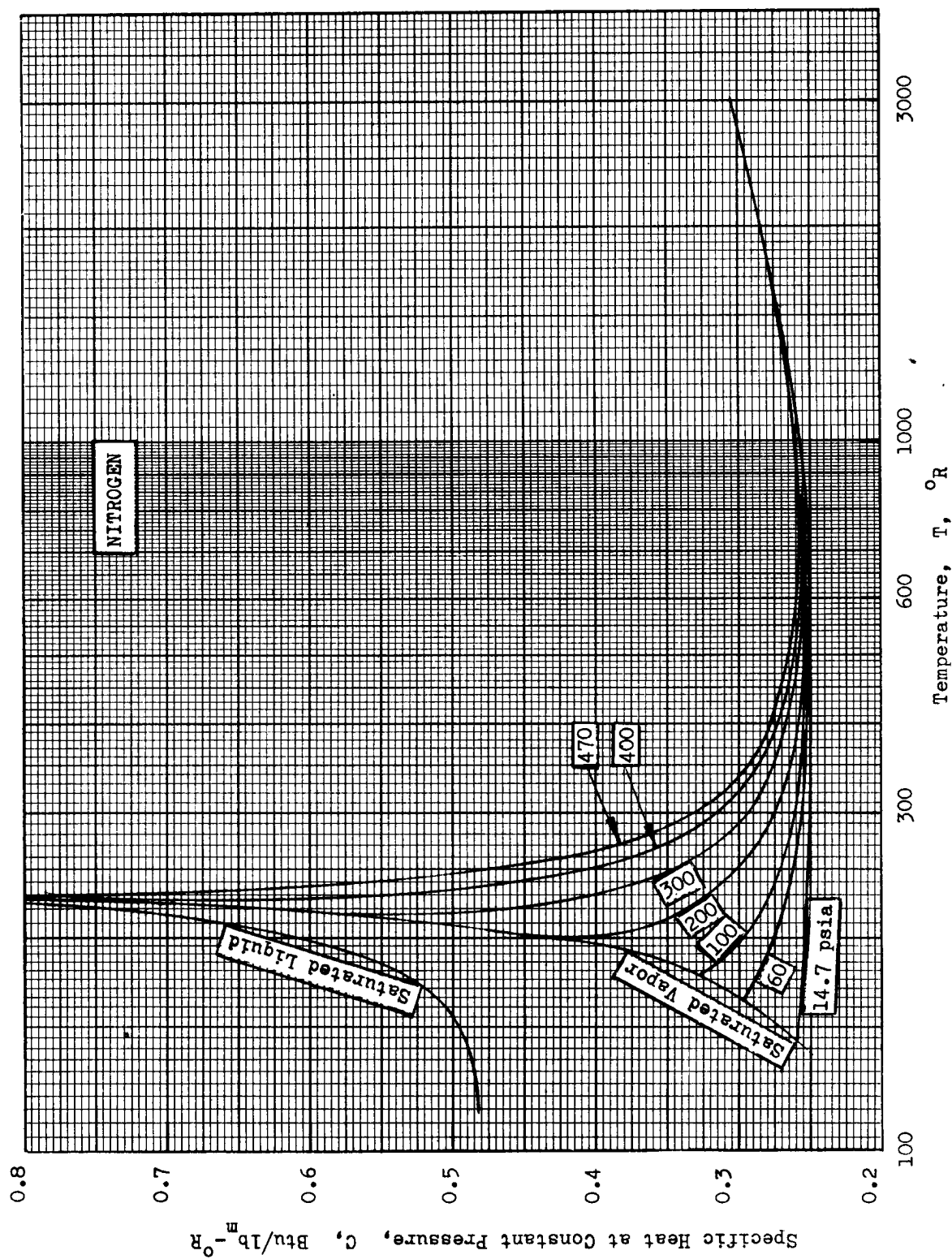


FIG. A-5 SPECIFIC HEAT AT CONSTANT PRESSURE OF NITROGEN

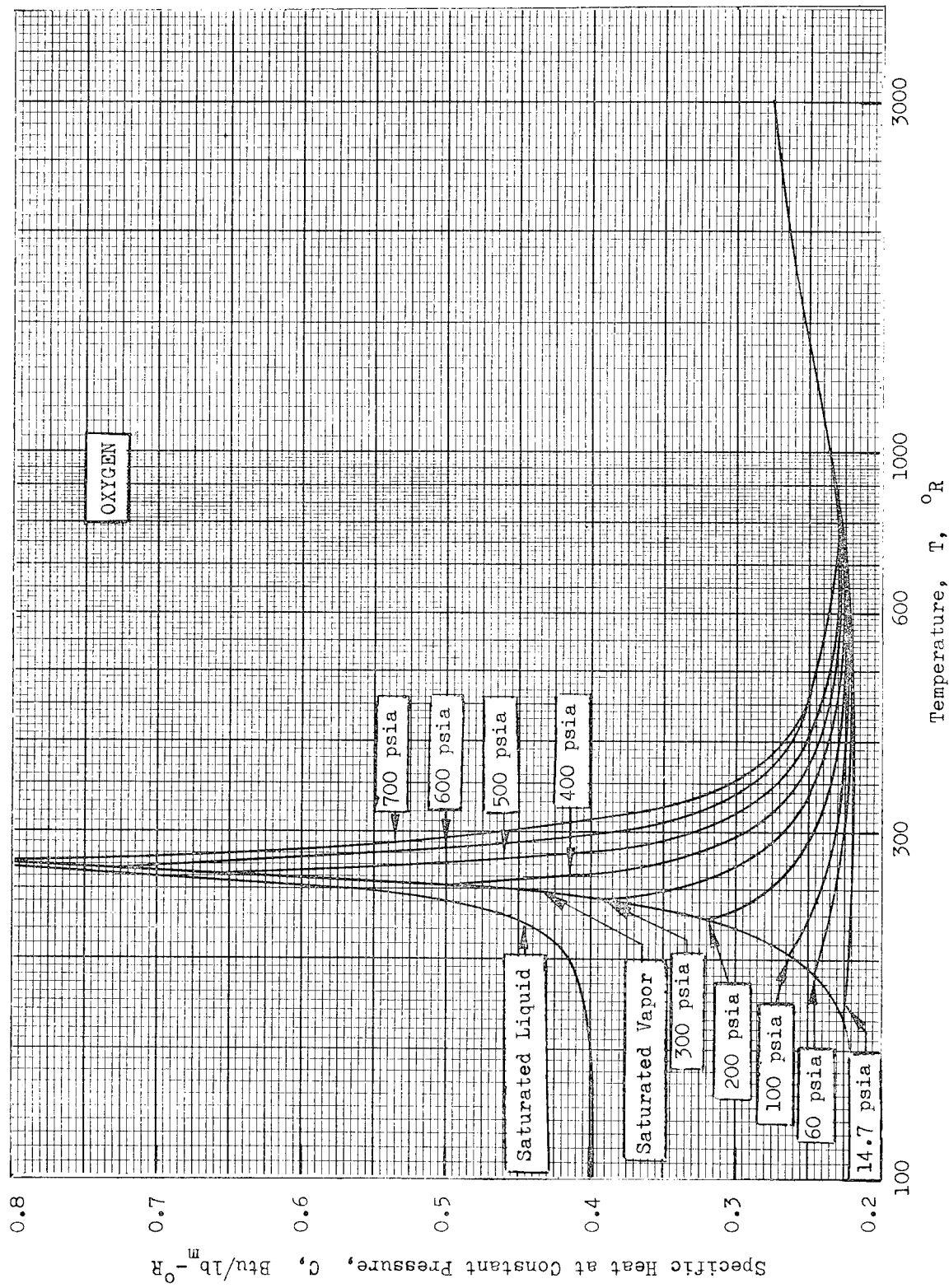


FIG. A-6 SPECIFIC HEAT AT CONSTANT PRESSURE OF OXYGEN

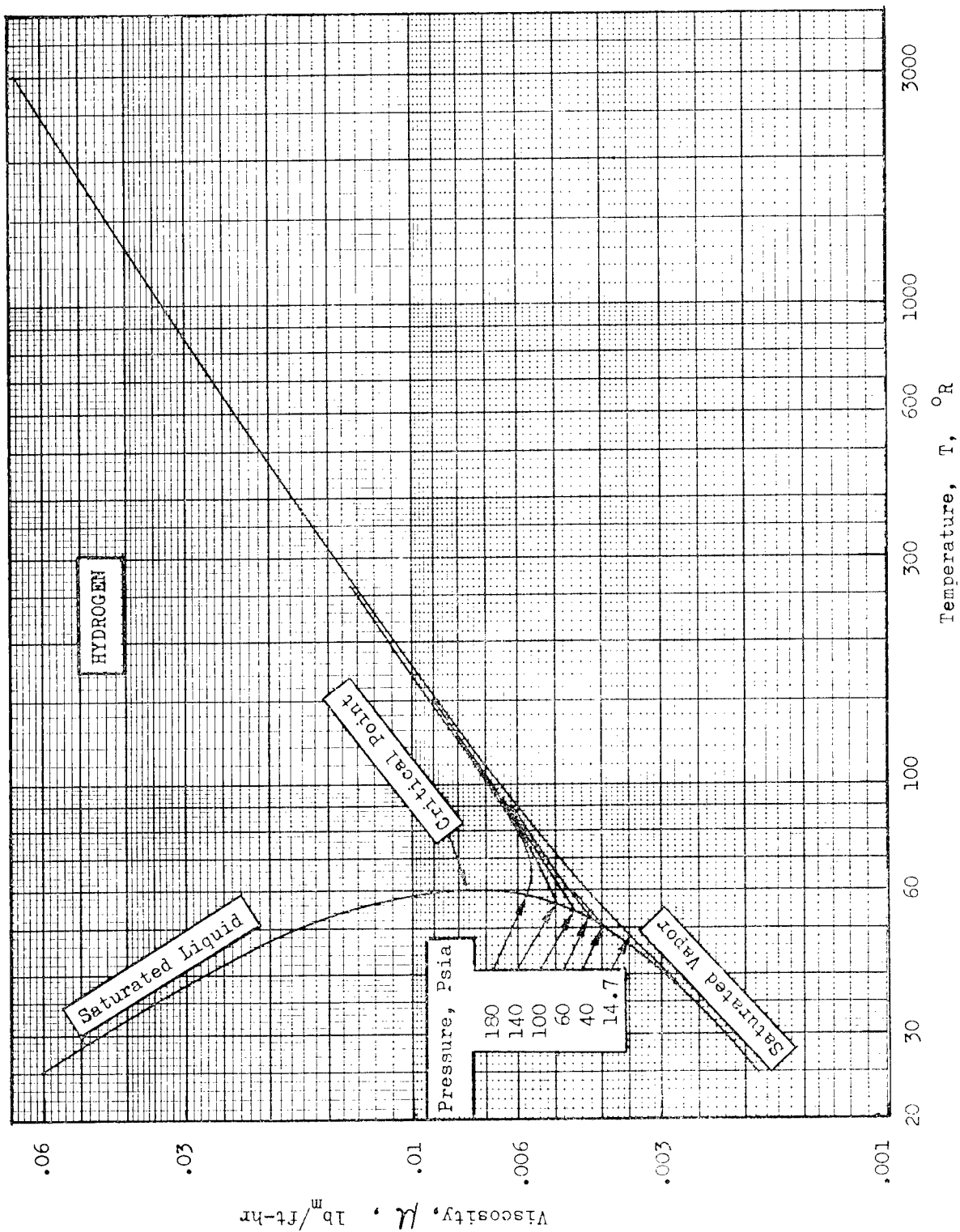


FIG. A-7 VISCOSITY OF PARA-HYDROGEN

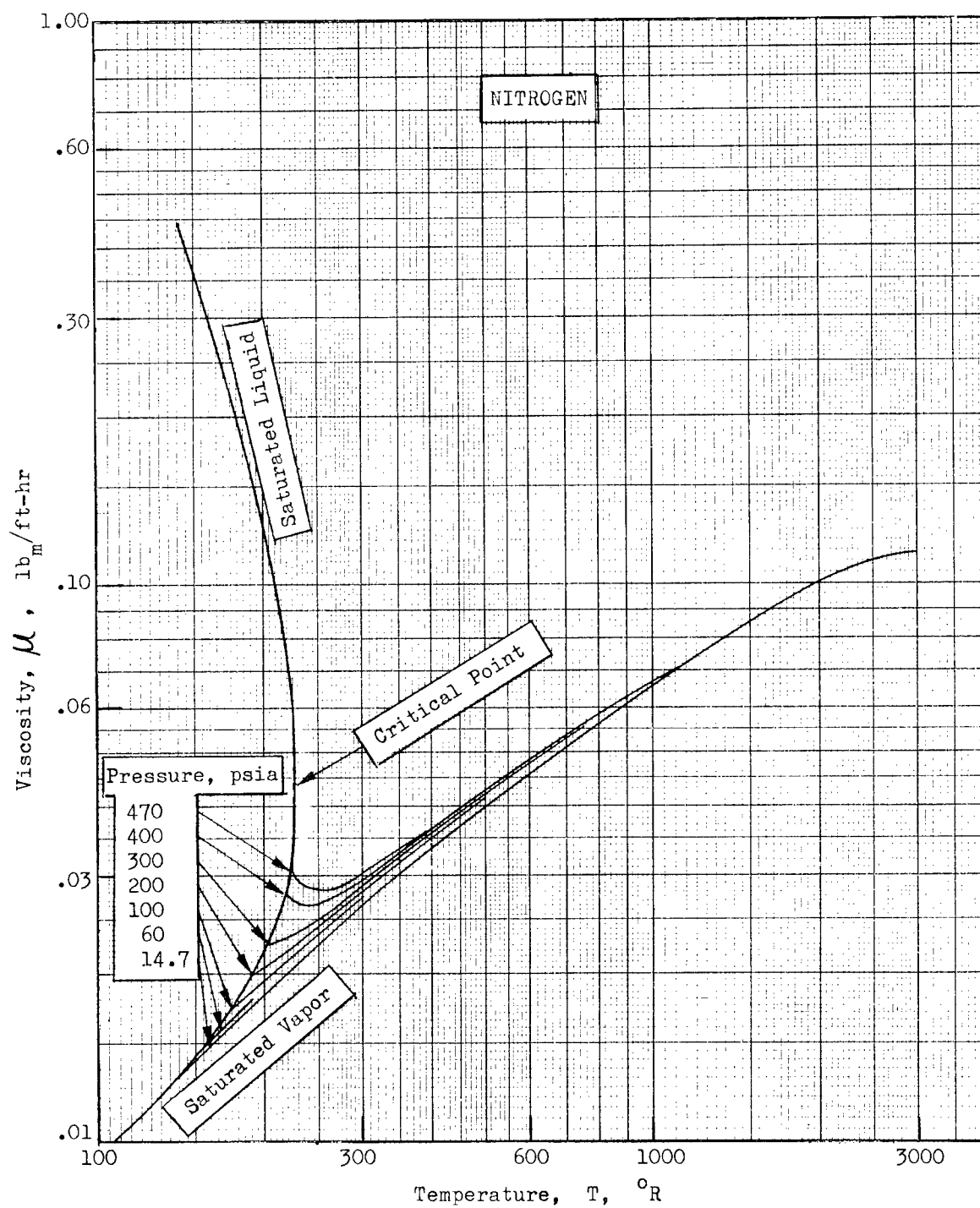


FIG. A-8 VISCOSITY OF NITROGEN

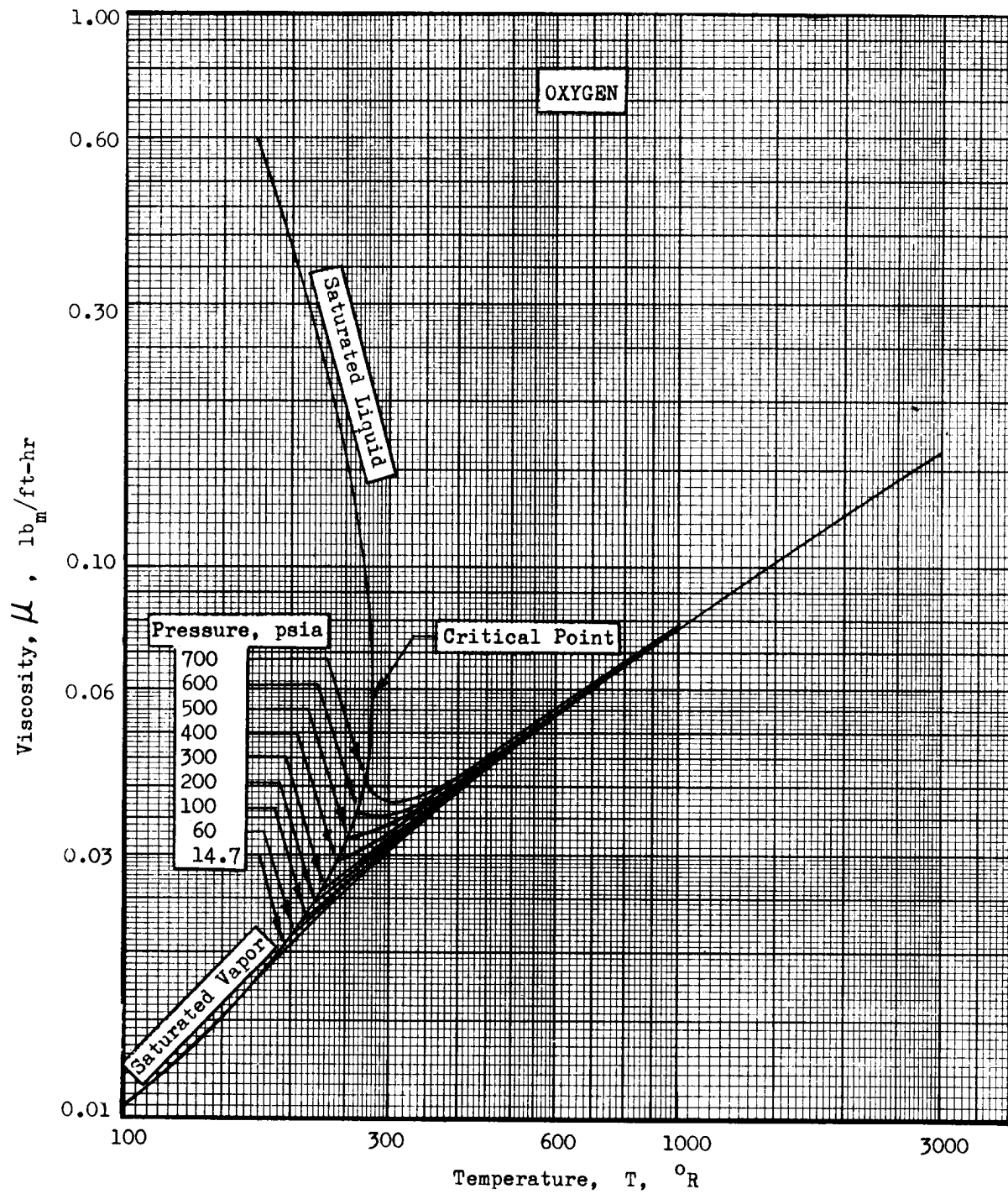


FIG. A-9 VISCOSITY OF OXYGEN

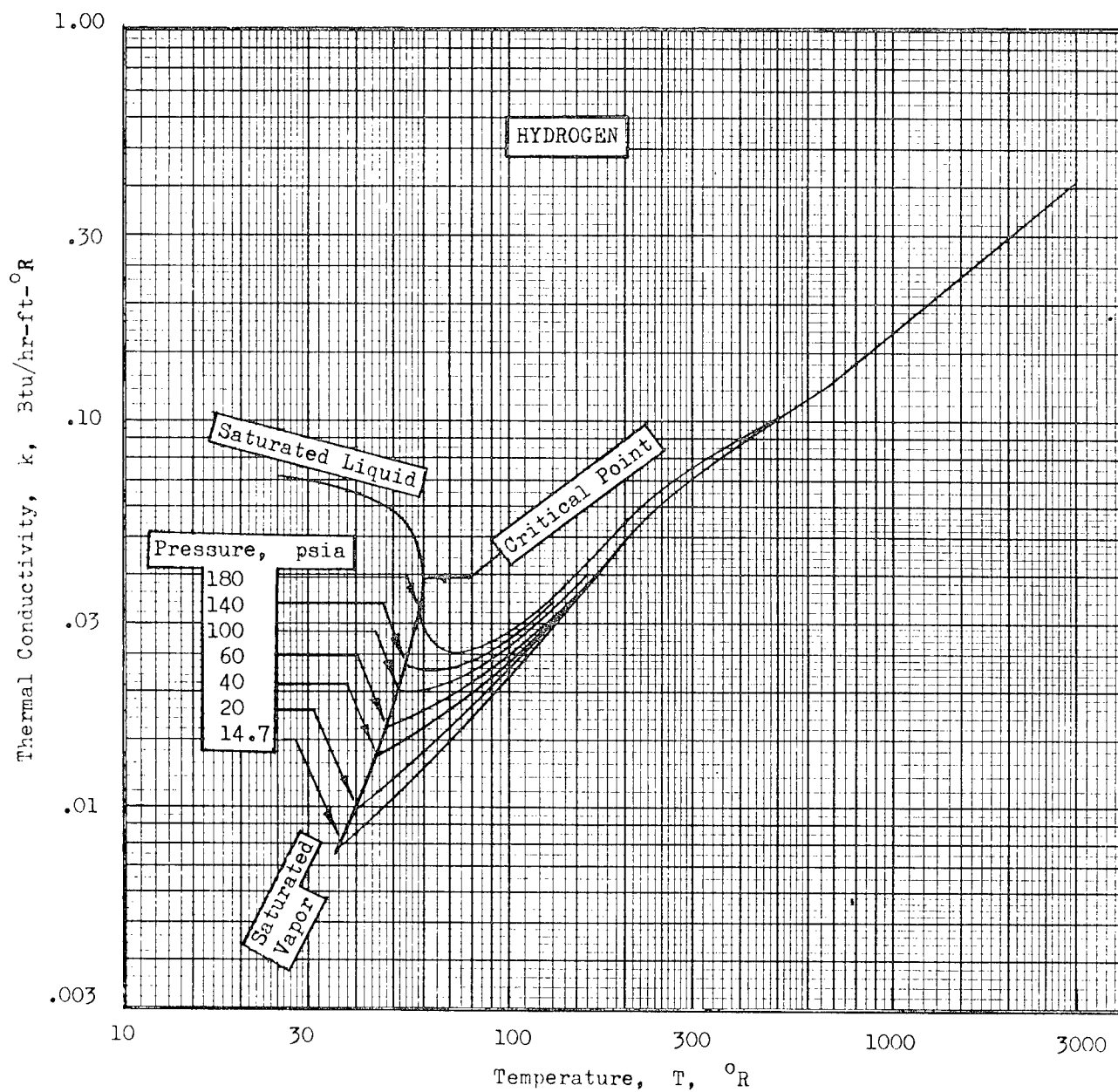


FIG. A-10 THERMAL CONDUCTIVITY OF PARA-HYDROGEN

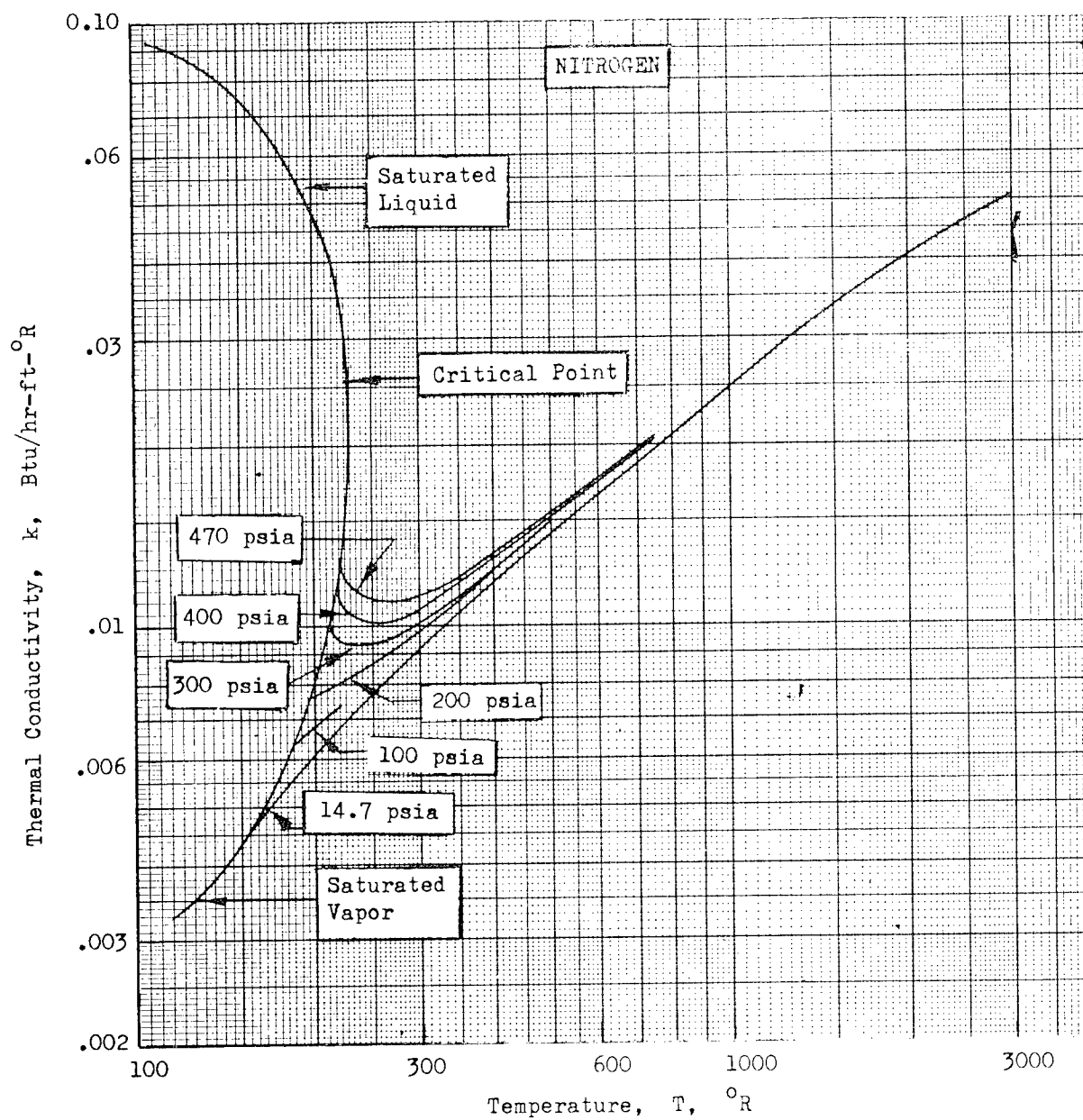


FIG. A-11 THERMAL CONDUCTIVITY OF NITROGEN

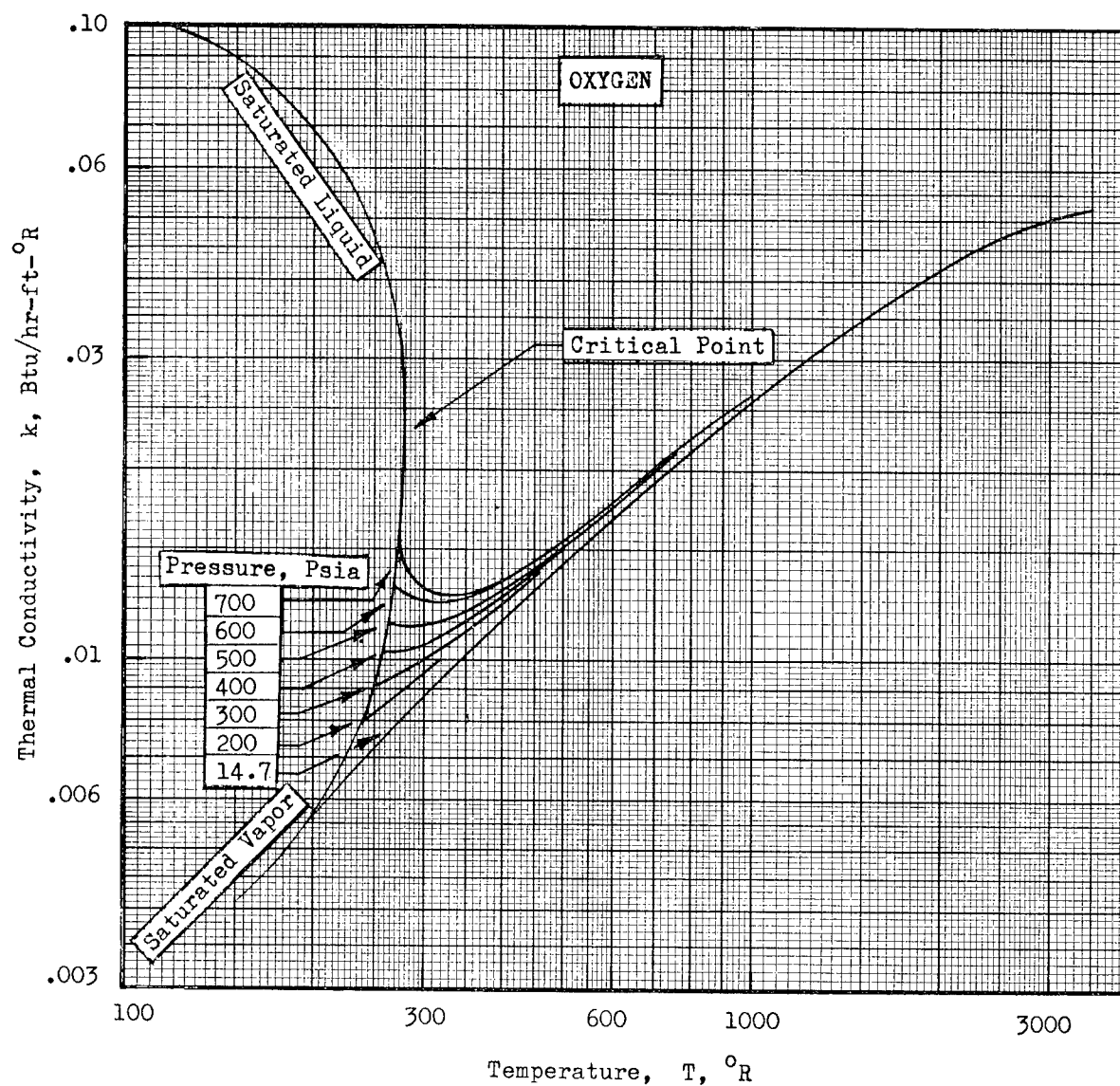


FIG. A-12 THERMAL CONDUCTIVITY OF OXYGEN

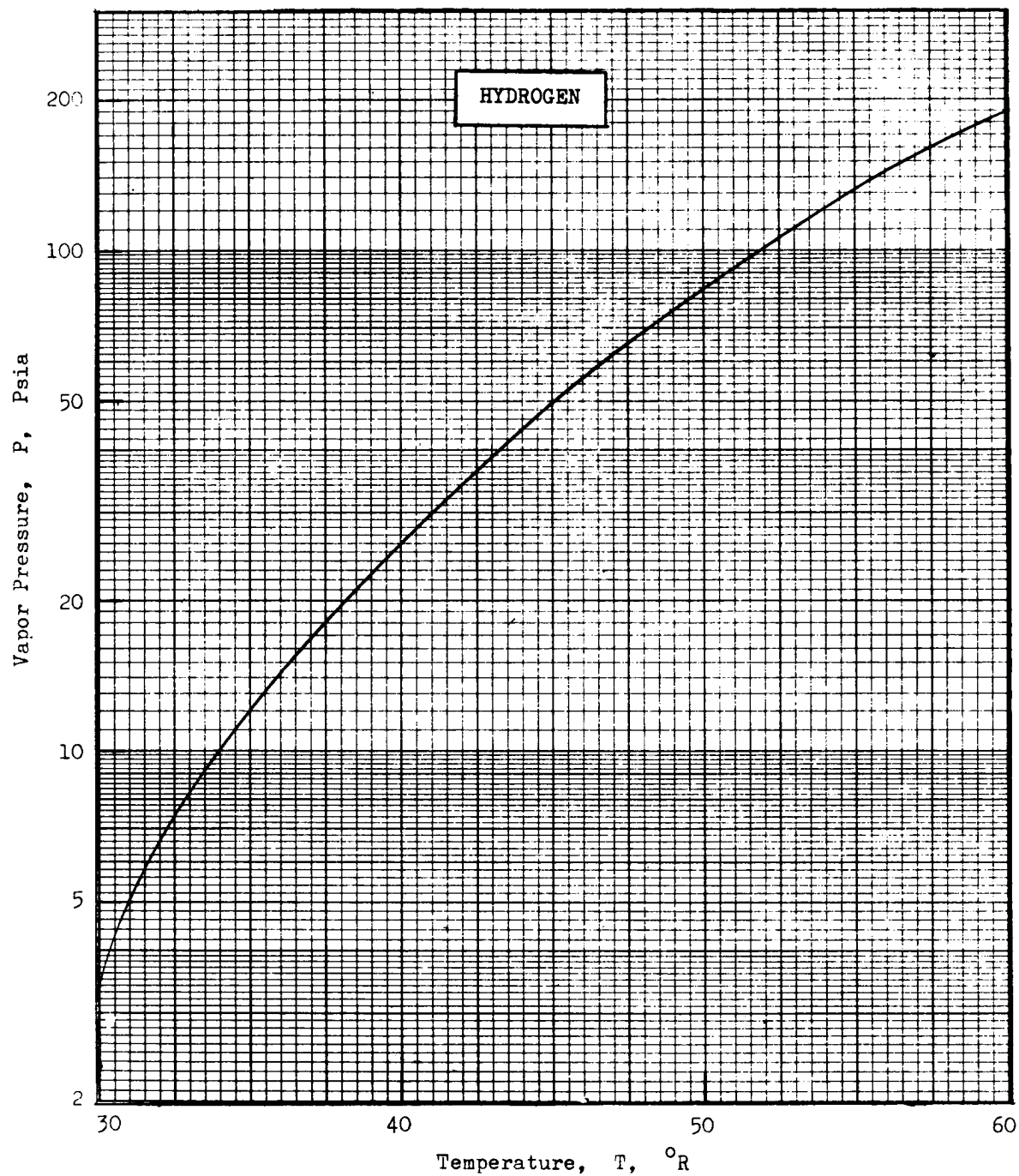


FIG. A-13 VAPOR PRESSURE OF PARA-HYDROGEN

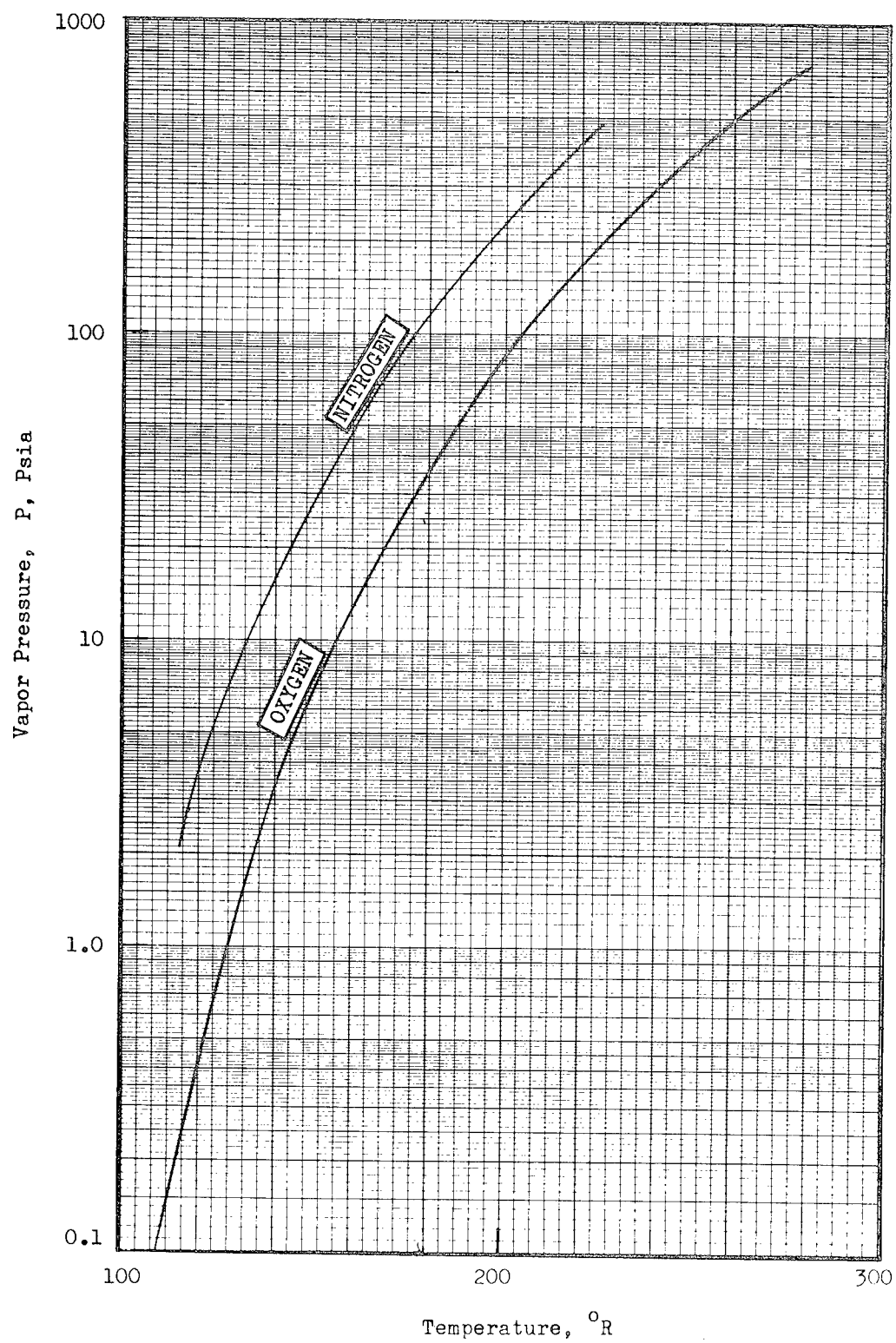


FIG. A-14 VAPOR PRESSURE OF NITROGEN AND OXYGEN

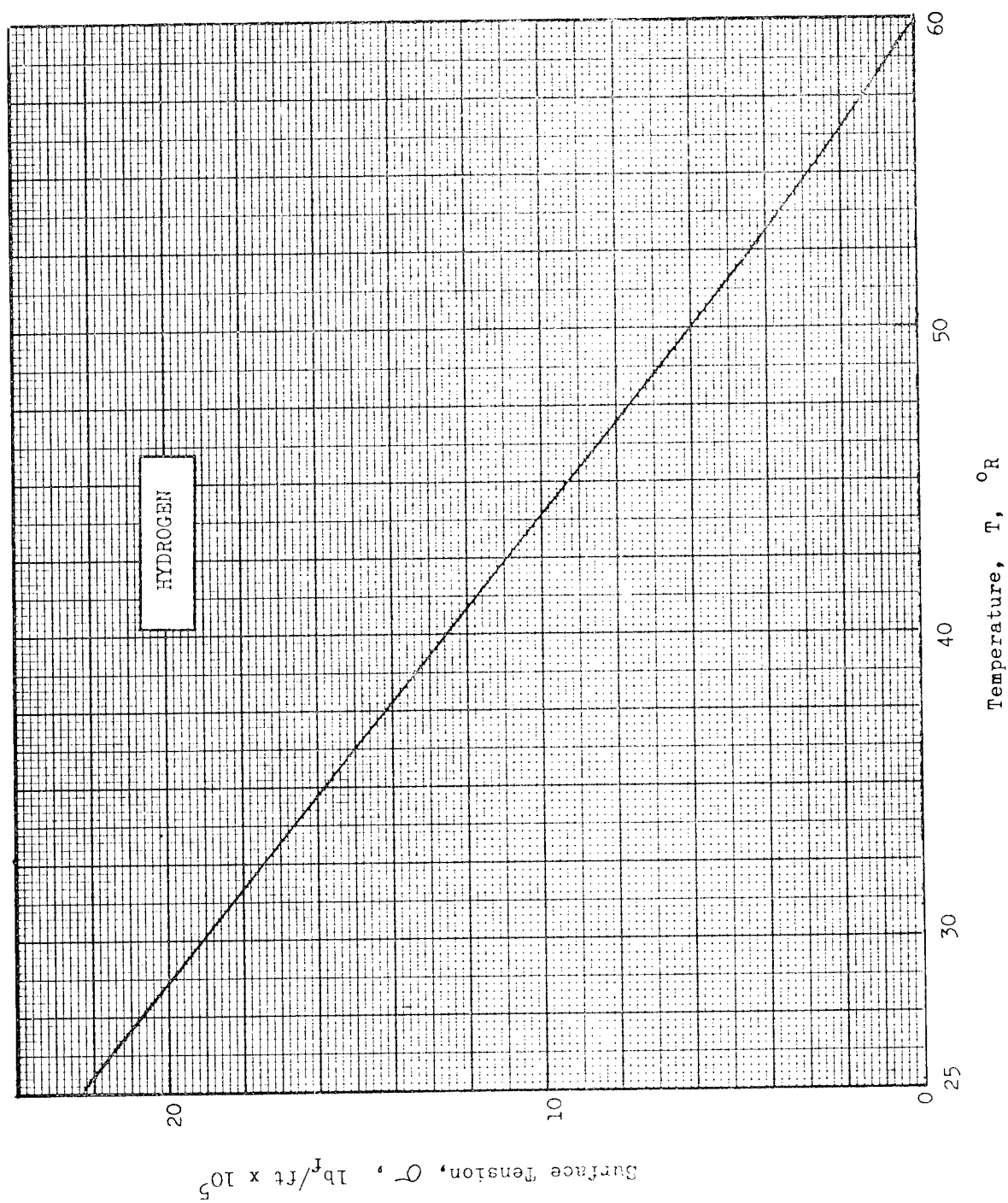


FIG. A-15 SURFACE TENSION OF PARA-HYDROGEN

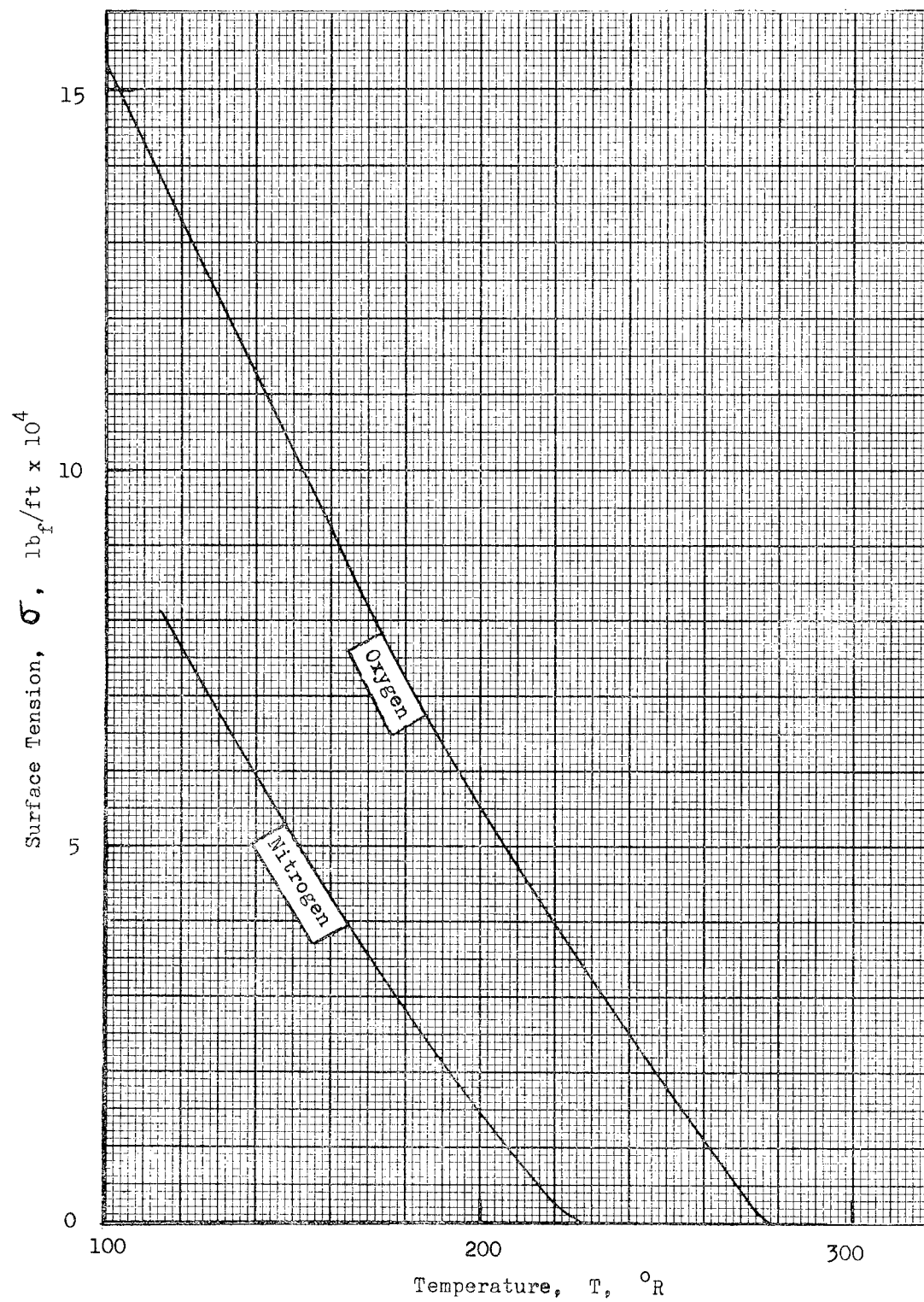


FIG. A-16 SURFACE TENSION OF NITROGEN AND OXYGEN

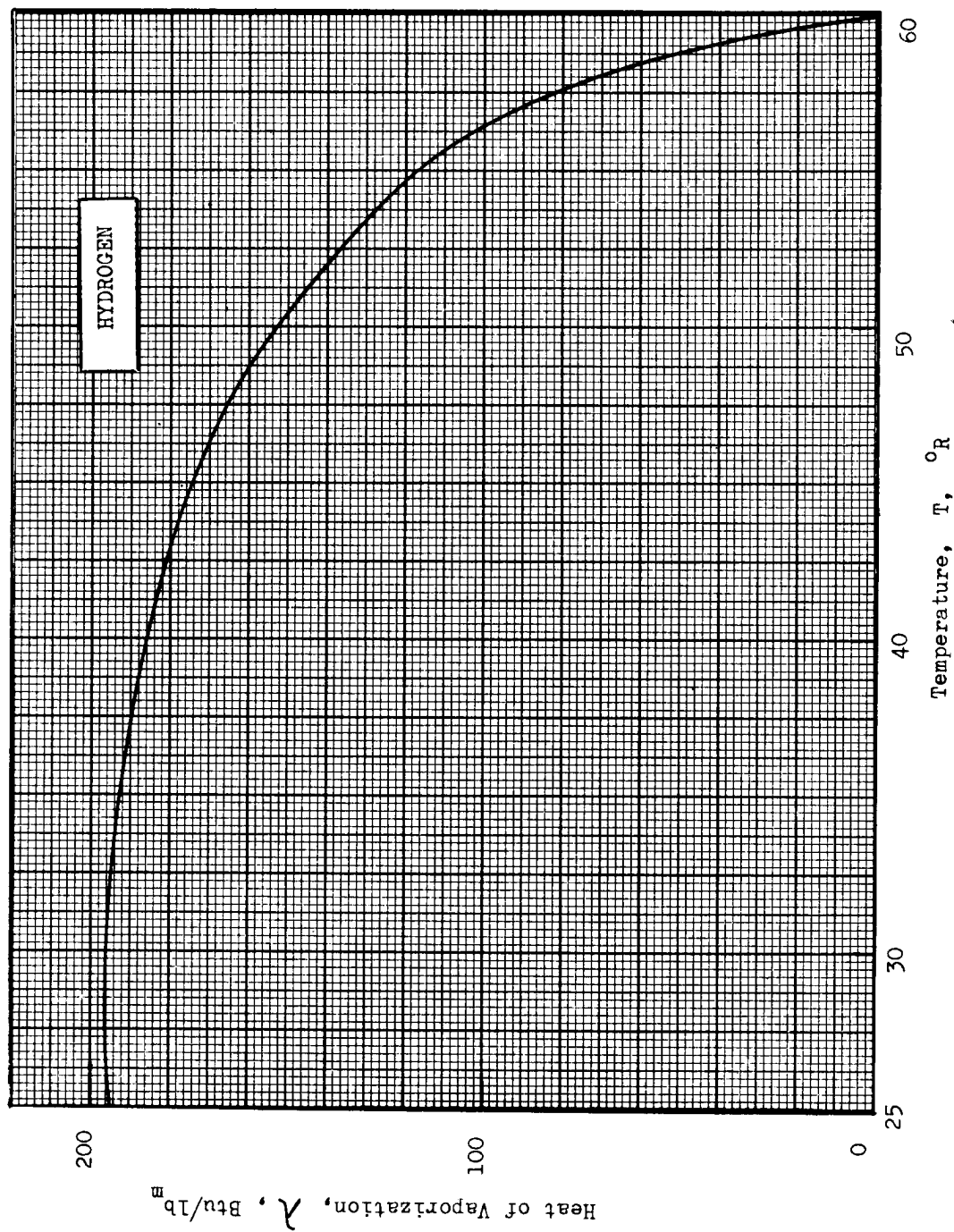


FIG. A-17 HEAT OF VAPORIZATION OF PARA-HYDROGEN

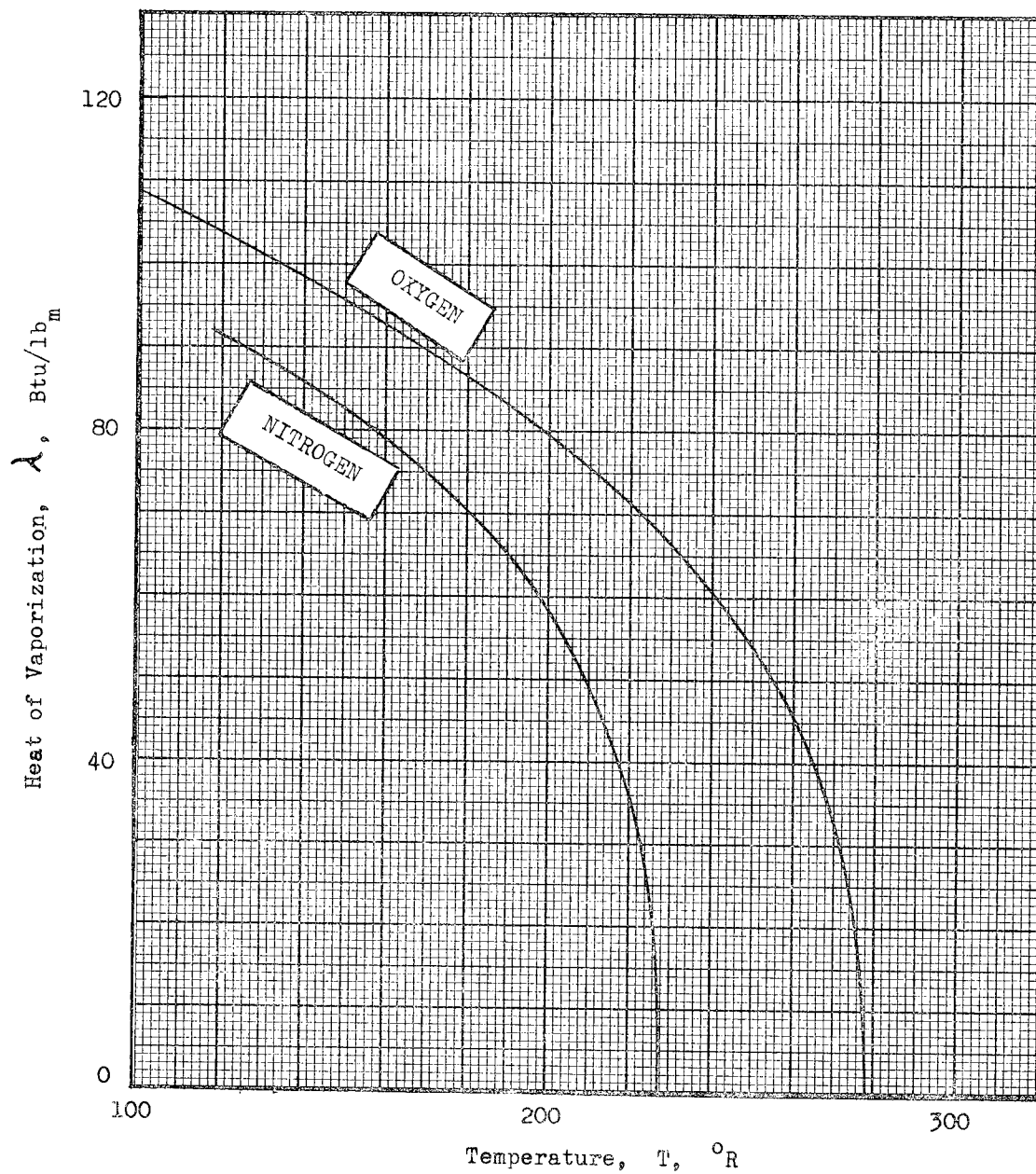


FIG. A-18 HEAT OF VAPORIZATION OF NITROGEN AND OXYGEN